EXPERIMENTAL VALIDATION OF A PRIMARY AFFERENT BASED SOMATOSENSORY NEUROPROSTHESIS

by

Christopher Albert Ayers

B.S. Electrical Engineering, Northeastern University, 2006

Submitted to the Graduate Faculty of

Swanson School of Engineering in partial fulfillment

of the requirements for the degree of

Doctor of Philosophy

University of Pittsburgh

2015

UNIVERSITY OF PITTSBURGH

SWANSON SCHOOL OF ENGINEERING

This dissertation was presented

by

Christopher Albert Ayers

It was defended on

September 21, 2015

and approved by

L.E. Fisher, Ph.D., Research Assistant Professor, Department of Physical Medicine and Rehabilitation

R.A. Gaunt, Ph.D., Assistant Professor, Department of Physical Medicine and Rehabilitation

H.R. Koerber Ph.D., Professor, Department of Neurobiology

G. Torres-Oviedo, Ph.D., Assistant Professor, Department of Bioengineering

Dissertation Director: D.J. Weber, Ph.D., Associate Professor, Department of Bioengineering and Department of Physical Medicine and Rehabilitation

EXPERIMENTAL VALIDATION OF A PRIMARY AFFERENT BASED SOMATOSENSORY NEUROPROSTHESIS

Christopher Albert Ayers, PhD

University of Pittsburgh, 2015

Losing a limb has a profound impact on the life of an individual. Unfortunately even the most advanced prosthetic limb pales in comparison to the dexterity and strength-to-weight ratio of a natural limb. Furthermore, artificial limbs cannot provide the exquisitely sensitive feedback provided by the body's natural sensors. For these reasons, the adoption rates for prosthetics remain low.

Recent advances in neurotechnology have provided researchers with the ability to stimulate through many independent electrodes. This technology can form the basis of future somatosensory neural interfaces (SSNI), replacing feedback once provided by skin and muscle with the state of a prosthetic limb encoded in patterned electrical stimulation. Suitable neural implant sites and electrode technologies for restoring sensation are the subject of active investigation.

One potential substrate for a SSNI are the dorsal root ganglia (DRG), enlargements of the spinal nerves that house primary afferent cell bodies. The DRG are compact structures located bilaterally outside the spinal cord but still isolated from movements and large muscles within the vertebral column. Unlike the peripheral nerves, the DRG are segregated from efferent flow so

afferents can be recruited by stimulation without the risk of producing uncomfortable contractions of residual muscles.

This dissertation evaluates the recruitment properties of electrodes implanted in the DRG. First, recordings from primary somatosensory cortex were used as the basis for evaluating primary afferent stimulation. Then, the effective lifetime of microelectrodes implanted in the DRG was characterized using recordings from the sciatic nerve. Subsequent instrumentation of many distal nerves enabled direct measurement of the selectivity and peripheral targets of recruited neurons. Finally the selectivity and dynamic range of epineural electrodes were characterized to demonstrate a path forward to clinical testing.

TABLE OF CONTENTS

LIST OF TABLES

LIST OF FIGURES

1.0 INTRODUCTION

Losing a limb is a profoundly disabling event that permanently separates individuals from their environs and limits their ability to affect it. There is as of yet no prosthetic that approaches the capabilities of the natural limb and so patients make do with crude approximations. Many are so disappointed with their artificial limbs that they choose to go entirely without.

The aim of this dissertation is to document the initial steps towards realizing the goal of a lower limb prosthesis augmented with restored sensory feedback. The etiology of limb loss and the significance of the problem within the U.S. will be discussed, with a focus on lower limb loss. Then, the shortcomings of current prostheses will be presented with the proposal that a better device, specifically one that provides artificial cutaneous and proprioceptive sensations, would significantly improve the quality of life of amputees. Available non-invasive solutions to sensory restoration and replacement will then be described. A new method will be proposed based on the recruitment of sensory neurons in the dorsal root ganglia. The main body of work, Chapters 2 through 5, covers experiments demonstrating the efficacy and viability of a DRG based somatosensory feedback interface. Finally, the conclusions from these experiments are summarized, with suggestions for future work.

1.1 SIGNIFICANCE AND MOTIVATION

1.1.1 Living with of Loss of a Limb

In the U.S., an estimated 1.6 million people were amputees in 2005, a number that is expected to more than double by 2050 [1]. Of these individuals, 65% were lower limb amputees, who struggle with mobility issues and are more likely than similar cohorts to fear falling [2]. The majority of lower limb amputations result from complications of peripheral vascular disease, often secondary to diabetes, in older individuals [1]. Upper extremity amputations are largely secondary to trauma, with a smaller population resulting from birth anomalies [1]. Upper limb amputees must contend with significant impact to their activities of daily living [3,4] as they cope with reduced dexterity and strength.

Prostheses run the gamut from cosmetic hands and feet to cable-actuated hooks to state-of-the-art robotic limbs [5,6], yet no single device satisfies all patient needs [7]. Most lower-limb prostheses are simple, passive devices but robotic devices are being developed that provide efficiency gains through powered push-off [6,8]. Conspicuously absent in more advanced devices is non-visual feedback, which in conventional upper limb devices is provided to the user by the cable and harness control system [9] and by stump pressure in lower extremity amputees. Although amputees successfully adapt to existing devices, high on the list of desired improvements is restored sensation [10]. Without significant progress in prosthetic limb technology, these individuals continue to endure severe reduction to their quality of life.

User satisfaction with prosthetic limbs has been investigated at length due to their high cost and low performance. Prosthetic usage is limited by poor device functionality, weight,

discomfort and a lack of sensory feedback [10,11]. Creating a replacement limb is difficult due to the required dexterity, degree of articulation, strength, and weight restrictions [5]. Prosthesis acceptance and amputation prognosis for both upper and lower extremities is generally better for more distal injuries [12]. One exception to this trend was noted in a study that found individuals with wrist disarticulations were less likely to use prosthetics [11]. The authors speculated that sensation provided by the residual limb was preferred over an insensate prosthetic hand.

1.1.2 Specific Issues Confronting Lower Limb Amputees

Lower limb amputees are nearly three times as likely to suffer from depression as a random age-matched cohort, even many years after amputation [13]. In this study, depression was attributed to social stigma associated with being an amputee. Other work has found a strong relationship between lack of balance confidence and abstention from social activities [14] which impacts quality of life and sense of wellbeing.

Lower limb amputees experience episodic residual and phantom limb pain, but unlike upper limb patients compensatory gait mechanisms are also a source of chronic pain [15]. Sequelae of amputation are osteoarthritis of the knee and hip of the intact limb and osteoporosis in the residual limb. Both conditions arise from preferential loading of the intact limb during gait [16]. Wheelchair use is uncommon, but is associated with an older population and increased levels of pain, and amongst bilateral amputees or individuals with higher level amputations [17].

1.1.3 Contribution of Feedback to Gait

The contribution of sensory feedback to gait has been demonstrated in a number of human studies and animal preparations. Many of these studies have been performed using decerebrate and spinal feline preparations to eliminate descending control of gait. The current consensus is that sensory feedback modifies commands generated by a central pattern generator as well as signaling gait phase transitions [18]. Proprioceptive feedback, via golgi tendon organs (Group Ib), in particular provides significant excitatory drive to ankle extensor muscles. In the absence of Group Ib input, either through unloading of the ankle extensors during stance [19] or the unanticipated removal of ground support [20], ankle extensor activity is significantly reduced until this feedback is restored [21]. Ankle extensor feedback is also used to signal the transition from stance to swing, which is used within the ipsilateral limb to coordinate muscle groups [22].

Primary muscle spindles (Group Ia) are thought to be the predominant carriers of kinesthetic sense. Tendon vibration produces fictive sensations of limb movement in human subjects [23] and has been shown to preferentially activate group Ia fibers to the exclusion of group Ib and group II [24]. Spindle primaries are modulated predominantly by changes in muscle length but also contain a strong fusimotor component [25] which increases sensitivity of the spindles during muscle shortening. In addition to feedback from tendon organs, the transition to swing phase is thought to be initiated by muscle spindles in leg flexors that have been stretched by extension of the leg at the end of stance [26].

1.1.4 Loss of feedback

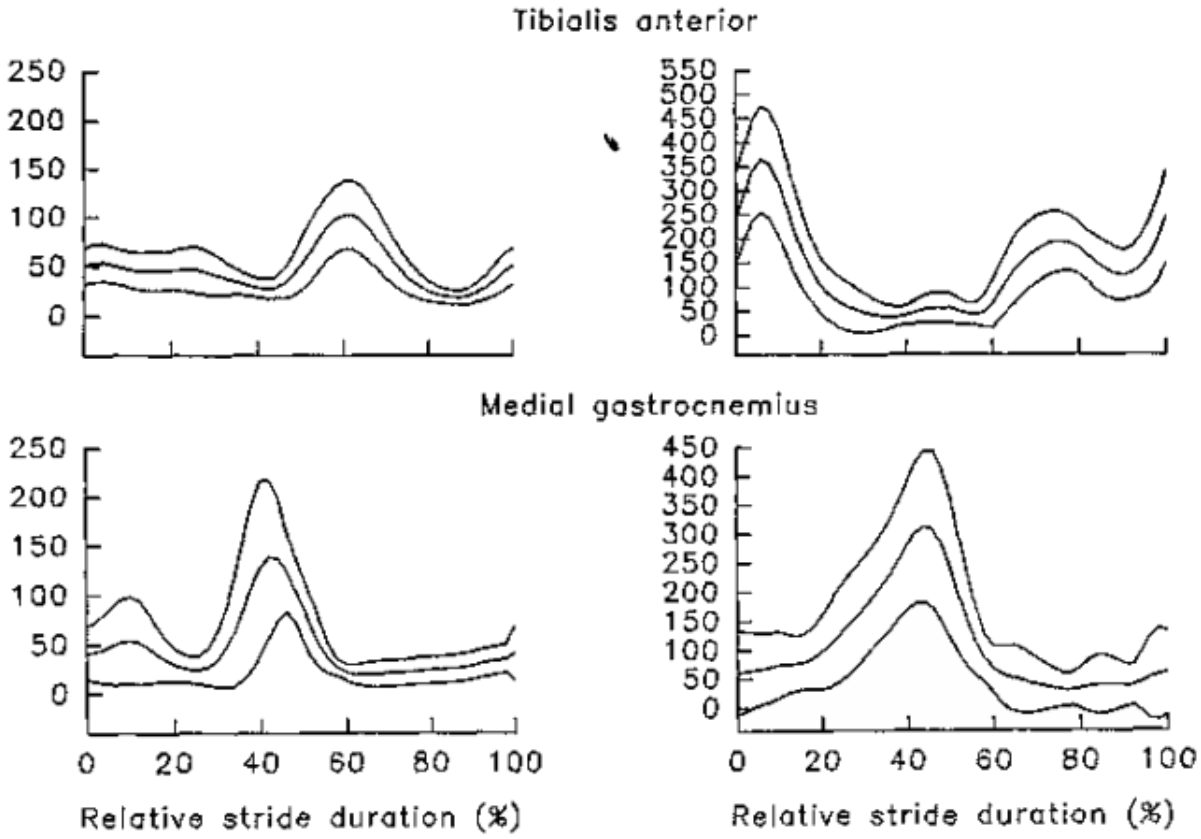

Figure 1.1 EMG from a deafferented patient during walking. Left: Deafferented subject Right: Control subject**.** Reproduced from [27].

Profound disruptions of gait and coordinated movements resulting from the lack of proprioception are readily demonstrated in non-amputees with neuropathies [28] or in locally anesthetized healthy subjects. A case study of a man deafferented below the neck found that he was only able to walk unassisted with tremendous focus and using adaptations typically found in

the elderly [27]. EMGs from this patient versus and a healthy control are shown in Figure 1.1. Compensatory gait mechanisms are reflected in the aberrant recruitment of the tibialis anterior at the beginning of the stride. Even younger, physically active, unilateral amputees have difficulty maintaining static and dynamic balance [29], a deficit attributed partially to the lack of proprioceptive feedback from the ankle. In the lower limbs of healthy subjects nearly a third of the excitatory drive of homonymous muscles was removed by acute afferent block [30] which demonstrates the strength of feedback pathways.

A study of two individuals with large fiber neuropathy in the upper limb found profound deficits in the production of simple coordinated movements, even with visual feedback [31]. Loss of feedback in able-bodied subjects through anesthetic block resulted in massive over production of grip force when handling known objects, despite the body's internal models that attempt to minimize force [32]. It is clear that sensory feedback is an essential part of motor control in both the upper and lower extremity.

1.1.5 Non-Invasive Feedback Mechanisms

Amputees receive a limited amount of sensory feedback from their artificial limbs. With conventional devices, feedback to amputees is provided by shear forces and pressure at the stump. Non-visual feedback in powered devices can be provided by motor vibration and sound emitted by the prosthesis. Subjects with osseointegrated devices gain additional vibratory feedback over those fitted with conventional devices [33], in a phenomenon known as "osseoperception".

There are a number of existing and emerging noninvasive technologies that have been designed to restore sensations of ground contact to amputees. In lower-limb amputees, transcutaneous stimulation has been used by the prototype "Sense-of-Feel" device to signal fore/aft center of pressure via transcutaneous electrical nerve stimulations (TENS). Users of this device were able to improve both weight distribution and step length symmetry [34]. Haptic feedback has been shown in able bodied individuals [35] and an amputee [36] to reliably transfer information about pressure on the sole of the foot to the thigh. Such a haptic system may improve balance in lower limb amputees by intuitively communicating center of pressure. As of yet, none of these methods have gained mass adoption. Even if ground reaction force feedback were integrated into existing devices it would still leave patients with a glaring lack of kinesthetic feedback.

1.1.6 Somatosensory Neural Interfaces (SSNIs)

Recent developments in neural recording and stimulation technology provide hope for novel solutions to sensory restoration. Commercially available high channel neurophysiology recording and stimulation equipment and multi-electrode arrays (MEAs) [37] enable researchers to focus on the development of therapeutic devices rather than electrode and amplifier fabrication. Advances in robotics technological have produced highly articulated prosthetic arms [5] and powered lower limbs [6] that can potentially utilize the large number of inputs from MEAs. The benefits of advanced prosthetic limbs may be moot, however, as using currently available devices is already difficult without the body's natural feedback [38].

Nerve stimulation has been suggested as a potential method for restoring feedback by transforming the kinematic state of a prosthetic device into the patterned stimulation of afferents. In exchange for a more invasive procedure, subjects could be provided with intuitive feedback that will reduce the learning curve of rehabilitation. Nerve stimulation of varying intensities and pulse rates can produce non-specific yet discriminable sensations (i.e. paresthesiae) that amputees can learn to distinguish [39]. These authors later used the same procedure to characterize the extent to which individual frequencies could deliver meaningful information [40]. Adaptation of the perceived sensations, perhaps due to mass activation of the nerve, ultimately prevented this method from being clinically useful. Nerve stimulation was refined shortly thereafter into a method capable of delivering "pure" or unimodal sensations named intraneural microstimulation (INMS) [41]. Using percutaneous electrodes inserted into the superficial nerves of restrained human subjects, the full suite of cutaneous and muscle afferents was diligently studied [42]. A notable limitation encountered by these investigators was the frequent inability of subjects to sense the recruitment of either individual spindle primaries or SA II (skin stretch) afferents. Microneurography and INMS provided a wealth of information on the behavior of primary afferents, however these techniques are not practical for use in an SSNI due to the difficultly of isolating an individual axon for extended periods of time [43].

As INMS studies have demonstrated, the periphery is an attractive substrate for a SSNI thanks to the accessibility of the nerves and the simplicity of the neural code. Many electrode technologies are designed for implantation in the peripheral nerve [42,43,44] but there are significant challenges with achieving both a highly selective and stable interface with peripheral nerves. Penetrating microelectrodes are able to achieve highly selective recruitment, but do so at the expense of stability. Non-penetrating epineural electrodes are stable but their large active

areas and distance from neurons necessitates the use of high intensity stimulation which reduces recruitment selectivity. Choosing a location within the peripheral nerve to implant an electrode is a compromise between emphasizing limb coverage (proximal) or selectivity (distal) [47] and subject to the constraints of the particular injury.

Most peripheral nerves contain both sensory and motor neurons, therefore stimulation must selectively recruit afferent over efferents axons. Activation of muscles drives natural feedback that may interfere with the intended artificial feedback, and furthermore may be uncomfortable. Muscle movement and nerve stretch put mechanical strain on implanted devices and additional precautions must be taken to avoid device failure [48]. Further, recording electrodes, used for myoelectric control of a prosthetic limb, may be contaminated by evoked EMG [49].

There have been a number of recent studies focused on clinical translation of SSNIs. MEAs have been implanted in the median and ulnar nerves of a human subject and were used to provide many individual tactile sensations referred to the missing hand [50]. Proprioceptive sensations were “infrequent”, a fact attributed to electrode placement being distal to major motor branch points. Epineural cuff electrodes, including the self-sizing spiral nerve cuff and flat interface nerve electrode (FINE), have likewise been implanted in the upper limbs of humans but have yet to produce proprioceptive sensations [51]. The only study involving indwelling electrodes to reliably evoke kinesthetic sensations is the work of Horch et al [52]. LIFE electrodes were implanted in upper extremity amputees to evoke both proprioceptive (finger movement) and force sensations. In sum, clinical studies of SSNI demonstrate that reorganization of the nervous system following long term amputation [53] does not prevent subjects from perceiving artificial sensations referred to their missing limbs. Furthermore, in the

studies described here a common secondary outcome of providing even coarse sensory feedback has been a reduction or extinction of phantom limb pain.

Unfortunately, nearly all studies of SSNIs focus on the upper extremity. Clippinger et al. implanted epineural electrodes on the sciatic nerve of 13 patients to provide both ground contact feedback and relief to phantom limb pain [54]. The bending moment produced by a piezoelectric crystal placed in the sole of the prosthetic foot was used to linearly modulate stimulation frequency. Thus, stimulation frequency was highest during stance onset and toe off and lowest at mid-stance. During swing phase stimulation was completely turned off. The users of this device self-reported more confidence when walking in the dark, walking over uneven ground, and climbing stairs. The reported outcomes were subjective, but still provided evidence of functional improvement even with this fairly simplistic feedback. This study also demonstrated that even several years post amputation, subjects had healthy residual nerves capable of responding to stimulation and evoking naturalistic sensations.

1.1.7 Dorsal Root Ganglia

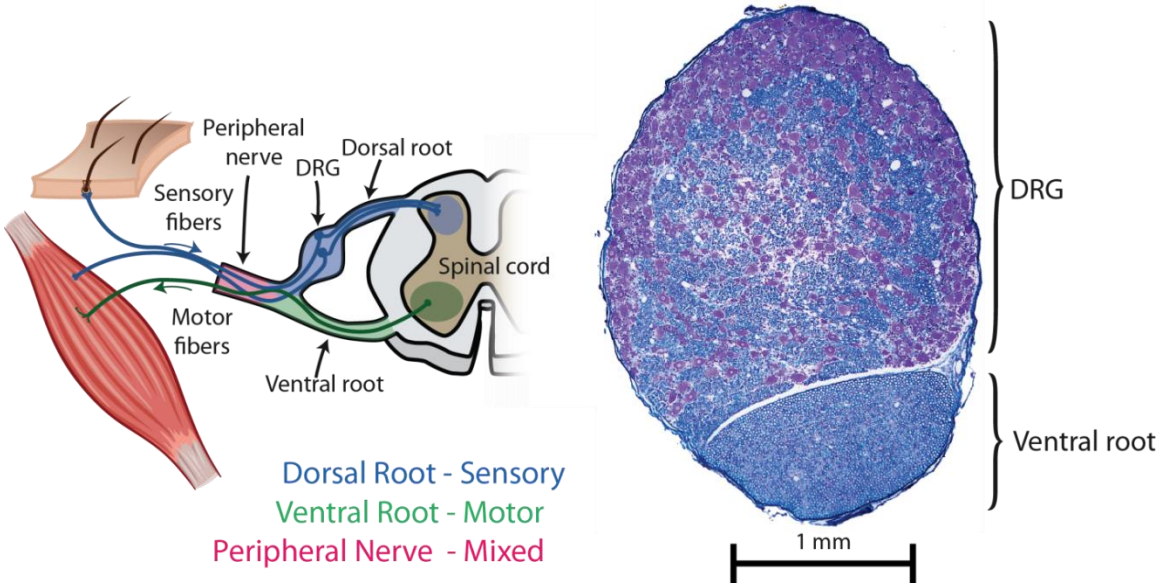

Figure 1.2 DRG Physiology. Left: Anatomy of the spinal roots and periphery. Right: Cross-section of an unimplanted right L6 DRG and ventral root. Tissue has been stained using Nissl (violet, cell bodies) and Luxol fast blue (myelin). Cell bodies tend to cluster near the exterior wall of the DRG.

One potential substrate for a SSNI are the dorsal root ganglia (DRG), enlargements of the spinal nerves that house primary afferent cell bodies (Figure 1.2). The DRG are compact structures located bilaterally outside the spinal cord but still isolated from movements and large muscles within the vertebral column. Electrodes implanted within the DRG are protected from damage and migration by the vertebrae. Unlike the peripheral nerves, the DRG are segregated from efferent flow so afferents can be recruited by stimulation without risking uncomfortable

contractions of residual muscles. Histology has shown that cell bodies of the DRG tend to cluster near the exterior, which may be useful for devices which need to record afferent activity.

Preserving the natural processing of sensory feedback is a distinct advantage of primary afferent based SSNIs over cortical ones. There is a large amount of prior work on primary afferent encoding models that could be leveraged by a DRG based SSNI [25,53,54]. These models can be used to encode the state of a prosthetic limb into patterned electrical stimulation of the DRG. Recruiting primary afferents preserves natural post-synaptic processing of sensory feedback, allowing information to diverge at spinal and supraspinal levels as would happen naturally. In contrast, a cortical based SSNI must contend with the comparatively poorly understood cortical encoding of proprioception, and if multiple regions are to be implanted multiple encoding schemes must be used. Cortical stimulation relies necessarily on access to the brain which greatly increases the surgical risk.

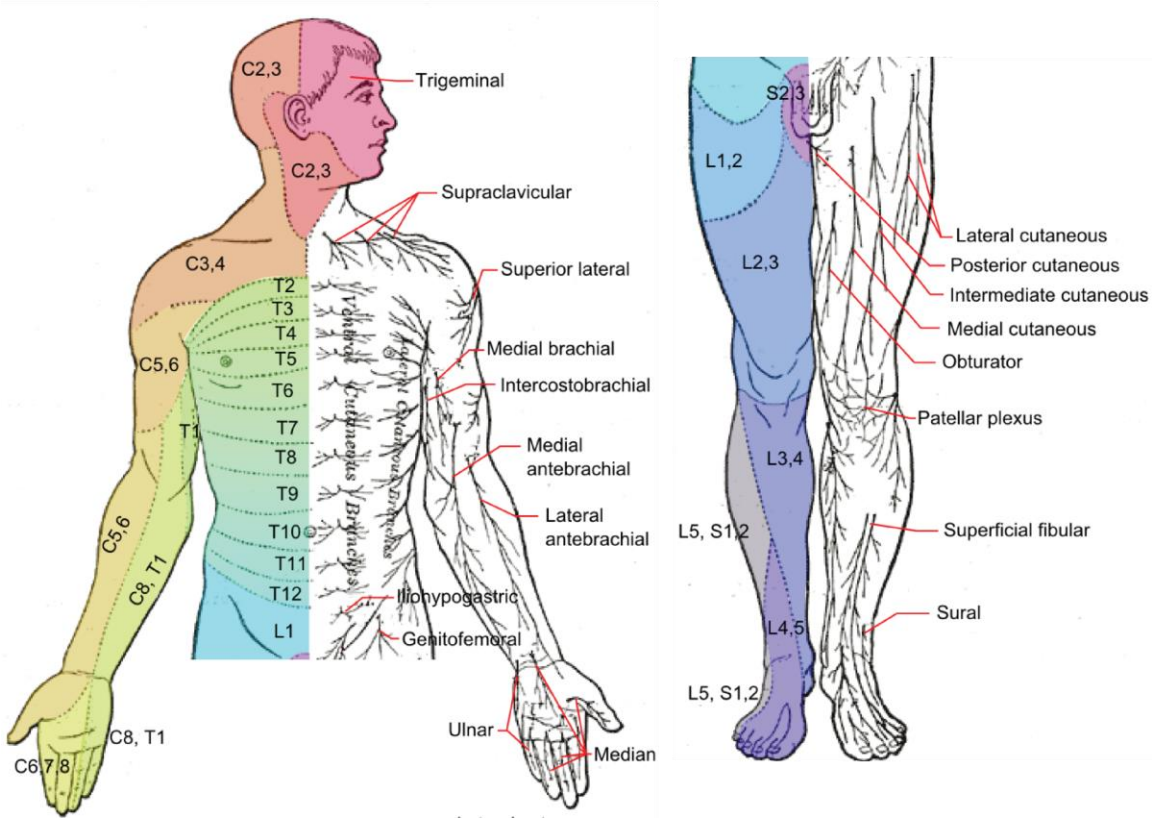

Figure 1.3 Dermatomes of the human body. Each color indicates the afferent flow from a patch of skin to a particular spinal segment. At each spinal segment are bilateral DRG containing the cell bodies of the ipsilateral dermatome. Reproduced from [57].

The afferent flow of the body is split in a segmental fashion across the population of ganglia, and the neurons within each ganglion only innervate a small portion of the limb (Figure 1.3). Restoring sensation to a trans-tibial amputee, for example, may require implanting the L3-S1 DRG. This is similar to the hindlimb of the cat which is innervated by 3-4 ganglia [58]. Studies have found varying degrees of somatotopy within the cross-section of the DRG, either based on rostral-caudal [59] or muscular [60] innervation patterns. Regardless, if the cells of the

DRG follow an organizing principle it is much more diffuse than can be found in somatosensory cortex or within distal peripheral nerves. A SSNI based on the DRG cannot guarantee *a priori* that sensations will be referred to a specific location within a dermatome and therefore such a device must allow clinicians to tune individual channels based on the distal targets of the recruited neurons. One strategy is to implant an array with many electrodes that cover an entire DRG to ensure adequate coverage of a diverse neural population. Current steering can also provide additional "virtual" channels of stimulation that recruit neurons not accessible by physical electrodes.

1.2 SSNI PERFORMANCE REQUIREMENTS AND ASSESSMENT

DRG primary afferent microstimulation (PAMS) is an attractive basis for a SSNI, but many practical concerns must be addressed prior to its use in human subjects. First, an animal model must be established to validate whether a DRG SSNI satisfies requirements for viable clinical translation. There are many requirements levied on an SSNI but several stand out: 1) it must be stable, reliably recruiting sensory neurons for many years post implantation, 2) it must be selective, able to recruit targeted neural populations to the exclusion of others, and 3) it must be safe, implantation of electrodes must cause minimal damage to the targeted neural structures, which may degrade residual function or be painful. These requirements are introduced here, and then investigated in depth in the chapters that follow.

1.2.1 Evaluating SSNI Function

One of the main difficulties confronting the development of a SSNI is the lack of a standard human or animal model to validate performance. Antidromic propagation of action potentials in the sciatic nerve has been used to characterize the selectivity of DRG PAMS and provide coarse estimates of the modality of recruited neurons [61]. However, measurements of nerve recruitment can't answer questions about the downstream integration of afferent activity necessary for proprioceptive feedback.

Models developed for other sensory systems may provide insight into developing a useful experimental paradigm. Auditory feedback can be readily tested using conditioned avoidance to fictive tones [62] and visual feedback can be verified using saccades to evoke phosphenes [63]. The development of paradigms to evaluate artificial auditory and visual feedback was enabled by the quantal nature of tones and phosphenes. Cutaneous sensations are quantal in nature as well: they are referred to a specific location and have a unimodal character such as vibration or pressure. There exist several primate models of artificial cutaneous feedback [62,63,64] that have shown detection of stimulation and discrimination between stimulation parameters.

Developing a model to test proprioception is more difficult as it relies on the congruent input of a physically distributed network of afferents. In particular multiple muscular (i.e. primary muscle spindles, secondary muscle spindles and golgi tendon organs) and cutaneous (i.e. SAII and SAIII [67]) afferents are all essential elements of conveying limb state information. Previous work has indicated that proprioception lacks an atomic component that can be easily interrogated, unlike vision, audition or even cutaneous sensation. Recruitment of individual muscle spindles fails to evoke conscious sensations of movement [42] but mass activation of

muscular afferents can produce sensations of assumed hand positions [68]. Trained animals have little difficultly detecting evoked cutaneous sensations but, despite the low recruitment threshold of muscular afferents, eliciting a behavioral response requires high intensity stimulation [69]. Artificial proprioceptive feedback has been evaluated using joint matching paradigms between the intact and missing limbs of amputees implanted with intrafascicular electrodes [70]. In another study from the same lab [71] it was noted that participants had to initially focus intently on the stimulation to perceive it, hinting at the subtly of the experience.

Recording from primary somatosensory cortex (area 3a) may provide a suitable basis for objective comparisons of proprioceptive encoding models. Area 3a has been shown to preferentially receive input from muscle spindles [72], suggesting that it is the first cortical region responsible for processing proprioceptive inputs. The general approach is to use recordings from the hindlimb region of area 3a [73] to find effective stimulation parameters, e.g. pulse rates and intensities, for DRG PAMS. A similar approach has been used to discriminate between stimulating electrodes implanted within the auditory nerve [74]. The advantage of this approach is that it may potentially be more sensitive to differences between limb state encoding models than behavioral reports from trained animals. The reliance of previous studies on conscious reports precluded the ability of researchers to characterize subconscious phenomena, which may form the better part of proprioception.

1.2.2 Stability

To be viable, implanted devices must remain efficacious for years without undue burden on the life of the patient. There are a large number of veterans who have recently lost limbs in

OIF/OEF [75], many undoubtedly in what should be the most productive years of their life. These are younger individuals who will require a device that can be serviced and potentially upgraded for decades without incident. Existing neural interfaces and electroceuticals provide examples of acceptable device life. The cochlear implant has an impressive record of stability with a 91.7% device survival rate after 11 years [76]. The deep brain stimulator uses implanted batteries designed with a four to five year lifespan, but the actual mean time to replacement was found to be only 32 months [77]. Once the battery is replaced patients can continue with treatment, and this is considered an acceptable compromise.

Changes at the electrode tissue interface have a large impact on the stability of a neural interface. Devices may fail for purely mechanical reasons, such as lead migration [78] or breakage. The choice of therapeutic targets isolated from large movements, such as DRG, can limit the likelihood of mechanical failures. Neuron migration and die off [79] is another major concern for penetrating microelectrodes arrays regardless of target. Microelectrode arrays owe their performance to their intimacy with neurons, which greatly decreases if the neurons move more than 200-300 μm from the electrode. Epineural electrodes are more likely to be stable over long periods of time because they do not penetrate neural disuse.

Devices should be robust to tissue changes without the expense and risk of revision surgery. For example, if targeted neurons migrate away from the electrodes or die the simplest method for restoring device functionality may be to increase stimulation intensity. Increasing intensity increases the size of the volume of tissue activated (VTA) potentially restoring the recruitment of previously targeted neurons or others that serve similar functions [80]. Some devices, such as dorsal column stimulators, employ multiple electrodes to steer current towards the appropriate therapeutic targets [81] a technique that can be used to adapt treatment to tissue

changes or electrode migration. Regardless of the method, devices should allow a clinician or trained patient to tune device performance after initial implantation to compensate for unforeseen changes.

1.2.3 Selectivity

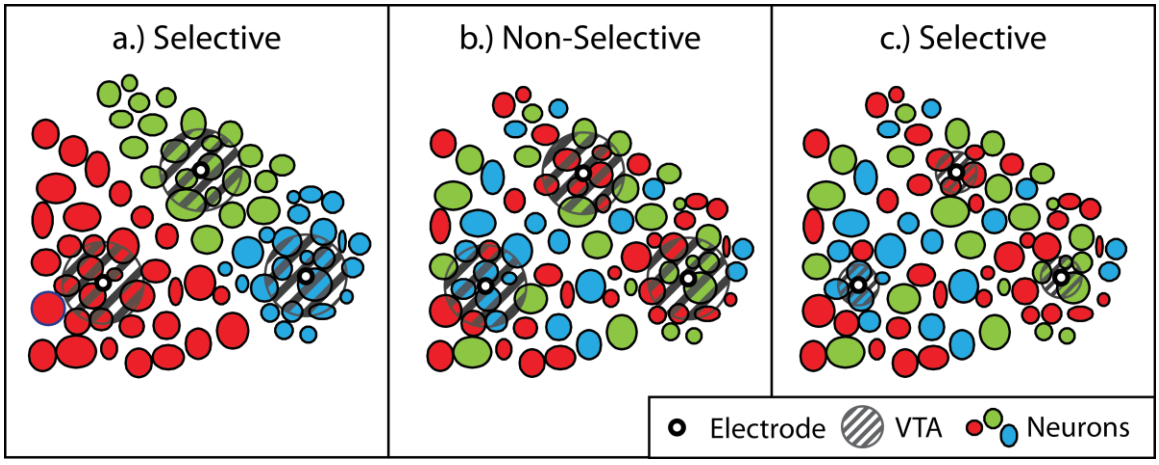

Figure 1.4 Selectivity conceptual diagram. Each electrode (white circle) is capable of recruiting a subset of neurons within its electric field, a region referred to as the volume of tissue activated (VTA). a.) If the VTA of a given electrode only includes neurons belonging to the same set (color), defined as the combination of modality and receptive field location, that electrode is said to be selective. b.) If the VTA of an electrode includes neurons from more than one set it is said to be non-selective. . In this example VTA remains the same as in a.) but neuron identities have been permuted. c.) Reducing the VTA by reducing intensity can result in more selective recruitment as compared to b.)

Selectivity is the ability to recruit one population of neurons to the exclusion of others. Recruitment selectivity is determined by the relationship between the volume of tissue activated

(VTA) and the neuron-electrode geometry (Figure 1.4). VTA is proportional to stimulation intensity and therefore high intensity stimulation can only be selective if the electrode is located within a homogenous neural population. Even a small VTA can produce non-selective recruitment if the electrode is very close to a diverse population of neurons. Recruitment may still be considered selective if different yet synergistic neural populations, such as those innervating synergistic muscles, are recruited.

Meeting selectivity requirements is a crucial determinant of the success of a neuroprosthesis. Typically, more selective stimulation is desired, however some neuromodulation devices, such as dorsal column stimulators [81], are non-selective in their recruitment. In the context of sensory restoration non-selective recruitment will likely result in less naturalistic sensation, and is therefore undesirable. The degree to which non-selective recruitment affects perception is unknown.

The difficulty of selectively recruiting neurons varies throughout the nervous system based on the underlying neural organization, or lack thereof. Neural interfaces based in primary somatosensory [65] and visual areas of cortex [63] rely upon the somatotopy and retinotopy of these regions respectively, in addition to the columnar organization of the cortex [82]. The cochlear implant relies on the well-defined tonotopic map of the auditory nerve [83] which facilitates selective recruitment of auditory fibers with similar tuning properties. Peripheral nerves can have a much more heterogeneous set of receptive fields and modalities, especially due to the comingling of afferent and efferent pathways. Therefore, the selectivity requirements for stimulating electrodes in peripheral nerve may be greater [45]. Because of the branching nature of peripheral nerves, however, it is possible to achieve a degree of selectivity at the expense of coverage by placing electrodes more distally [47].

Selectively recruiting neurons within the DRG is a uniquely challenging problem. The DRG contains cutaneous, proprioceptive, and nociceptive afferent modalities all of which can be further divided into specific receptor classes (e.g. for proprioception: primary muscle spindles vs golgi tendon organs) each of which convey different information about the limb. There is only a coarse somatotopy [57,58] within an individual DRG unlike the other sensory modalities or even other locations within the somatosensory neuraxis. Specific populations of neurons, either in terms of projected location or specific sensation, therefore cannot be targeted *a priori* with DRG PAMS.

1.2.4 Safety

Penetrating microelectrodes arrays are well suited for selective recruitment of neurons because they are able to focally deliver small amounts of current [84]. Unfortunately, implanting a foreign object in neural tissue is an inherently destructive process. Electrode insertion results in mechanical damage to the tissue followed by an acute immune response [85]. Indwelling electrodes provoke glial scarring which isolates the electrode from the neurons it is attempting to recruit [79] and, in the periphery, shifts the fiber composition towards smaller fibers [86]. These factors have led to degradation and eventual failure of contemporary microelectrodes, which has limited clinical testing of these devices.

For clinical translation of a DRG SSNI epineural electrodes might be an appropriate substitution. Non-penetrating electrodes have been favored for clinical translation due to their overall biocompatibility (e.g. vagal nerve stimulators [87] phrenic pacers [88] bladder control [89]). Epineural electrodes can be designed to conform to neural tissue to minimize the gap

between neurons and the active region to increase recruitment selectivity. Existing minimally invasive surgical techniques for accessing the spinal cord [90], and specifically for implanting DRG with epineural electrodes for pain management [91], can potentially be adapted for implanting epineural arrays on the DRG for sensory stimulation. Clinically approved epineural stimulation leads, such as those used for sacral root stimulators [89], may be amenable to use in sensory feedback easing the clinical translation process.

1.3 RESEARCH OBJECTIVES AND CHAPTER SUMMARIES

The promise of DRG PAMS was demonstrated in acute studies showing recruitment of medium and large diameter fibers [61]. This body of work extends that line of inquiry to further establish whether or not DRG PAMS could serve as the basis of a somatosensory neuroprosthesis. This dissertation was motivated by the desire to both develop a model to validate sensory feedback and to characterize to what degree DRG stimulation satisfies the three SSNI requirements discussed in Section 1.2, namely stability, selectivity and safety. Chapters are organized in the chronological order that each experiment was completed.

Early investigations sought to establish an objective means of assessing the performance of DRG PAMS. **Chapter 2** describes an early success that used cortical recordings to discriminate between stimulation on different electrodes of a MEA. This experiment demonstrated that PAMS could drive activity in primary somatosensory cortex using the same pathways as natural feedback. This work also demonstrated a degree of recruitment selectivity based on separation between electrodes.

A later effort to characterize the long term stability of penetrating MEAs in the DRG is described in **Chapter 3.** This study focused on the ability of DRG PAMS to recruit large and medium diameter fibers over time by analyzing compound actions potentials recorded from the sciatic nerve. It was shown in four cats that DRG PAMS could recruit fibers of interest for up to 24 weeks.

Lacking from the approaches used in **Chapter 2** and **Chapter 3** was an understanding of the peripheral targets of neurons recruited by DRG PAMS. A new paradigm is developed in **Chapter 4** in which recruitment curves for many distal nerve branches were generated for each stimulation electrode. The recruitment curves were then used to demonstrate that microelectrodes implanted in the DRG were able to selectively recruit a diverse range of fibers over the entire hindlimb. It was argued that the coverage and selectivity of DRG PAMS within the L7 DRG alone might have been sufficient to restore sensation to a trans-tibial amputee.

Chapter 2 through **Chapter 4** demonstrate that penetrating microelectrodes in the DRG are able to form the basis of a sensory neuroprosthesis, however these may not be amenable to clinical translation due to the inherent safety and longevity issues of penetrating electrodes (see Section 1.2.4). **Chapter 5** describes an experiment performed using the methodology of **Chapter 4** but with epineural rather than penetrating electrodes. Recruitment selectivity with the epineural electrodes was characterized and shown to approach that of penetrating electrodes in some instances. Representation of the hindlimb within the recruited afferent population was found to be qualitatively similar as well. In some instances entirely different nerves were recruited with each of the epineural electrodes on an array, suggesting that it is possible to increase the number of electrodes.

2.0 EFFECTS OF SPATIAL AND TEMPORAL PARAMETERS OF PRIMARY AFFERENT MICROSTIMULATION ON NEURAL RESPONSES EVOKED IN PRIMARY SOMATOSENSORY CORTEX OF AN ANESTHETIZED CAT.

The contents of this chapter are published as: *Hokanson JA, Ayers CA, Gaunt RA, Bruns TM, Weber DJ (2011) Effects of spatial and temporal parameters of primary afferent microstimulation on neural responses evoked in primary somatosensory cortex of an anesthetized cat. Conf Proc IEEE Eng Med Biol Soc 2011:7533–7536*. My contribution to this work was assisting in conducting the experiments, writing the data management and analysis code, and producing all the presented results and figures.

2.1 INTRODUCTION

Acceptance and usefulness of modern prosthetics is limited by their lack of sensory feedback [88,89]. To overcome this limitation, patterned microstimulation of primary afferent neurons is being explored as a way to transmit sensory information into the central nervous system (CNS). Recent work in amputee patients has already shown that electrical stimulation with intrafascicular electrodes in peripheral nerves evokes painless sensations of touch and joint movement that were perceived to originate in the phantom limb [49].

The dorsal root ganglia (DRG) provide a compact target for accessing large populations of somatosensory fibers with high density arrays of microelectrodes. Previous studies have shown that penetrating microelectrodes in the DRG can provide selective activation of various types of muscle and cutaneous afferents [61]. A challenging problem is how to create effective patterns of stimulation in the array of inputs provided by the electrodes. The amplitude and rate of stimulation can be varied independently on each electrode, resulting in an extremely large parameter space for creating feedback patterns.

The goal of this study was to examine how variations in the basic parameters that define a multichannel pattern affect both the threshold for evoking a response and the range over which the response is readily distinguished from other inputs. Various patterns of primary afferent microstimulation (PAMS) were applied via penetrating microelectrodes in the lumbar DRG of anesthetized cats. We quantified the response to stimulation using the firing rates of neurons recorded on an array of microelectrodes in primary somatosensory cortex (S1).

Although it is not possible to know what type of sensation (if any) is represented by each S1 response, our goal was to examine the extent to which these responses differ across variations in the stimulus parameters. Stimuli that evoke similar responses in S1 are presumed to carry similar information. However, if variation in a particular stimulus parameter (e.g., pulse rate) leads to a large modulation in the cortical response, then variation of that parameter is viewed as an effective mode of conveying information to the brain (e.g., see [94]).

This paper presents some initial results regarding threshold and discriminability as a function of the following stimulus parameters: pulse amplitude, rate, and electrode location. Interactions between these parameters are observed in determining stimulus threshold. High classification accuracy between independently activated stimulus locations suggests they can be

used as separate pathways for providing feedback. Results also demonstrate interesting interactions in the neural response evoked by multichannel stimulation.

2.2 METHODS

Results shown are from a single experiment. Experimental procedures were performed in accordance with the University of Pittsburgh IACUC.

2.2.1 Experimental Procedures

Isoflurane (1-2%) was used to maintain the cat in a surgical anesthetic plane, and after some preliminary surgery to expose the DRG, the cat was placed in a stereotaxic frame. Vitals were monitored continuously and kept within normal ranges. Electrode arrays (Blackrock Microsystems) were placed in the L6 and L7 DRGs as well as hindlimb area of S1 cortex (post-cruciate gyrus). Stimulation was conducted on 30 channels, 14 in L6 and 16 in L7 (see Figure 2.1A), one or two at a time using an MS-16 stimulus isolator (TDT). Cortical recordings (48 channels) were sampled at 25 kHz using an RZ system (TDT) and manually thresholded to determine times of multi-unit spiking activity.

Stimulation pulses were biphasic with a 200 μs cathodic phase followed by a half amplitude 400 μs anodic phase with a distant return electrode. Discrete stimulation patterns were applied to 1 of 30 electrodes at a time and consisted of a 300 ms train of pulses having a fixed amplitude and pulse rate, followed by a 700 ms quiescent period without stimulation. A total of

360 different patterns were tested (3 intensities [5, 10, 20 μA] and 4 pulse rates [10, 100, 300, and 1000 pulses per second; pps] at 30 different electrode locations) with 10 repetitions for each pattern. Single repetitions of each pattern were tested in random order.

We also tested a limited number of 2-channel stimulation patterns using the same stimulus pulse rates and amplitudes as described above. In each 2-channel trial, the same stimulus pattern was applied synchronously to both electrodes in the pair. The S1 response to 2-channel stimulation was compared to the responses evoked by single channel stimulation on each electrode in the pair. This test was done to examine interactions in the neural responses evoked by the inputs applied at two different locations.

2.2.2 Data Analysis

The cortical response was evaluated as the spike count in a 50 ms bin starting 10 ms after the onset of a stimulation train. We used a Naive Bayes classifier with leave-one-out cross validation to determine differences in the S1 responses evoked by different stimulus patterns. Differences were considered significant if they exceeded a 99% confidence interval on chance (> 78% classification accuracy over the 20 total repetitions, 10 from each pattern). The cortical population was used for classification with the exception of Figure 2.1B in which single cortical channels were used.

2.3 RESULTS

2.3.1 Thresholds for evoking S1 responses

Figure 2.1A shows the electrode locations that were tested in each DRG. The numbers indicate the lowest stimulation amplitude at each site that evoked a significant response in S1 as compared to baseline. Over 30% of channels (11 of 30) evoked a response at the lowest amplitude (5 μA; at least one pulse rate). A similar percentage of channels (10 of 30) required much higher currents (20 μA) to evoke a response. A small number of channels did not evoke a response at any of the levels tested, although those electrodes may have been outside the ganglia. Note that the differences are unlikely to reflect variability in the thresholds for recruiting neurons in the DRG (Gaunt et al. 2009), but may instead reflect differences in the pattern of connectivity from the DRG to S1. Also note that some clustering of thresholds is apparent in both arrays, which may indicate a certain level of somatotopic organization of sensory fibers within each DRG [95].

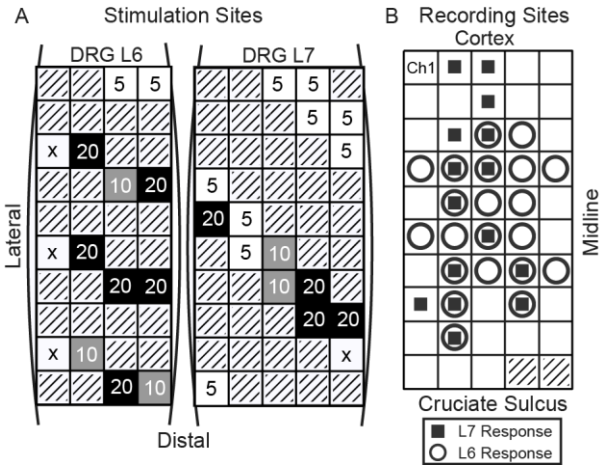

Figure 2.1: Spatial Effects of single channel stimulation. A: Spatial layout of the stimulus amplitude threshold (μA) for evoking a significant cortical response (vs. baseline) on each tested stimulus channel for the L6 and L7 DRGs. Threshold at any stimulus rate counted as being at threshold for the reported stimulus amplitude. An 'x' indicates that no stimulus amplitude/rate pair was sufficient to elicit a cortical response. Gray boxes represent disconnected channels. B: Spatial pattern of responses in S1 to 5 μA stimulation. Circles and squares indicate that a response was elicited by at least one electrode in the L6 or L7 DRG, respectively.

Of the 48 channels in S1, 26 showed significant responses vs. baseline from stimulation at 5 μA on at least one stimulus channel (see Figure 2.1B). Eleven of these channels were responsive only to stimulation in L6, 5 were responsive only to L7, and 10 channels recorded responses evoked by stimulation in both locations.

Figure 2.2 illustrates the interaction between stimulation pulse rate and amplitude on the threshold for evoking a cortical response vs. baseline. With 5 μA stimulation applied at 10 pps, only 4 DRG electrodes evoked a significant response in S1. More than twice as many stimulation channels evoked a response at 5 μA when higher pulse rates were used. A similar but smaller effect was observed for 10 μA stimulation pulses, whereas no effect was observed at 20 μA.

Although higher amplitude stimulation was most effective in surpassing the threshold needed to evoke an S1 response, it is clear that high pulse rate stimulation is also effective at facilitating stronger responses in S1.

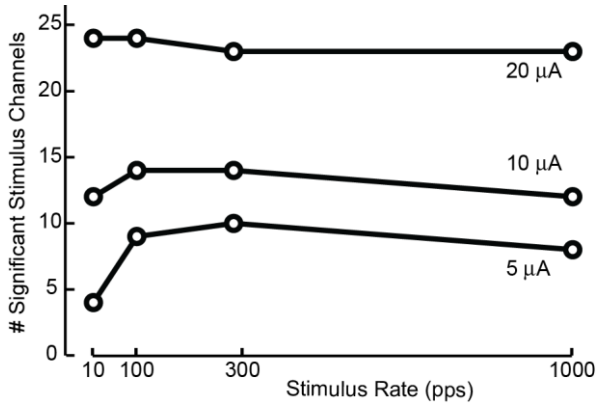

Figure 2.2: Interaction between stimulation pulse rate and amplitude on threshold for evoking a response in S1. Number of stimulus channels that evoked a discriminable response in cortex as a function of stimulus pulse rate for 5, 10, and 20 µA pulses.

2.3.2 Effects of stimulation location

We examined how the discriminability of the S1 response varied with the relative location of two stimulation sites in the DRG arrays. Figure 2.3A shows examples of the neural response averaged for stimulus patterns (10 repetitions each) that were applied at channels 1 and 3 (566 µm apart) in the L7 DRG. The averaged responses appear qualitatively similar but were discriminated reliably by a Naive Bayes classifier with 90% accuracy (18/20).

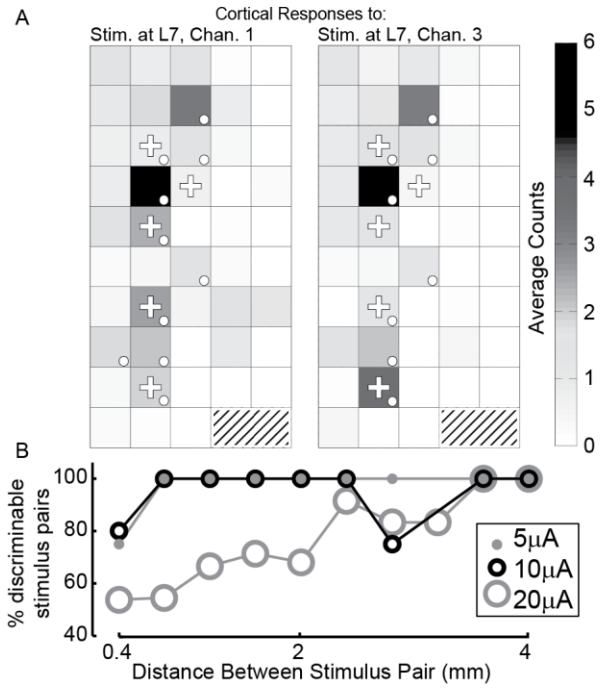

Figure 2.3: Discriminability of S1 responses evoked by stimulation at different locations, and amplitudes. A: Examples of the average cortical response to stimulation on channels 1 (left) and 3 (right) in the L7 DRG at 5 μA and 100 pps. Shown is the average spike count observed 10 – 60 ms following stimulus onset. Dots denote channels showing a significant response; plus symbols (+) indicate channels used for classification. Although they have similar average responses, they can be classified with 90% accuracy. B: Percentage of channel pairs that evoked discriminable S1 responses as a function of the separation distance between the 2 stimulation sites (rate = 100 pps). Only stimulus electrodes that evoked significant responses vs. baseline were included. Pairings were kept within arrays. Distances have been grouped to nearest 0.4 mm.

Figure 2.3B shows the percentage of stimulation pairs that evoked discriminable responses in S1 as a function of the distance separating the two stimulation sites (rate = 100 pps in all cases). At 5 and 10 μA, the cortical response was sufficient to discriminate between the stimulus pairs at most distances, with a slight decrease for adjacent stimulus sites as well as one outlier pair separated by 2.8 mm at 10 μA. At 20 μA, the recruitment of a much larger number of

primary afferent neurons resulted in S1 response patterns that were difficult to distinguish from each other when coming from nearby stimulus electrodes. For discriminable stimulus pairs, and across all distances, the average classification accuracies were 97%, 93%, and 90%, for stimulation amplitudes 5, 10, and 20 μA, respectively.

2.3.3 2-channel stimulation effects

Figure 2.4 shows examples of responses evoked on two S1 channels during single and 2-channel stimulation. The S1 channel in Figure 2.4A did not respond to stimulation on either of the channels independently, but responded strongly when the same two channels were stimulated together. This type of response suggests a convergence of excitatory inputs activated by channels 3 and 6 (1.44 mm apart), such that the combined activation was sufficient to evoke a response in S1. In Figure 2.4B, a response was evoked by stimulation on channel 3, but the response disappeared when paired with stimulation on channel 25. This pattern of responses suggests an inhibitory effect of channel 25 on the response evoked by channel 3. In total, 5.5% of the responses to 2-channel stimulation were similar to Figure 2.4A and 14.8% of the responses were similar to Figure 2.4B.

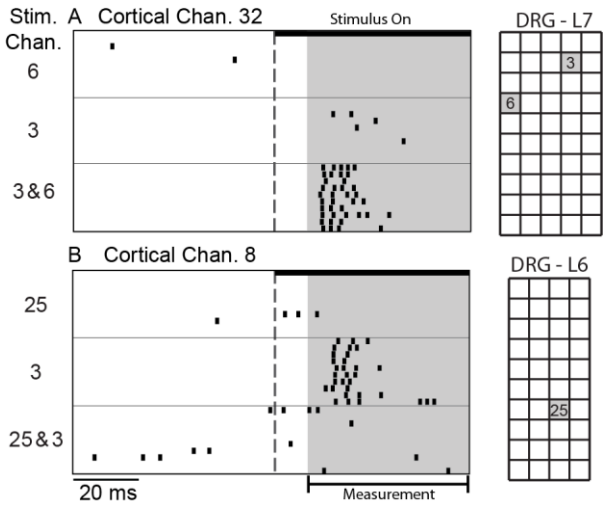

Figure 2.4: Two examples of S1 responses to single and 2-channel stimulation at 5µA. A: This S1 channel did not respond to stimulation at channel 6 or 3; concurrent stimulation on channels 3 and 6 evoked a vigorous response (rate = 1000 pps). B: This S1 channel responded to stimulation on channel 3, but not 25. When both channels were stimulated, the response was nearly eliminated (rate = 100 pps).

2.4 DISCUSSION

2.4.1 Providing Sensory Feedback

The primary aim of this work was to investigate means of providing sensory feedback to the nervous system through patterned microstimulation of primary afferent neurons. Although the response of most primary afferents to external stimuli is fairly well understood, details of how these afferent inputs are integrated in the CNS and their effects on higher-order neural networks are less clear. The manner in which these afferent inputs are integrated is a crucial determinant of the information conveyed by the combined activation of these inputs. Electrical microstimulation

of primary afferents can yield insight into how to design stimulation patterns that are effective in conveying information to the CNS, even if they are not naturalistic.

The focus of this paper is on understanding how basic patterns of stimuli differentially activate a population of neurons in S1. We are assuming that if stimuli evoke similar cortical responses, then they convey similar information to the brain. Stimuli that evoke distinct responses, as determined by classification with machine learning algorithms, are presumably discernible by the brain as being different as well. At this point, we cannot conclude that distinct responses in S1 indicate differences in evoked percepts. Future studies will test for perceptual differences using psychophysical discrimination experiments.

2.4.2 Results: Implications for sensory neural prosthetics

One of the challenges with using multichannel microelectrode arrays to provide sensory feedback is figuring out how to encode information in the high dimensional input space that is available. The basic parameters of stimulation include pulse amplitude, pulse rate and electrode location and variations in each of these parameters affects the recruitment of neurons. Our results demonstrated that the threshold for evoking a response in S1 was highly dependent on these three parameters. Interactions among these parameters may greatly reduce the effective size of the input space. For example, interactions between stimulation amplitude and pulse-rate (Figure 2.2) indicate one mode of dimensionality reduction; at high stimulation amplitudes, variations in pulse rate are less effective in evoking distinct responses. Similarly, interactions between stimulus amplitude and electrode locations (Figure 2.3) indicate that the spatial resolution may be reduced as the stimulus amplitude is increased.

It is generally accepted that effective stimulation parameters will vary with stimulus location due to the recruitment of a different neural population. There may exist other dependencies between our stimulus parameters which could be used to inform stimulus design. For example, stimulus channels that primarily activate muscle spindles may require spatial summation to sufficiently activate the cortex [42]. High threshold stimulus channels may be more effective if coactivated rather than simply increasing stimulus amplitude. With more data we plan on building statistical models that characterize these dependencies.

Rate/amplitude interactions suggest paradigms that model perceived intensity as a function of stimulus rate at a fixed amplitude [49] might not generalize to other amplitudes. A desire to selectively activate neurons means that lower stimulation amplitudes would be preferred. Low stimulus amplitudes, however, might limit the range of perceived intensities due to the decrease in responsiveness at high frequencies (Figure 2.2). This potential tradeoff is something that our experimental model would examine.

Results such as those shown in Figure 2.3 can be used to inform the design of electrode array geometries. Ochoa and Torebjörk mention that artificial stimulation almost never led to natural touch due to inappropriate or insufficient recruitment [96]. This may be improved by maximizing the number of effective stimulus channels. In this experimental context, this would correspond to maximizing the number of discriminable stimulus channels for different arrays designs. Since we can discriminate between a majority of neighboring electrodes (Figure 2.3) at low amplitudes, this suggests the need for denser arrays, or possibly more complicated stimulation paradigms such as current steering.

With some exceptions, the majority of somatosensory stimulation feedback studies have examined the use of single channels in isolation. Thoroughly examining groups of stimuli is

difficult because of the staggering number of channel combinations. Figure 2.4 indicates that interactions between stimulus sites exist. Future work can elucidate to what degree these interactions are at the site of recruitment versus convergence of inputs, the dependence of these interactions on the stimulus parameters, and ultimately how multiple channels can be used to increase the amount of deliverable feedback information.

3.0 CHRONIC RECRUITMENT OF PRIMARY AFFERENT NEURONS BY MICROSTIMULATION IN THE FELINE DORSAL ROOT GANGLIA

The contents of this chapter are published as: *Fisher LE, Ayers CA, Ciollaro M, Ventura V, Weber DJ, Gaunt RA (2014) Chronic Recruitment of Primary Afferent Neurons By Microstimulation in the Feline Dorsal Root Ganglia. Journal of Neural Engineering vol. 11, no. 3, p. 036007, Jun. 201* My contribution to this work was co-conducting the experiments, writing the data management code, and reviewing the text.

3.1 INTRODUCTION

There has recently been a great deal of progress in the mechanical design of prosthetic limbs for amputees, with development of high degree-of-freedom devices, such as the Modular Prosthetic Limb (Johns Hopkins University, Applied Physics Laboratory, Baltimore, MD, USA) and the DEKA arm (DEKA Research and Development Corp, Manchester, NH, USA) [5,93]. These devices have the potential to reproduce much of the functionality of the intact limb and may also be instrumented with sensors that monitor joint position, torque, and fingertip pressure to allow restoration of sensory feedback. Sensory feedback is crucial for motor control, and one of the major impediments to adoption of advanced prosthetic technologies is this lack of sensation

[94,95]. Remarkably, simple body-powered prostheses are often preferred over the more advanced devices, in large part because of the sensory feedback provided by the harness and control cable [100]. Without cutaneous and proprioceptive feedback from the limb, users of these advanced devices must rely mainly on visual feedback for information about limb orientation and grip force [100].

There is a growing body of evidence that suggests it may be possible to restore sensory function by electrically stimulating the peripheral nerves that remain intact in the limb above the level of amputation. Multiple studies have demonstrated that stimulation of peripheral nerves results in activation of neurons in primary somatosensory cortex (S1). In one study, Utah slant electrode arrays were implanted in the median, ulnar, and radial nerves of a monkey, and somatosensory evoked potentials were recorded in S1 via an electrode grid on the surface of the brain [45]. While this method did not provide information on the modality or perceived location of the stimulus, it did demonstrate that short latency (less than 20 ms) cortical responses occurred after stimulation in the peripheral nerves. In a recent study from our lab, Utah electrode arrays were implanted into S1 and the lumbar dorsal root ganglia (DRG) of a cat, and stimulus pulses were patterned to replicate the firing of action potentials recorded in the DRG during leg movements [101]. In some cases, multi-unit cortical responses to patterned electrical stimulation were similar to the cortical responses recorded during passive leg movement.

Additional studies in humans have demonstrated that peripheral nerve microstimulation evokes sensory percepts that are localized to specific regions of the hand and forearm [68,90,98]. In one study, longitudinal intrafascicular electrodes (LIFEs) were implanted in the median nerve stumps of three amputees. In all three individuals, electrodes were identified that could selectively elicit distally referred sensations of either thumb pressure or elbow flexion/extension

[70]. Further, the magnitude of those sensations was related directly to the frequency of stimulation. This study suggested that there is great potential for restoring sensory function to amputees via electrical stimulation. However, long-term studies have not been performed to test the chronic stability of LIFE or other peripheral nerve interfaces for sensory restoration.

This paper describes the testing of microelectrode arrays implanted chronically in the DRG to stimulate primary afferent neurons to restore sensory function. The DRG are attractive targets for achieving a stable peripheral neural interface for a number of reasons. The spinal roots provide the potential for a mechanically stable anatomical location for the implantation of penetrating electrodes because they may be less prone to the stretching and movement that occurs in the more distal regions of peripheral nerves [99,100]. Further, they can be accessed by minimally invasive surgical techniques that are used commonly during procedures such as neuroma removal or spinal root decompression [101,102]. Additionally, because the dorsal and ventral spinal roots offer complete segregation of sensory and motor functions, respectively, electrodes placed in the DRG will activate sensory neurons. Anatomical selectivity can be achieved through the use of multiple microelectrodes, implanted in the spinal roots at different vertebral levels [58]. Through the use of multi-electrode arrays and varied stimulation parameters, it may also be possible to activate proprioceptive or cutaneous fibers in isolation to elicit distinct sensations [107]. Previous work from our lab has demonstrated that it is possible, in an acute preparation, to selectively activate either Group I, Group II, or Aβ primary afferents with penetrating microelectrode arrays in the L6 and L7 DRG, and to produce cortical responses that resemble the natural response to changes in limb position [59,104].

The goal of this study was to examine the chronic stability and selectivity of the response to microstimulation via penetrating microelectrodes in the DRG. Floating microelectrode arrays

(Microprobes for Life Science, Gaithersburg, MD, USA) were implanted chronically in the L6 and L7 DRG of four cats and the stability and selectivity of the response to stimulation was monitored for up to six months after implantation. Initially, many electrodes elicited both Group I and Group II/Aβ responses with low thresholds. Over time, thresholds increased, the number of electrodes that elicited a response decreased, and there was fluctuation in the conduction velocity and shape of the responses elicited by individual channels. There were, however, still 9 implanted electrodes across three arrays that continued to evoke a response at 24 weeks after implantation, suggesting that it is possible to achieve a long-term chronic interface with the DRG as part of a sensory neuroprosthesis.

3.2 METHODS

The ability to activate sensory neurons in the DRG was assessed by measuring the electroneurogram (ENG) in the sciatic nerve in response to microstimulation of the L6 and L7 DRG using floating microelectrode arrays (FMAs). All procedures were approved by the University of Pittsburgh Institutional Animal Care and Use Committee.

3.2.1 Implanted microelectrodes and nerve-cuff

Four adult male cats (4.3-5.2 kg) were included in this study. Prior to implantation of stimulating and recording electrodes, anesthesia was induced with ketamine, followed by intubation and administration of isoflurane (1-2%) for the duration of the procedure. Blood

pressure, oxygen saturation, expired CO_2, and body temperature were monitored throughout the procedure and kept within normal physiological ranges.

Figure 3.1 shows a schematic of the implanted electrodes and hardware used during this study. In each cat, a five-contact spiral nerve-cuff electrode (Ardiem Medical, Indiana, PA, USA) was implanted around the left sciatic nerve to record the antidromic ENG response to microstimulation in the DRG. Contacts were 1 mm wide platinum bands spaced 4 mm apart along the length of the nerve. The proximal, distal, and central contacts were tied together to act as a reference, and ENG signals were recorded from the second and fourth contacts differentially with respect to the reference. Two sutures were tied loosely around the cuff to ensure that it remained in place for the duration of chronic experiments and the lead wires were tunneled under the skin to a percutaneous port centered on the back between the iliac crests.

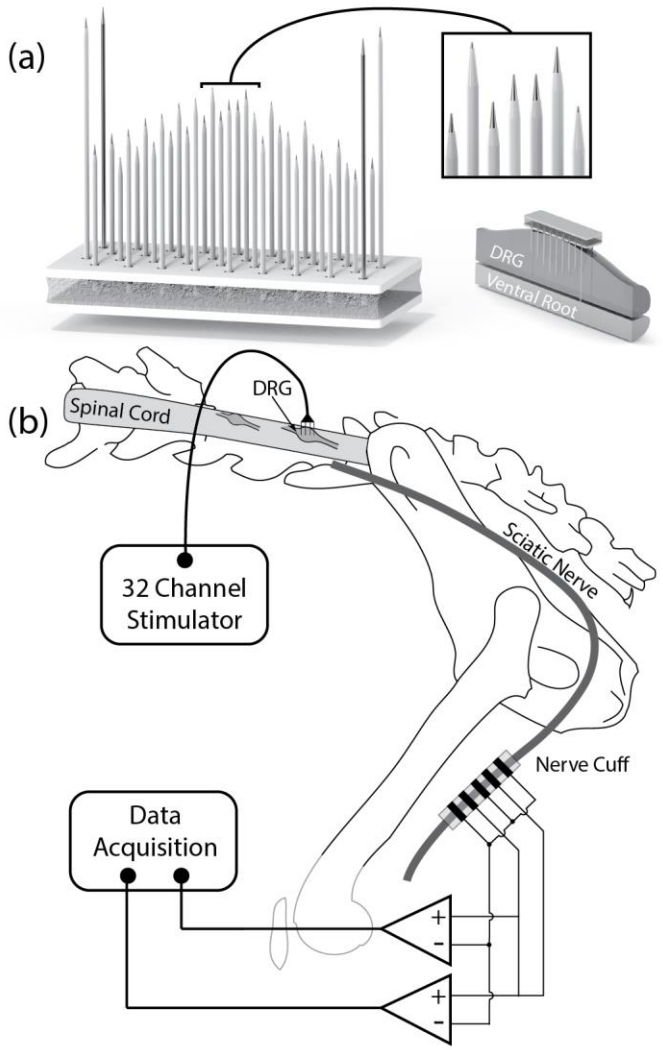

Figure 3.1 Chronic testing experimental and instrumentation setup. (a) Rendering of the 32-channel floating microelectrode arrays implanted in the L6 and L7 DRG of 4 cats. Electrode shank lengths spanned the depth of the DRG and exposed tip lengths varied from 30 to 120 µm. Each array also included two ground electrodes and two reference electrodes at the corners (3.0 mm length). (b) Diagram of the experimental setup. Microstimulation in the DRG generated compound action potentials which propagated antidromically along the sciatic nerve and were recorded differentially via a nerve-cuff electrode.

A dorsal laminectomy was performed to expose the left L6 and L7 DRG, and a 32-channel FMAs was implanted in each one. The platinum-iridium electrodes of each FMA (Figure 3.1a) had a variety of lengths designed to span the depth of the DRG (1.2, 1.4, 1.6, and 2.0 mm) and exposed tip sizes of 30, 60, 90, and 120 µm (mean±std pre-implant impedance for each site size: 144±128 kΩ, 62±57 kΩ, 31±28 kΩ, 14±13 kΩ), allowing us to examine the effect of tip size and impedance on the selectivity and stability of microstimulation. The array implanted in the L6 DRG of Cat C had slightly longer electrode shanks (2.4, 2.6, 2.8 and 3.0 mm) than all other arrays, although care was taken to ensure that the electrodes were implanted appropriately into the DRG. During implantation of all arrays, a custom vacuum holder attached to a micromanipulator was used to position the array over the DRG during visualization with a surgical microscope. The array was positioned so that its long axis was aligned with the proximal/distal axis of the spinal root. A pneumatic inserter with 1.5 mm of travel (Blackrock Microsystems, Salt Lake City, Utah) was used to rapidly insert the array through the epineurium into the DRG. Following initial insertion, electrophysiological recordings were performed to verify sensory responses evoked by manipulation of the left hindlimb. Single-unit action potential recordings were acquired from the implanted FMA, sampled at 25 kHz, and digitized via a neurophysiology recording system (RZ2, Tucker-Davis Technologies, Alachua, FL). Based on the quality of these recordings and visualization of the array under a surgical microscope, repeated impacts were applied with a pneumatic inserter that had 1 mm of travel until the array was sufficiently inserted into the DRG. This procedure was necessary because many of the electrodes were longer than the available travel of the inserter, and therefore required multiple impacts to achieve full insertion into the DRG. Rapid insertion was required as the DRG is covered in a tough perineurium that is difficult to penetrate using slow insertion methods. Lead

wires were tacked to the spinal dura with 8-0 silk sutures and routed to a percutaneous port between the iliac crests. A stainless steel ground wire (AS636, Cooner Wire Company, Chatsworth, CA), which acted as the stimulation return, was fixed to the iliac crest with a bone screw. In some animals, a layer of silicone rubber was poured over the arrays to minimize adherence of connective tissue (Kwik-Cast, WPI, Sarasota, FL). A baseplate was attached to the dorsal fascia and iliac crests and all lead wires and external connectors were passed into a protective plastic backpack mounted to the baseplate via percutaneous posts.

3.2.2 Stimulation and data acquisition

At regular intervals after implantation, the stability and selectivity of the response to stimulation was measured during anesthetized recording sessions. During these sessions, anesthesia was induced and maintained by intramuscular injection of dexmedetomidine (0.04 mg/kg). Stimulus pulses were applied at 33 pulses per second through randomly selected individual electrodes within each FMA while antidromic propagation of compound action potentials (CAPs) was recorded via the nerve-cuff. All stimuli were 200 μs cathodic-leading, charge-balanced biphasic pulses, with current amplitudes of 2, 5, 7, 10, or 15 μA. The anodic phase of each stimulus pulse was 400 μs and half the amplitude of the cathodic phase. Current amplitudes were chosen based on results of our previous study of the acute response to DRG microstimulation, as well as to maintain stimulation safety, to avoid activating spinal reflexes that could cause muscle contraction and movement artifact, and to constrain the duration of experiments and minimize the time under anesthesia [61]. ENG signals were amplified (gain = 10,000) and band-pass filtered (300-10,000 Hz) with a differential amplifier (Model 1800, A-M

Systems, Sequim, WA, USA), digitized and sampled at 300 kHz with a data acquisition board (USB-6259, National Instruments, Austin, TX, USA).

At the end of most experimental sessions, electrode impedances were recorded at 1 kHz using one of two multi-channel potentiostat systems (niPOD, NeuroNexus Technologies, Ann Arbor, MI, USA or CompactStat, Ivium Technologies, Eindhoven, The Netherlands). Similarity of the impedance results for these two systems was confirmed via unpublished *in vitro* testing of all electrodes in an FMA placed in a saline bath. Electrode impedances were used to track changes in the electrode tissue interface. We expected that changes to the electrode surface as a result of electrochemical reactions during stimulation (e.g. pitting) would result in a higher electrode surface area and a corresponding decrease in impedance. Alternatively, increases in electrode impedance might correspond to encapsulation of the electrode tip.

3.2.3 ENG analysis

This study relied on the antidromic propagation of CAPs along the sciatic nerve as a measure of recruitment in the DRG and a surrogate for the orthodromic action potentials traveling into the central nervous system. Stimulus-triggered averaging (Figure 3.2) was performed on the filtered ENG signals to isolate evoked responses. A set of automated techniques was used to determine the presence or absence of CAPs within the signal. The conduction velocity for each CAP was measured from its propagation delay between the stimulating and recording electrodes. Based on these conduction velocities, the fiber type of the recorded axons was inferred, and selectivity was determined based on the ability to activate only Group I or Group II and Aβ fibers.

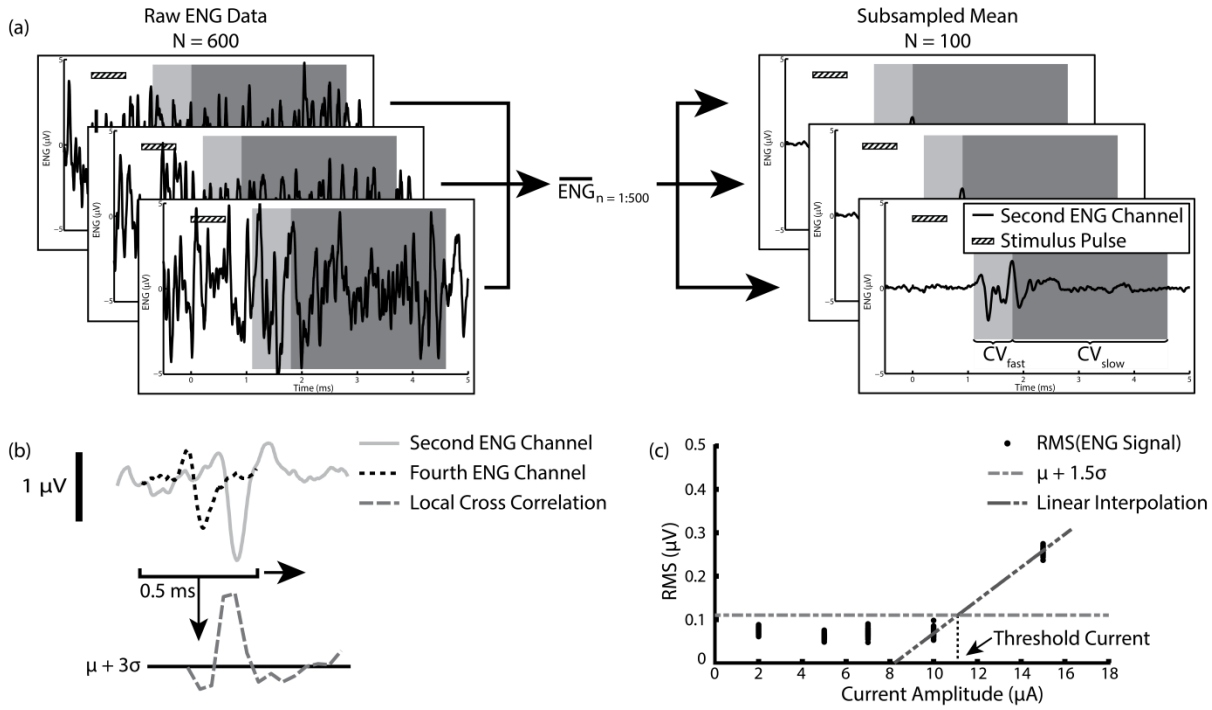

Figure 3.2 The procedure used to analyze ENG data and identify the presence of CAPs. (a) Stimulus-triggered averaging and subsampling were performed to reduce the noise in the ENG signal and quantify the variability in the CAPs. Based on the differences in conduction velocity of CV_{fast} and CV_{slow} fiber types, as well as the propagation delay between the second and fourth contacts within the nerve-cuff electrode, time windows (gray boxes) were created to differentiate CV_{fast} and CV_{slow} fiber types. (b) A sliding 0.5 ms window of signal from the fourth contact within the cuff was cross-correlated with signal from the second contact. If the local cross-correlation surpassed the mean plus three standard deviations of the cross-correlation of the noise, a CAP was identified. (c) For signals that included a CAP, the RMS of the signal was calculated at each current amplitude. RMS signals above the mean plus 1.5 standard deviations of the noise signal were identified as supra-threshold. Linear interpolation was used to determine the threshold current amplitude

3.2.4 Stimulus-triggered averaging

ENG signals typically have low signal-to-noise ratio with a great deal of contamination from both neural and non-neural bioelectric sources. To reduce the amplitude of this noise and reveal the underlying CAPs evoked by stimulation, stimulus-triggered averaging (Figure 3.2a) was performed on all ENG recordings. For every electrode within the FMA, 600 repetitions of each stimulus amplitude were applied. A subsampling procedure was performed to generate a distribution of average responses to these stimuli by repeatedly averaging (100 times) random selections of 500 of the 600 responses to stimulation. These distributions were used to perform statistical tests and determine differences in the magnitude of the ENG response under different stimulus conditions. All of the methods described below rely on these subsampled stimulus-triggered averages, rather than the raw ENG signal.

3.2.5 Measurement of conduction velocity and fiber type

For a neural interface to successfully restore sensory function, it should selectively activate multiple sensory modalities, especially proprioceptive and cutaneous sensations, in a controlled manner. Primary afferents can be loosely segregated into separate populations based on their axonal diameters and corresponding conduction velocities, though those populations have some overlap [105,106,107]. In the cat, Group I proprioceptive afferents, which are sensitive to muscle length, stretch velocity, and force, typically have conduction velocities between 75 and 120 m/s, while Group II proprioceptive afferents, which are sensitive primarily to muscle length, typically have conduction velocities ranging from 33 to 60 m/s [105,106]. For

Aβ cutaneous afferents, conduction velocities typically range between 45 and 80 m/s [111]. For this study, primary afferents were segregated into two groups based on these conduction velocities and corresponding sensory modalities: fibers with fast conduction velocities between 75 and 120 m/s (CV_{fast}), representing mainly Group I proprioceptive afferents, and fibers with slower conduction velocities between 33 and 75 m/s (CV_{slow}), representing a mix of Group II proprioceptive and Aβ cutaneous afferents. Other primary afferents, such as Group III, Aδ and C fibers have smaller diameter axons and produce lower amplitude ENG signals that are difficult to discriminate, and were therefore not considered in this study [61]. By measuring the conduction velocity of CAPs traveling through the nerve-cuff electrode, it is possible to infer the most likely sensory modalities of the activated neurons. To measure conduction velocity, the distance between the stimulating and recording electrodes was estimated using, a supra-threshold stimulus pulse (15 μA) in the DRG that elicited an obvious ENG response. By measuring the time delay between the peaks in the recorded ENG signals for the second and fourth contacts within the nerve-cuff electrode (which were separated by 8 mm), it was possible to calculate the conduction velocity of the stimulated fibers. Further, by measuring the time delay between the stimulus onset and the peak of the CAP, it was possible to estimate the distance from the stimulating electrode to the nerve-cuff electrode. Based on the conduction velocities for CV_{fast} and CV_{slow} fibers, this distance was used to estimate time windows (gray boxes in Figure 3.2a, Figure 3.3, Figure 3.6) in which those fibers would conduct CAPs through the nerve-cuff electrode. For all subsequent recordings, ENG responses were classified as either CV_{fast} or CV_{slow} based on the time window in which they occurred.

3.2.6 Estimation of stimulus threshold

Throughout this study, the threshold current required to elicit a response to stimulation was used as a means of quantifying selectivity and stability. To quantify threshold, it was necessary to detect the presence or absence of CAPs in the noisy ENG signal. All steps in the detection process were performed on the subsampled, stimulus-triggered averaged data. First (Figure 3.2b), the local cross-correlation (LCC) was calculated between the signals recorded from the second and fourth contacts of the nerve-cuff electrode. The process for calculating LCC is described in detail elsewhere [61], but briefly, the cross-correlation was calculated between the signal recorded from the second contact and a 0.5 ms window of the signal recorded from the fourth contact. The 0.5 ms window for the fourth contact was moved through either the CV_{fast} or CV_{slow} time window in 50 μs steps, and the peak of the cross-correlation was calculated. This peak was compared to the cross-correlation of a 0.5 ms window of noise with another window of noise that was the size of the CV_{fast} or CV_{slow} time window. If the peak of the LCC exceeded three standard deviations above the cross-correlation of the noise, the trial was identified as containing a CAP. Only electrodes that demonstrated CAPs in response to 15 μA stimulation were flagged as responding to stimulation. For those electrodes that elicited CAPs in response to 15 μA stimulation, the average signal power (RMS) was calculated (Figure 3.2c) for the time windows corresponding to CV_{fast} or CV_{slow} fibers at all tested current amplitudes. A one-tailed Student's t-test was used to determine whether the RMS of the signal within the CV_{fast} or CV_{slow} time window was above threshold. Threshold was defined as 1.5 standard deviations above the RMS of a 1 ms window of unstimulated noise. The accuracy of the method was determined by calculating the false positive and false negative rates when comparing the results with those of an

expert human observer for a randomly selected subset of 200 responses. The threshold value was chosen because it produced low rates of both false positives (2%; mainly from CAPs that straddled the CV_{fast} and CV_{slow} time windows) and false negatives (6%; mainly from very low amplitude CAPs). Because only a limited number of stimulus current amplitudes were tested during this study, we estimated the threshold value by linearly interpolating (Figure 3.2c) between the highest subthreshold current amplitude and the lowest supra-threshold amplitude.

3.2.7 Selectivity and stability of recruitment

Chronic stability and selectivity of the response to stimulation are especially important for a sensory stimulation neuroprosthesis. Tuning of stimulus parameters to achieve meaningful sensory feedback is likely to be a time-intensive process involving psychophysical metrics. As such, an ideal sensory interface should activate a distinct sensory modality, localized to the same peripherally referred location, with the same current amplitude from day to day. While it is impossible to infer what perceptions might have been evoked by a given stimulus in this study, the threshold response to stimulation and the type of fiber activated by that stimulation provide useful metrics for assessing efficacy. Selectivity for a given electrode was quantified as the difference in stimulation thresholds for activation of CV_{fast} and CV_{slow} fibers. Counts were made of the number of electrodes that selectively activated either CV_{fast} or CV_{slow} fibers and statistical analyses were performed to determine the effects of factors such as implant location (L6 vs. L7 DRG) and electrode size on the stability of recruitment.

To quantify the stability of the response to stimulation, the threshold for activation of CV_{fast} and CV_{slow} afferents was monitored over time. However, it was difficult to make a

statistical comparison of threshold values across factors that may affect the stability of stimulation (i.e. time, cat, implant site, electrode size, fiber type, electrode impedance) because of a ceiling effect caused by limiting stimulation to 15 µA. In the case when an electrode did not generate a response at or below 15 µA, it was treated as a missing observation. Because of their dependence on the factors of interest, missing observations were not distributed randomly throughout the data set. The probability of observing a missing value depended clearly on time post-implantation, making simple statistical techniques like analysis-of-variance unreliable. To circumvent this problem, a related quantity was analyzed: the probability (P_{15}) of electrodes generating CAPs when stimulated at or below 15 µA. Intuitively, one can think of P_{15} as the probability that a given electrode would elicit a CAP, and changes in the P_{15} reflect changes in the ability to elicit a response at or below 15 µA. Below is a short description of the procedure used to analyze P_{15} and the stability of the response to stimulation. For a more detailed treatment, see *Appendix A*.

3.2.8 Logistic regression model of P_{15}

To study the change in P_{15} of each implanted electrode array with respect to various factors of interest such as time, tip size, and fiber type, a logistic regression was performed on the data set, using the model:

$$\text{logit}\big(P_{15}(s,g,t)\big) = \log\left(\frac{P_{15}(s,g,t)}{1-P_{15}(s,g,t)}\right) = \alpha_{s,g} + \beta_{s,g} \times t; \qquad (1)$$

where $P_{15}(s,g,t)$ is the probability that an electrode with tip size s elicits a CAP for fibers of type g, when stimulated with a current less than or equal to 15 µA. This model assumes that, on

the logit scale, the probability of a CAP is linear in time, with different intercepts, $\alpha_{s,g}$, and different slopes, $\beta_{s,g}$, for each of the 4×2 combinations of tip size and fiber type. Likelihood ratio (LR) tests revealed that the slopes were not significantly different from one another, suggesting the relative effect of time was the same for all electrodes and fiber types. However, the intercepts were significantly different ($p<0.05$), suggesting that different tip sizes and fiber types had different effects on the probability of producing a CAP at the time of implantation. Furthermore, the intercepts could be decomposed into separate additive effects of fiber type and tip size, i.e. there was no interaction effect between these factors. Therefore, the final model for $P_{15}(s, g, t)$ was

$$\text{logit}\big(P_{15}(s, g, t)\big)=\alpha_g + (\gamma_0 + \gamma_1 s) + \beta t, \qquad (2)$$

where $\alpha_1 = 0$ so that α_2 measured the differential effect between CV_{fast} and CV_{slow} fibers, $\gamma_1 s$ was the linear effect of tip size *s*, and βt was the linear effect of time *t*, which was the same for all electrodes and all fiber types.

Impedance values were also considered as a factor that may affect P_{15}, however we found no relationship between changes in impedance and changes in threshold. As such, that factor was not included in the final formulation of the response rate model.

3.3 RESULTS

The goal of this study was to examine the chronic stability and selectivity of microstimulation in the lumbar DRG of anesthetized cats using penetrating microelectrode arrays. FMAs were

implanted in the left L6 and L7 DRG of four cats, and the threshold response to stimulation and number of responding electrodes were tracked over time.

3.3.1 Typical responses to stimulation

Figure 3.3 shows the responses to stimulation through two electrodes from one L6 DRG array. Figure 3.3(a) shows the response to stimulation at different current amplitudes through a single electrode on a single day. In this case, a CV_{fast} response (in the light gray box) was first observed at a stimulation amplitude of 10 µA, followed by a more complex combination of CV_{fast} and CV_{slow} responses (in both light and dark gray boxes) at 15 µA. Figure 3(b) shows the response evoked by a different electrode at 15 µA at times ranging from 9 to 134 days after implantation. On many days, a CV_{fast} response was visible, while on some later days (e.g. days 51, 64, and 119), there was an additional slower response that straddled the CV_{fast} and CV_{slow} time windows. These types of responses were typical, with recruitment of one fiber type and, for some electrodes, additional recruitment of a second fiber type at higher amplitudes. In many cases, as in Figure 3.3(b), a response was visible at early time points, but that response changed or disappeared and returned again at later time points. Figure 3.4 shows plots of the threshold response to stimulation within the first four weeks after implantation for each electrode in the L6 arrays of cats B, C, and D. These plots were typical of the response for both L6 and L7 arrays, and show a high degree of variability in thresholds as well as a significant reduction in the number of electrodes that responded to stimulation at amplitudes up to 15 µA over the first month after implantation.

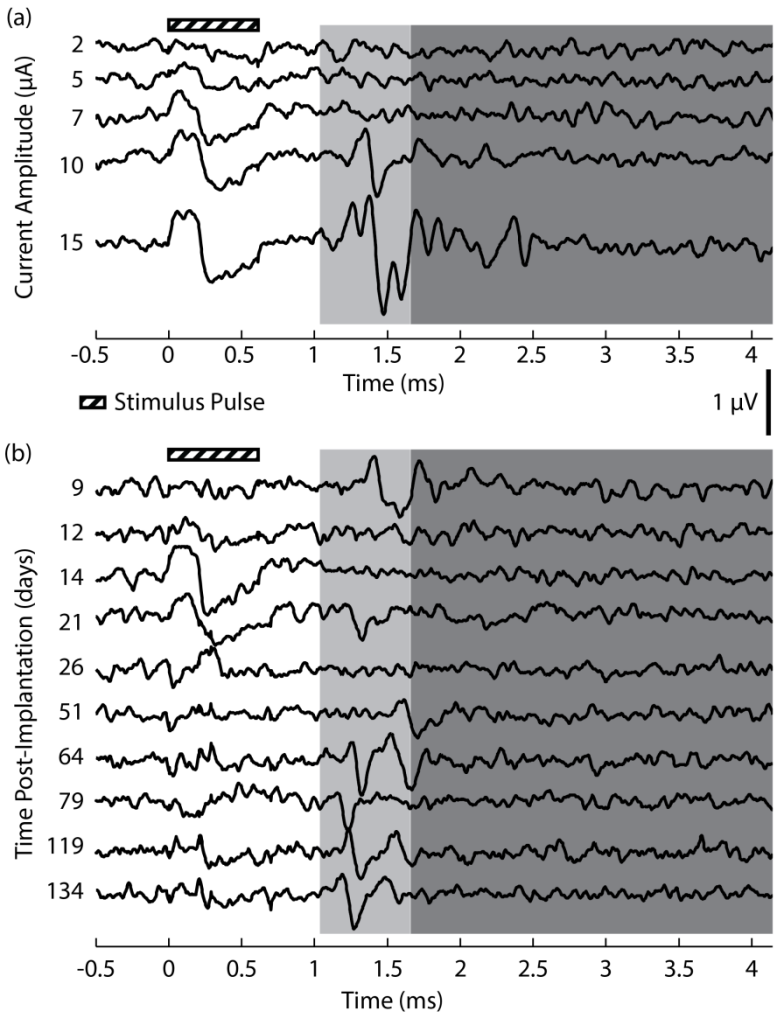

Figure 3.3. Typical ENG responses to stimulation. (a) The ENG signal recorded in response to stimulus pulses with current amplitudes of 2, 5, 7, 10, and 15 μA, applied through a single FMA electrode at time t = 0. There is a response visible in the CV_{fast} interval (light gray box) at current amplitudes of 10 μA, along with a complex longer latency response in the CV_{slow} time window (dark gray box) at 15 μA. (b) The ENG signal recorded in response to 15 μA stimulus pulses applied through a single FMA electrode at t = 0 on multiple days after implantation. At 9 days post-implantation, there is a CV_{fast} response that disappears at later time points. Starting at 51 days after implantation, there is a response that straddles both the CV_{fast} and CV_{slow} time windows. At time points between 64 and 134 days after implantation, there is also a response in the CV_{fast} time window.

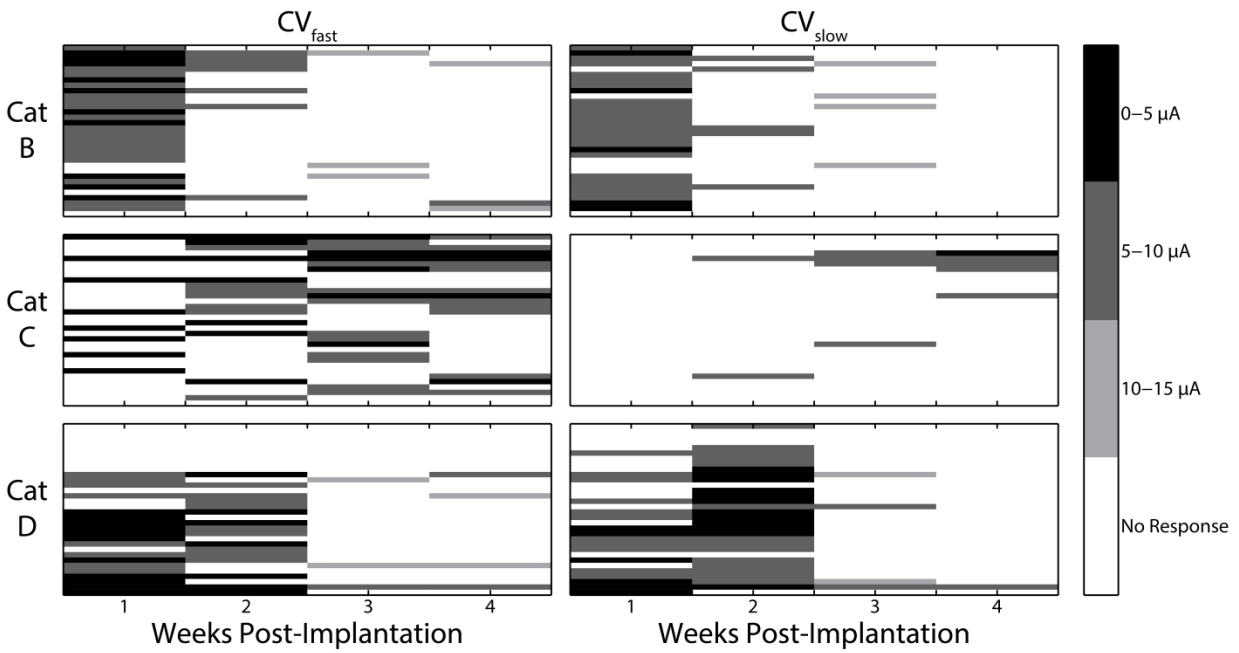

Figure 3.4 Thresholds in the CV_{fast} and CV_{slow} time windows for all electrodes in the FMAs implanted in the L6 DRG of Cats B, C, and D. Each row of the color maps corresponds to an electrode, and the color of the box corresponds to the minimum current amplitude that produced a CAP. White boxes correspond to electrodes that did not produce a CAP at stimulus amplitudes up to 15 µA. There is a high degree of variability in threshold current amplitude, although thresholds tend to be lower at early weeks than later weeks. Additionally, the number of electrodes that produce a CAP decreases over time. Data from Cat A are not included in this plot because testing did not begin until Week 4.

3.3.2 Threshold stability over time

Table 3.1 Data collection intervals for all cats and reasons for terminating experiments

	Array location	First time point (weeks after implantation)	Last time point (weeks after implantation)	No. of sessions	Reason for termination
Cat A	L6	4	26	13	No response to stimulation
	L7	4	11	10	Lead broke
Cat B	L6	1	6	9	Lead broke
	L7	1	6	9	Lead broke
Cat C	L6	1	24	12	End of study
	L7	1	24	12	End of study
Cat D	L6	1	4	5	Infection
	L7	1	4	3	Infection

Figure 3.5 shows, for each cat and each implant site, the expected probabilities that electrodes would generate CAPs when stimulated at or below 15 μA, as functions of the number of weeks post-implantation, electrode tip size, and fiber type. The shaded areas are 95% pointwise confidence bands for the expected P_{15}. For clarity, only the smallest and largest tip sizes are shown. Table I shows the time windows over which responses were tracked in each of the four cats. Note that not all electrode arrays were tested at each time point after implantation, and that testing with Cat A did not begin until four weeks after implantation. Typically, longitudinal tracking ended either as a result of gross array failure caused by damage to the leads near the connector or because of a lack of response to stimulation (limited to 15 μA in most

cats). Electrode impedances provided a useful tool for diagnosing lead damage and gross electrode failure, as impedances for all electrodes in an FMA would suddenly exceed 2 MΩ after leads broke. In Cat D, the experiment was terminated at four weeks post-implantation because of an infection at the percutaneous connector site.

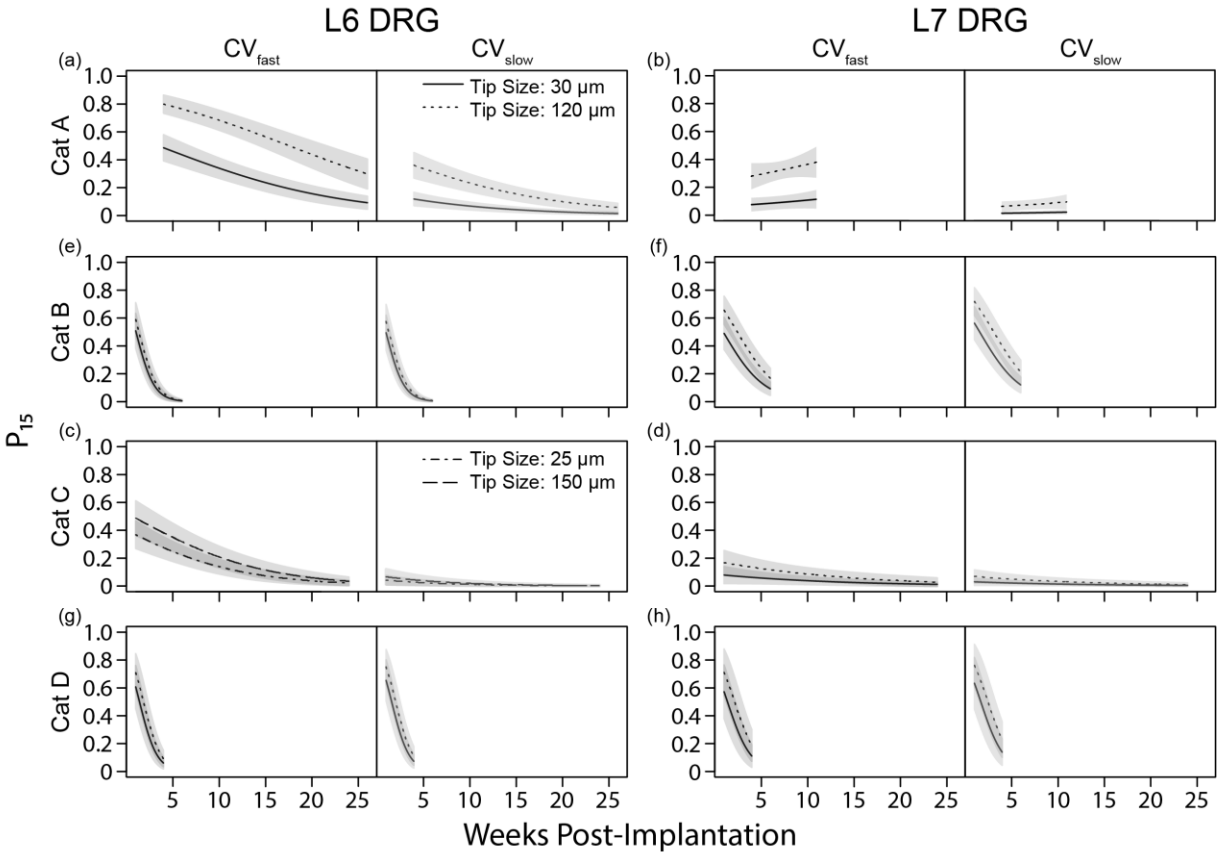

Figure 3.5 P_{15} for the largest and smallest electrodes in each implanted array across the time post-implantation. The implant periods ranged from 4 weeks (Cat D) to 26 weeks (Cat A). Shaded bands are 95% pointwise confidence intervals. The P_{15} value for all arrays except the L7 DRG array for Cat A decreased over time, suggesting that the threshold for stimulation was increasing. For all arrays, larger electrodes had a higher P_{15} than smaller electrodes. Also, CV_{fast} fibers had a higher P_{15} than CV_{slow} fibers, suggesting CV_{fast} fibers were activated more often.

In all cats, there were multiple electrodes on each array that evoked a CAP in the nerve-cuff electrode. In the first week post-implantation, there was typically a high number of electrodes that evoked responses (3 cats; CV_{fast}: 105 out of 192 electrodes; CV_{slow}: 83 out of 192 electrodes) with average thresholds of 5.1±2.3 μA for CV_{fast} and 6.3±2.0 μA for CV_{slow} fibers. Four weeks after implantation, the number of electrodes that elicited a response in both the CV_{fast} or CV_{slow} time windows decreased (4 cats; CV_{fast}: 64 out of 256 electrodes; CV_{slow}: 30 out of 256 electrodes) and the mean threshold current amplitude for responsive electrodes increased to 9.2±3.6 μA for CV_{fast} fibers and 11.2±2.6 μA for CV_{slow} fibers. Cumulatively across Cats A and C, there were 9 electrodes that continued to evoke a response to stimulation at 15 μA up to 24 weeks after implantation.

Overall, P_{15} decreased with time for all cats, both CV_{fast} and CV_{slow} fiber types, and all electrode tip sizes, except for the L7 DRG in Cat A (Figure 3.5(b)), where the P_{15} remained constant. The rates of decrease in P_{15} were remarkably different for different cats, as were the initial P_{15} values after implant. However, there were systematic patterns in the change in P_{15}. First, larger electrodes had higher P_{15} values than smaller electrodes, as illustrated by the dotted and solid curves in each panel of Figure 3.5, for all 16 combinations of cat, fiber group, and implant site. This suggests that larger electrodes achieved activation of both CV_{fast} and CV_{slow} fibers more often than smaller electrodes. Although this result was statistically significant only for the L6 and L7 arrays for Cat A (two-sided test p-values: $p<0.001$), the L7 array for Cat B ($p=0.014$), and borderline significant for the L7 array for Cat C ($p=0.073$), the probability that this systematic difference happened by chance is very low. Comparing the curves in each pair of adjacent panels, the P_{15} of the electrodes for Cats A and C were significantly higher for CV_{fast} than CV_{slow} fibers (two-sided test: $p<0.001$ for L6 and L7 arrays for Cat A, $p<0.001$ and $p=0.006$

for L6 and L7 arrays, respectively, for Cat C). The estimated effects for Cats B and D were not statistically significant. These results suggest that more electrodes recruited CV_{fast} than CV_{slow} fibers. Finally, for all four cats, the P_{15} of electrodes implanted in L7 decreased less sharply than the P_{15} of electrodes implanted in L6. Notably, there was no significant decrease for the L7 implant in Cat A. This result was statistically significant for Cats A and B (one-sided p-value: $p<0.001$), and borderline significant for Cats C and D ($p=0.053$ and $p=0.067$, respectively). Impedances remained constant over the course of the study, and there was no relationship between decreased P_{15} values and changes in impedance.

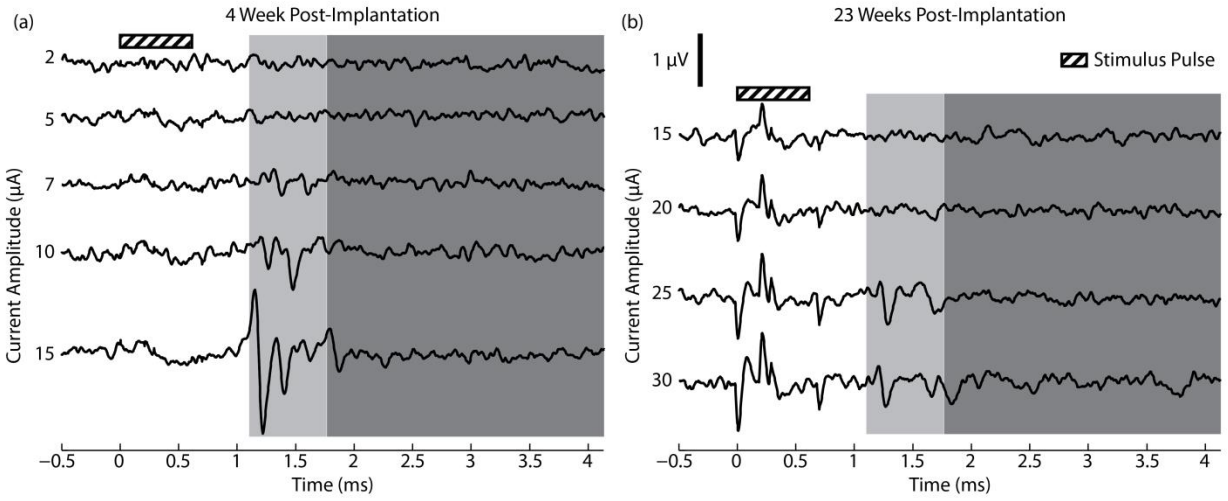

Figure 3.6. Early and late ENG response to stimulation on an electrode. (a) The ENG signal recorded in response to stimulus pulses with current amplitudes of 2, 5, 7, 10, and 15 μA, applied through a single FMA electrode at time t = 0, 4 weeks after implantation. There is a large CVfast CAP in response to stimuli at 10 and 15 μA. (b) At 23 weeks, the same electrode did not elicit a response at 15 μA but a CVfast response was evoked at 25 μA.

In Cat C, further testing at higher current amplitudes was performed at 23 weeks after implantation to determine if the reduced response rate was a result of increased thresholds or some other problem such as lead breakage. At that time point, only 2 electrodes were still responding to stimulation at 15 μA. However, when the current amplitude was increased to 30 μA, an additional 23 electrodes elicited responses to stimulation. As can be seen in Figure 3.6, many of those responses at higher amplitudes appeared similar in shape to the responses elicited by lower amplitude stimulation at earlier time points. Because of the time constraints of the experiment, this testing procedure at higher amplitudes was only performed once in Cat C.

3.3.3 Selectivity of stimulation

To assess the selectivity of stimulation of CV_{fast} and CV_{slow} fibers, the threshold current amplitudes for eliciting those responses were compared for each electrode. Figure 3.7(a-b) show the percentage of electrodes that elicited a response and selectively activated only CV_{fast} or CV_{slow} fibers and the threshold for activation. Figure 3.7(c-d) show the percentage of electrodes that elicited a response and activated both CV_{fast} and CV_{slow} fibers, but activated one fiber type at a lower current amplitude than the other. Also shown is the difference in threshold for activation of CV_{fast} or CV_{slow} fibers for those electrodes. These plots demonstrate the dynamic range for selectively stimulating one fiber type when the threshold for the other fiber type was at or below 15 μA. Figure 3.7(e) shows the total percentage of electrodes that elicited a response and were selective for either CV_{fast} or CV_{slow} fibers. These results demonstrate that it was more common for electrodes to selectively activate only CV_{fast} fibers than to activate only CV_{slow} fibers. For those channels that activated both fiber types, CV_{slow} fibers were more commonly activated at

lower current amplitudes than CV_{fast} fibers. The mean difference in estimated stimulation threshold (i.e. dynamic range) between CV_{fast} and CV_{slow} fibers was 2.6±2.3 µA for electrodes that activated CV_{fast} fibers first, and 3.2±2.8 µA for electrodes that activated CV_{slow} fibers first. Overall, there was a high degree of variability in the number of CV_{fast} and CV_{slow} fibers activated selectively, with approximately the same proportion of each fiber type activated selectively at early time points, but with more CV_{fast} than CV_{slow} fibers activated at time points after 6 weeks.

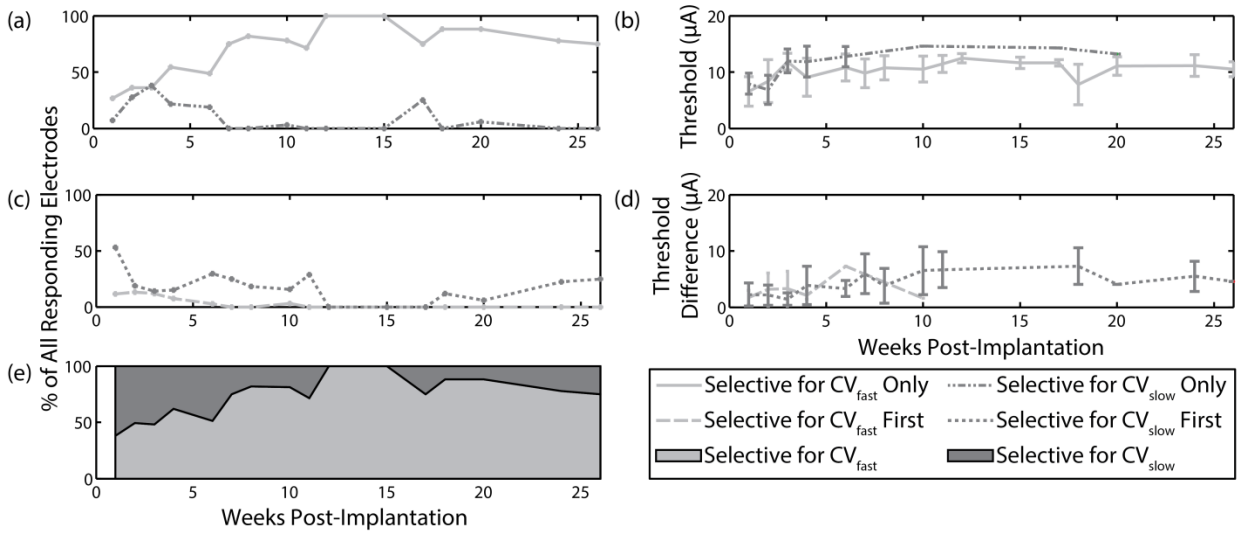

Figure 3.7 Summary of selectivity data for all electrodes implanted in all cats. (a-b) The percentage of responding electrodes and the average thresholds for electrodes that only elicited either a CV_{fast} or CV_{slow} CAP. (c-d) The percentage of responding electrodes that elicited both CV_{fast} and CV_{slow} CAPs, as well as the difference in threshold for their responses. (e) The total percentage of responding electrodes that selectively elicited either a CV_{fast} or a CV_{slow} response.

3.4 DISCUSSION

The goal of this study was to assess the chronic stability and selectivity of primary afferent recruitment using penetrating microelectrode arrays in the DRG. Based on the results of this study, it is clear that it is possible to achieve selective activation of both CV_{fast} and CV_{slow} fiber types with chronically implanted electrodes. However, the likelihood of recruiting only CV_{slow} fibers declined over time. We also found that, within the first week after implantation, thresholds for activating both CV_{fast} and CV_{slow} fibers were very low, averaging between 5.0 and 6.5 µA. These thresholds are higher than those from our previous work in acute experiments, where activation of DRG neurons occurred at an average of 2.7±1.3 µA [61]. This difference in thresholds can likely be attributed to differences in stimulating electrode technology, variations in data analysis methodology, and the assumed tissue response that likely occurred during the one week delay before the first set of data was collected in the current study. These thresholds are generally similar to those reported to evoke a sensory percept in human subjects via intraneural peripheral nerve stimulation with LIFEs or microneurography needle electrodes [69,108].

During the first month after implantation, mean thresholds increased and the number of electrodes that elicited a response to stimulus pulses up to 15 µA decreased. Further testing in one animal at higher amplitudes (up to 30 µA) demonstrated continued responses to stimulation on many electrodes (23 out of 64) at 23 weeks after implantation. The decreased P_{15} and the restored response at higher current amplitudes suggest that a ceiling effect was occurring as a result of the limit that was chosen for the maximum stimulus amplitude to test in this study. We chose to limit the maximum amplitude to 15 µA for several reasons. First, we wanted to reduce

the risk of tissue damage associated with high amplitude stimulation. While safety limits have not been determined for DRG microstimulation, studies of intracortical microstimulation in cat brain suggest that intensities as low as 20 μA (4 nC/phase) may cause neuronal damage [113]. Second, we wanted to avoid recruitment of spinal reflexes during testing. Lastly, we needed to impose a limit on the number of stimulus amplitudes tested on each of the 64 electrodes to limit the total time each animal spent under anesthesia. In future testing, it may be beneficial to use closed-loop algorithms such as binary search to intelligently choose stimulation parameters and avoid the ceiling effects of the current experimental protocol. Such an intelligent algorithm would need to identify the presence or absence of CAPs in real-time, and could potentially be designed to perform only enough stimulus repetitions to confidently identify a CAP from the noisy ENG signal. Alternatively, it may be appropriate to rely on a behavioral response from awake animals as a means to detect stimulation thresholds [114].

A variety of factors may have contributed to the decrease in P_{15} over time, such as migration of cells away from the electrodes, mechanical failure of electrode leads, accumulation of a tissue encapsulation layer around the electrodes, or damage to the electrodes as a result of electrochemical reactions during stimulation. Additionally, the variability observed between the P_{15} values in L6 and L7 DRG may be attributed to differences in anatomical structure, surgical access, and implant technique. The lack of a relationship between impedances and P_{15} values suggests that there were not significant changes in the electrode-tissue interface over time, and the observed changes in threshold may be a function of changes in the location or density of neurons near the electrode tips. Future studies should include histological analysis of neural tissue near the electrodes to explore the consistency of the placement and orientation of the electrodes with respect to the DRG as well as the biological response to the electrodes. As with

microelectrode implants at other locations in the nervous system (e.g. periphery, cortex, etc.), the longevity and stability of neural interfaces with the DRG may be improved by further development of technologies such as flexible electrodes or chemical agents to suppress immune response and promote neural growth [115].

From the ENG data it is not possible to identify whether the same set of neurons were activated by each electrode from day to day. When the response to stimulation disappeared and reappeared over time, the activated neuron pool certainly changed, but in cases such as in Figure 3.3(b), where a CV_{fast} response occurred at each time point from 64 to 134 days after implantation, it is unclear whether those responses were always from the same set of neurons. However, for the CV_{fast} response in Figure 3.3(b), as well as many other examples across all animals, the size, shape, and time delay of the CAP appears to be consistent over time. As Figure 3.4 makes clear, though, there is a great deal of fluctuation in the response to stimulation within the first month after implantation. With respect to the implementation of a sensory neuroprosthesis, it is unclear how these fluctuations would translate to perceived sensation. It seems likely that, over the first month after implantation, the rapid changes in response would lead to variability in sensation, but, as in the case of Figure 3.3, the perceived sensation may stabilize over time. Future work will require significant effort to characterize the perceived sensation as a result of stimulation over time.

Throughout this study, activation of CV_{fast} or CV_{slow} fibers was used as a representation of the ability to selectively recruit different sensory modalities. Based on the data in Figure 3.5 and Figure 3.7, it seems that, initially, the thresholds for CV_{fast} and CV_{slow} activation were similar and that approximately equal numbers of electrodes selectively activated CV_{fast} and CV_{slow} fibers. At later time points, however, more electrodes elicited CV_{fast} than CV_{slow}

responses. Further, those electrodes that elicited a CV_{slow} response were more likely to elicit a CV_{fast} response at slightly higher amplitudes, suggesting the dynamic range for selectively activating CV_{slow} fibers may be limited. Models of the response to stimulation in the DRG predict that medium diameter (i.e. CV_{slow}) fibers will be recruited in a slightly higher proportion than large diameter (i.e. CV_{fast}) fibers [116]. Additionally, our previous work with acute implantation of penetrating electrodes in the DRG demonstrated that approximately equal proportions of CV_{fast} and CV_{slow} fibers were activated [61]. Those results largely agree with the initial phase of this study, although further work should be devoted to studying the difference in CV_{fast} and CV_{slow} responses at later time points after implantation.

Overall, this study represents the first example of a chronic microstimulation interface with the DRG and suggests that the DRG is an appropriate target for interfacing with the peripheral nervous system to restore sensory function after injury, though it will likely be necessary to develop electrode technologies that can provide a more stable interface with the nerve. There are, however, some important limitations that should be noted with respect to this study. First, the study relies on antidromic propagation of CAPs to evaluate the effectiveness of sensory stimulation, and classifies sensory modality based on conduction velocity. While this approach provides a good first approximation for the efficacy of a sensory neuroprosthesis, further testing in awake animals is needed to determine if the animals can detect stimulation at the threshold amplitudes found in this study. It will be impossible to evaluate with certainty the qualia of sensory percepts experienced by the animals, but ultimately we would like to assess sensations evoked by stimulation of proprioceptive and cutaneous afferents. Human studies will be needed to definitively answer these and other questions about the percepts evoked by DRG microstimulation.

A second limitation of the study is the relatively small sample size. Out of eight FMAs implanted in the DRG of four cats, only three lasted to the end of the study without suffering gross array failure such as lead breakage or infection. This certainly limits the predictive power of the study and does not allow for generalization of the ability to evoke responses in other animals. It should be noted, however, that in all of the arrays that did not suffer gross mechanical failure (Cat A: L6; Cat C: L6 and L7), there remained multiple electrodes that could elicit CAPs at least 24 weeks after implantation. These results demonstrate that it is possible to evoke responses via microstimulation of the DRG with chronically implanted penetrating electrode arrays for an extended period of time after implantation.

An additional limitation of this study results from the intrinsic characteristics of the ENG signal. The CAPs recorded from the ENG signal often contain multiple overlapping responses, which can sum both constructively and destructively. This summation may result in the appearance that the response to stimulation is actually either larger or smaller than the individual superimposed responses would be. Because the procedure for estimating threshold relied on the RMS of the ENG signal, this may have resulted in slight under- or overestimation of the stimulation threshold. Since this effect would only affect the linear interpolation procedure used to estimate threshold, but likely would not affect the LCC procedure for detecting CAPs, it is unlikely to have a significant effect on the results presented here.

A final limitation occurs because of the anatomical structure and innervation of the hindlimb. In this study, stimulating electrodes were implanted in the L6 and L7 DRG, and ENG recordings from the sciatic nerve were used to detect the response to stimulation. While many neurons whose cell bodies are in the L6 and L7 DRG have axons that project through the sciatic nerve, some may have projections through the femoral nerve or may exit the sciatic nerve above

the level of the cuff, making them undetectable with this method. This may have contributed to the observed differences in P_{15} for electrodes implanted in the L6 and L7 DRG, or may have resulted in a slight underestimation in the overall number of electrodes that elicited a response to stimulation.

Despite these limitations, this study presents the first example of a chronic neural interface with the DRG for sensory stimulation. These results demonstrate that it is possible to activate multiple populations of primary afferents independently with penetrating arrays implanted in the DRG, and that responses can be elicited by microstimulation up to 26 weeks after implantation. These findings suggest that the DRG are potentially feasible sites for sensory neural interfaces. Future work will include detailed histological analysis of the tissue near the tips of the implanted electrodes in order to gain additional insight into the failure modes and to develop improvements to the electrode design that may extend the usable life and functionality of these devices. Further future work should focus on behavioral testing of the response to stimulation, as well as testing of alternative stimulus waveforms, pulse widths, and paradigms that might further improve selectivity and allow for tuning of the type of fibers activated by individual stimulating electrodes [117].

3.5 CONCLUSIONS

This study presents results from the first chronic implantation of stimulating electrodes in the DRG as part of a neuroprosthesis for sensory stimulation. Over 26 weeks after implantation, a subset of electrodes elicited CAP responses in the sciatic nerve at stimulation amplitudes of 15

μA or below, though the number of electrodes that responded to stimulation decreased and threshold for eliciting a response increased over time. In one cat, only two electrodes still elicited a response at 23 weeks after implantation at 15 μA, but when the stimulation amplitude was increased to 30 μA, over twenty additional electrodes elicited a response. Based on CAP conduction velocity, it was possible to selectively activate both CV_{fast} and CV_{slow} primary afferents via many of the implanted electrodes, though the percentage of electrodes that selectively activated CV_{slow} fibers decreased over time. These results suggest that the DRG is a viable anatomical location for chronic stimulation as part of a sensory neuroprosthesis, and that the approach merits further study.

4.0 MICROSTIMULATION OF THE LUMBAR DRG RECRUITS PRIMARY AFFERENT NEURONS IN LOCALIZED REGIONS OF LOWER LIMB

Patterned microstimulation of the dorsal root ganglion (DRG) has been proposed as a method for delivering tactile and proprioceptive feedback to amputees. Previous studies demonstrated that large and medium diameter afferent neurons could be recruited separately, even several months after implantation. However, those studies did not examine the anatomical localization of sensory fibers recruited by microstimulation in the DRG. Achieving precise recruitment with respect to both modality and receptive field locations will likely be crucial to create a viable sensory neuroprosthesis. In this study, penetrating microelectrode arrays were implanted in the L5, L6 and L7 DRG of four isoflurane-anesthetized cats instrumented with nerve cuff electrodes around the proximal and distal branches of the sciatic and femoral nerve. A binary search was used to find the recruitment threshold for evoking a response in each nerve cuff. The selectivity of DRG stimulation was characterized by the ability to recruit individual distal branches to the exclusion of all others at threshold. 84.7% (N=201) of the stimulation electrodes recruited a single nerve branch, with nine of the 15 instrumented nerves selectively. The median stimulation threshold was 0.68 nC/phase and the median dynamic range (increase in charge while stimulation remained selective) was 0.36 nC/phase. These results demonstrate the ability of

DRG microstimulation to achieve selective recruitment of the major nerve branches of the hindlimb suggesting that this approach could elicit focal percepts in a limb.

4.1 BACKGROUND

In the U.S., an estimated 1.6 million people living with amputation in 2005, a number that is expected to more than double by 2050 [1]. Of these individuals, 65% had a lower limb amputation, struggle with mobility issues and are more likely than similar cohorts to fear falling [2]. Adding to these numbers are the more than 700 veterans of OIF/OEF that have lost limbs, many who have lost multiple limbs [118]. While lower-limb prostheses typically have higher adoption rates than upper-limb prostheses [119], there are still a number of significant problems with current devices that limit their adoption. One major limitation is the lack of sensory feedback provided by these devices. Without direct sensory feedback from the prosthetic limb, the user must infer information about limb state from the pressure exerted on the residual limb by the prosthetic socket. Reduced sensory feedback can make many activities such as stair climbing and walking on uneven terrain difficult and dangerous with a prosthetic limb [120]. These problems could be reduced by haptic interfaces [35] that deliver cutaneous feedback to the residual limb as a substitute for sensory inputs lost in the missing limb.

Electrical stimulation of afferent fibers in residual nerves has been proposed as a method to provide sensory feedback to amputees. An early approach to creating a somatosensory neuroprosthesis was suggested by Clippinger et al.[54], which used frequency-modulated stimulation of the sciatic nerve to provide sensation of the pylon bending moment during early

and late stance. Although the authors reported that patients had used their devices for up to six years, the technology appears to have been abandoned, as there have been no subsequent reports since the initial publication in 1982. Contemporary studies using epineural electrodes have demonstrated successful recruitment of sensory neurons in distal peripheral nerves in humans with arm amputation [51]. Similar epineural electrodes have been shown to provide selective recruitment of lower limb muscles during functional neuromuscular stimulation (FNS) of knee extensors and hip flexors [121] as well as ankle plantar- and dorsiflexors [122]. Despite these successes, epineural electrode placement on peripheral nerves is a compromise between the competing interests of recruitment selectivity, limb coverage, and robustness to mechanical stresses. In particular the more proximal trunk nerves used to achieve the greatest limb coverage contain a mixture of motor and sensory pathways making selective recruitment of afferents to exclusion of efferents difficult.

The degree of selectivity required to produce useful sensory feedback is currently unknown, though it is expected that more focal stimulation will result in more natural sensation. Intraneural microstimulation (INMS) has been used to demonstrate that recruitment of even individual cutaneous afferents can produce conscious percepts [42]. The same subjects could not detect the recruitment of single muscle spindles suggesting that mass activation of spindles may be required for salience. Thus, proprioceptive feedback may require selectivity at the population level, i.e. recruitment of many spindles from the same muscle) though, even paresthesias resulting from non-selective recruitment can be modulated to convey discriminable sensations [39].

The dorsal root ganglion (DRG) is an attractive target for sensory neuroprostheses, owing to its anatomical segregation of sensory afferents from motor efferents, its mechanical stability, and its inclusion of both cutaneous and proprioceptive afferents. Three to four ganglia account for

the innervation of an entire limb [58], while a DRG at a single spinal level may provide access to the entire sensory representation of the foot. It is anticipated that existing minimally invasive surgical techniques [90] can be adapted for implanting epineural electrodes on the DRG. We have previously shown that microstimulation of the DRG can recruit primary afferent neurons at low intensities both acutely [61], and over several months after implantation [123]. While these studies suggest that DRG microstimulation may be an appropriate technique for sensory feedback, they provide limited information on the specific sensory modality of recruited neurons or their distal innervation patterns. Single unit recordings [124] and tracer studies [125] within the DRG have revealed a heterogeneous distribution of afferents lacking somatotopy. Further investigation is required to determine whether the lack of clear somatopic organization of fibers within the DRG will limit its utility as a substrate for clinical devices.

In this study, we report on the selectivity and dynamic range of microstimulation and the distribution of projected fields in the L5, L6, and L7 DRG via recordings from many of the proximal and distal branches of the femoral and sciatic nerves. Instrumentation of multiple distal nerve branches has been used previously to directly assess the selectivity of peripheral nerve stimulation [126] in the same way that EMG has been used to measure the selectivity of FNS [127]. This technique can be applied to the study of DRG microstimulation by recording from major nerve trunks of the hindlimb and their distal branches during stimulation. Recording the response to microstimulation in a large number of distal nerve branches allows for approximate determination of the receptive field and fiber type.

4.2 METHODS

Acute experiments were performed in four anesthetized male cats (E-H). All experimental procedures were performed under the approval of the University of Pittsburgh IACUC.

4.2.1 Electrode Implantation Procedures

Isoflurane (1-2%) was used to maintain the animals at a surgical anesthetic plane throughout the experiment and vitals signs were monitored continuously. Distal nerve branches (Figure 4.1) were instrumented with two-contact nerve cuffs, which were either custom made or purchased (Microprobes, Gaithersburg, MD). Both types of electrodes were made from split silicone tubing with circumferential fine-wire stainless steel electrodes with an interelectrode spacing of 3 or 4 mm. The nerve cuff inner diameters ranged from 1 mm to 3 mm depending on the size of the targeted nerve. The sciatic and femoral nerves were instrumented with 5-pole nerve cuffs (Ardiem Medical, Indiana, PA), which had an interelectrode spacing of 4 mm. Proximal, center, and distal contacts were shorted together and were used as a reference in a virtual tripole configuration when recording from the second and fourth contacts within the cuff [61].

Where possible, nerves projecting to members of each major muscle group innervated by the sciatic and femoral trunks were instrumented. The sciatic branches innervating the hamstrings were often too proximal to instrument safely, although a cuff was implanted around the nerve innervating biceps femoris in cat G. It was not possible to instrument the branch of the common peroneal nerve innervating ankle dorsiflexors without reflecting the biceps femoris tendon, however the common peroneal nerve was always instrumented proximal and distal to this

important branch point. Nerve identities were determined using known anatomical landmarks and verified by stimulation using a voltage-controlled stimulator (Grass, Warwick, RI) and finding coarse motor thresholds. Sensory nerves, such as the sural and the sciatic cutaneous branch, were tested to the maximum stimulation intensity (20 V) to verify that there were no evoked movements. After nerve cuff implantation, the left L5, L6 and L7 DRG were exposed via laminectomy and the cat was placed in a spinal frame for duration of the experiment. Motor thresholds were measured again after transfer to the frame to verify that the cuffs still made adequate contact and that the instrumented nerves were still intact. Penetrating microelectrode arrays (cats E&F 32-Channel FMA Microprobes, Gaithersburg, MD;cats G&H 32-channel Utah arrays, Blackrock Microsystems, Salt Lake City, UT) were inserted into the L5, L6, and L7 DRG. A stainless steel screw in the iliac crest was used as the return for stimulation.

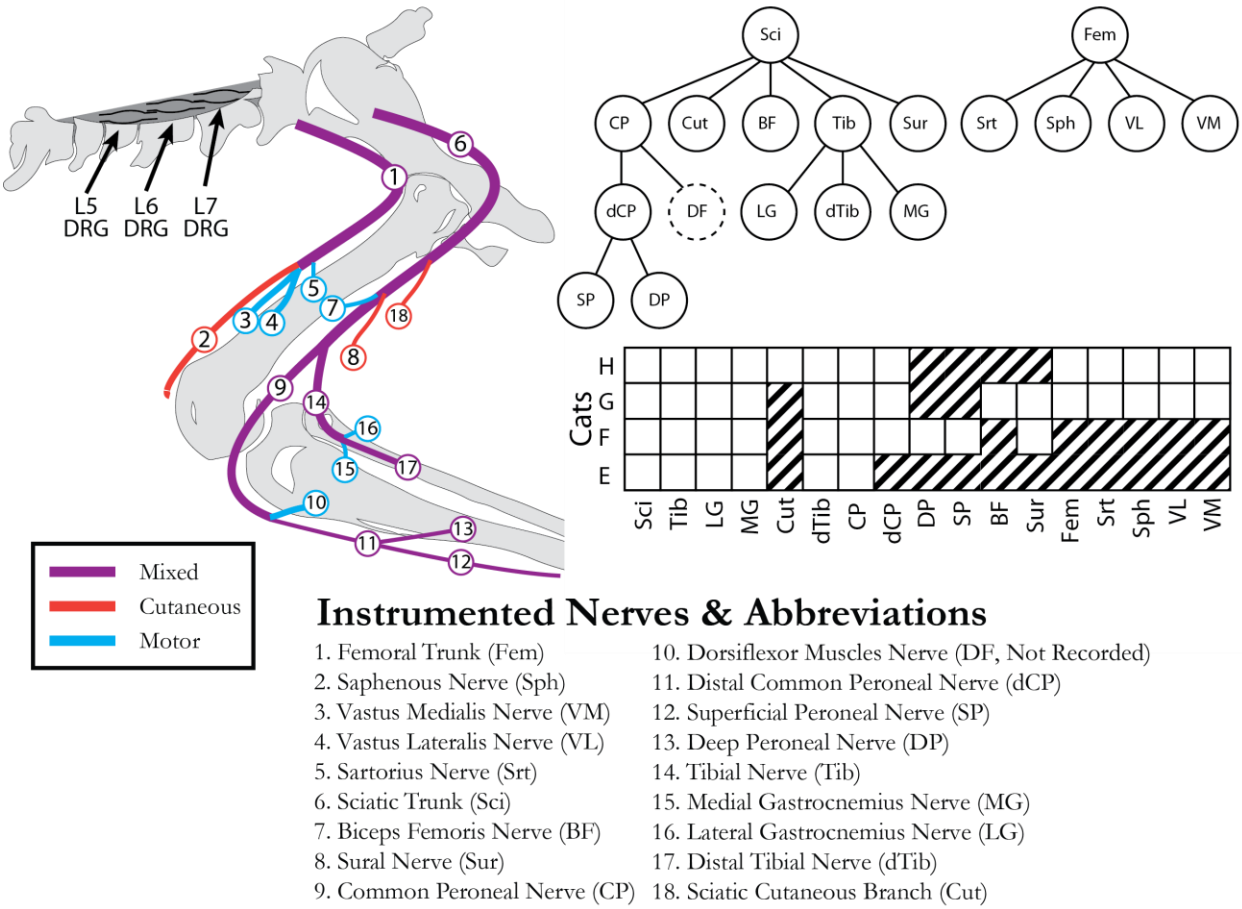

Figure 4.1 Schematic of nerve cuff location in the left hindlimb. The femoral and sciatic trunks were each implanted with a 5-pole cuff, while all other nerves received bipolar cuffs. In experiment H a custom book electrode was implanted on three of femoral nerve branches. The common peroneal and tibial nerve were both implanted with a proximal cuff, close to the initial branch point, and a distal cuff. The ankle dorsiflexor nerves tended to be deep and could not be implanted without significant dissection of the limb, but activity could be inferred by differential activation of the proximal and distal portions of the common peroneal nerve.

4.2.2 Experiment Design

The objective of these experiments was to identify the minimum stimulus intensity in the DRG that elicited activity in any of the instrumented nerve cuffs (threshold), and whether or not activity occurred in one or more nerves (selectivity) at threshold. In the event of non-selective recruitment any synergies between recruited motor nerves (e.g. nerves innervating multiple heads of the quadriceps) were identified. Finally, the range of intensities over over which recruitment was selective (dynamic range),was characterized.

Electroneurogram (ENG) signals from both the 5-pole and bipolar cuffs were collected using a Grapevine Neural Interface Processor (NIP) (Ripple, Salt Lake City, Utah), amplified using differential headstages and digitized at 30 kHz. Stimulation was performed using two IZ2 16-channel stimulus isolators (TDT, Alachua, FL) and custom written LabVIEW software. Stimulation artifacts were generally small and could be blanked out in software using a 1 ms window, which did not exceed the minimum conduction latencies of the most proximal nerves. Following blanking, ENG data were high-pass filtered at 300 Hz. Custom software was written in C++ and Matlab (Mathworks, Natick, MA) to capture and display stimulus triggered ENG recordings from all cuff electrodes, to detect responses, and to coordinate a binary search for threshold as a function of the injected charge.

Experiment duration was a significant concern due to the time required to collect recruitment data for the many individual nerves and stimulation electrodes. Furthermore, the low SNR of nerve cuff recordings dictated that a large number of stimulus repetitions be used (N = 600) in order to resolve responses near threshold. Significant effort was spent minimizing experiment duration. An initial survey across all electrodes was performed at a high intensity

(2.46 - 4.38 nC/phase) at a stimulation frequency of 58 pulses/second (pps). Individual stimulation pulses were either a cathodic-leading 200 μs pulse with a 400 μs half-amplitude anodic phase (cats: E&F) or a cathodic-leading 82 μs per phase symmetric biphasic pulse (cats: G&H) Pulse width was shortened in the latter two experiments to prevent artifact from obscuring short latency ENG responses in the most proximal nerve cuffs. The intent of this survey was to identify DRG stimulation electrodes that evoked compound action potentials in any nerve branch. Stimulation electrodes that did not recruit any nerves during the survey trial were not tested further. For electrodes that did evoke responses, only the nerves recruited during that survey trial were considered for further evaluation. The longest latency response recruited by each stimulation electrode was used to set the stimulation frequency for the remainder of testing to minimize the duration of testing. Multichannel headstages allowed for recording from multiple nerve cuffs simultaneously, which allowed threshold searching to be performed for multiple nerves in parallel (see below) rather than sequentially.

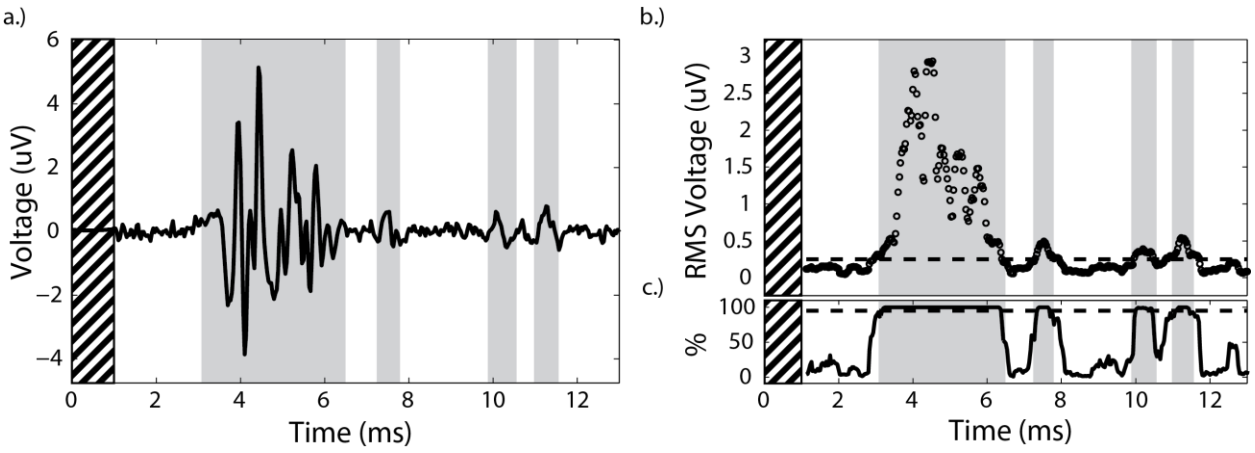

Figure 4.2 ENG response detection algorithm. a.) Example survey trial stimulus triggered averaged (N=600) showing compound action potentials from the common peroneal nerve. Initial hashed section of time denotes 1 ms blanking period. Detected responses are highlighted in grey. b.) Average windowed RMS (250 us width, 25 us step) values. Dashed line denotes 99% confidence interval on baseline mean which was used as the detection threshold. C.) To reduce the effect of outliers 200 individual averages were generated using 80% of the stimulus repetitions (480) drawn with replacement. For an RMS time window to be considered significant 95% (190) of averages drawn in this manner had to exceed the 99% confidence interval upper bound.

A binary search over stimulation intensity was performed on each stimulation electrode to determine the recruitment threshold of each instrumented nerve to a user-specified minimum resolution, which was adjusted between 0.08 nC/phase and .41 nC/phase as time allowed. During the online threshold search, responses were detected (Figure 4.2) by comparing the windowed RMS (250 μs duration, 25 μs step size) of stimulus triggered averages between baseline and stimulation epochs. Baseline data were divided into intervals of the same duration as the stimulation interpulse interval for statistical comparison. RMS values exceeding both 0.5 uV and 3-4 standard deviations of the mean windowed baseline RMS values for two consecutive

windows were accepted as responses. In cats E & F the 600 possible stimulus repetitions was divided into three subsets of 150, 175, and 275 repetitions. After each subset of stimulus repetitions was collected the detection algorithm was a run, and if a response was detected the remaining subsets were not collected. The intent was to reduce the time needed to test at higher stimulation intensities where the ENG SNR was high and 600 repetitions were unnecessary to detect a response.

All analyses presented in this paper are based on responses detected using a non-parametric bootstrap approach, because runtime efficiency and experiment duration were not limitations. First, a 99% confidence interval about the baseline mean was calculated by bootstrapping averages using 80% of the windowed baseline RMS repetitions (N=480) into 200 separate draws. These numbers were chosen to balance computation time and detection sensitivity. The upper bound of the resulting 99% confidence interval was used as the detection threshold for the post-stimulation interval. Next, 200 averages were generated using 80% of the stimulation repetitions (N=480) drawn with replacement. For a time window to be considered significant, 95% of the resulting averages (N=190) had to be superthreshold during that time window. This second step was designed to reduce the effect any outliers had on detection. Finally all responses for each nerve had to fall within a 250 μs window of the responses detected during the survey trial for that same nerve to be considered valid. The 250 μs buffer was added to the survey response time windows to accommodate the anticipated preferential recruitment of slower medium diameter fibers at perithreshold intensities [59,112,119]

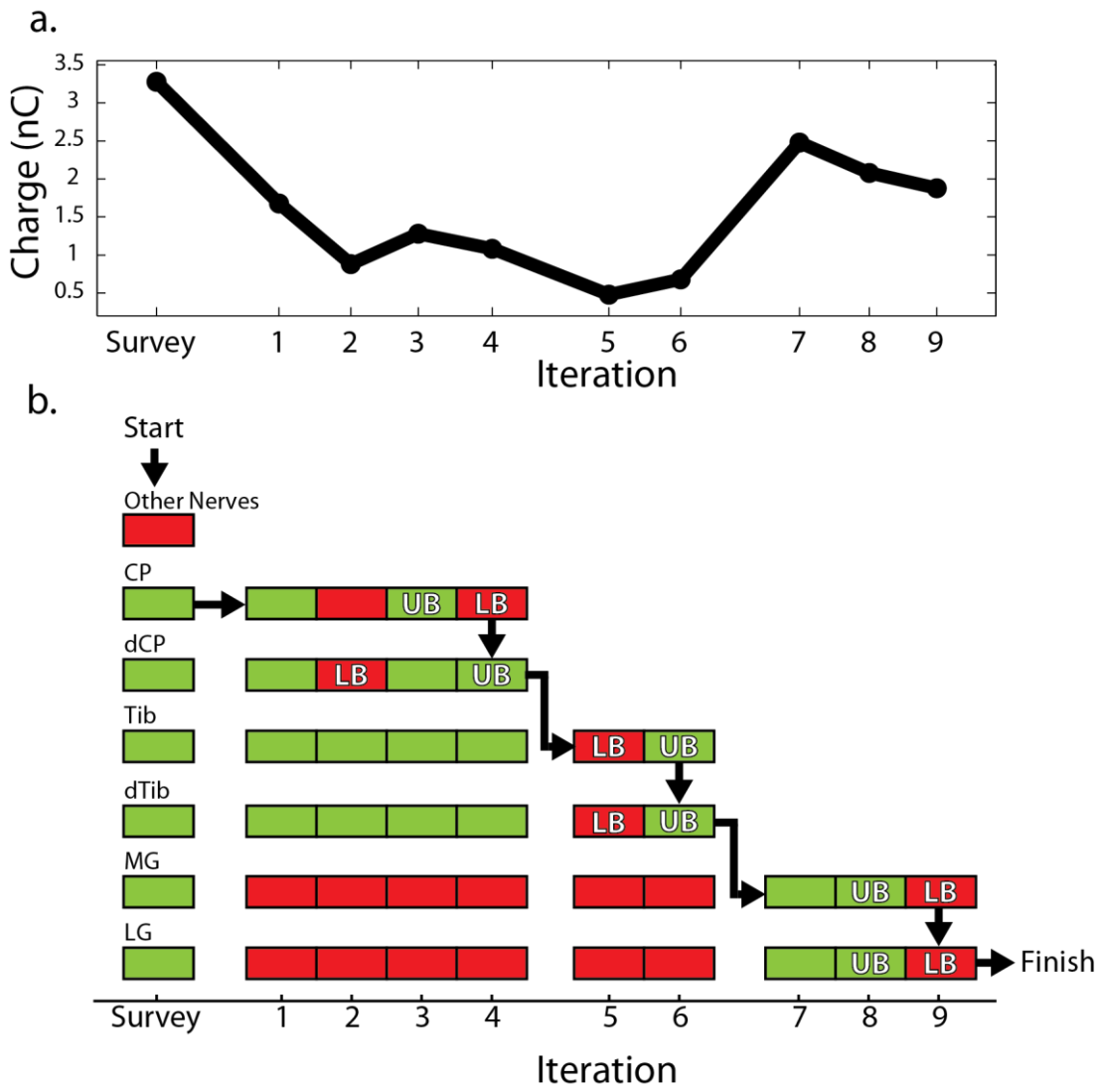

Figure 4.3 Example binary search. A binary search over stimulation intensity was used to find the threshold each of nerve recruited by each DRG stimulation electrode. a.) The charge injected at each iteration of the binary search. b.) Whether a response was detected (green) or not (red) in each nerve at each stimulus intensity. The survey amplitude was used to determine which nerves were recruited by this electrode to limit the scope of the search. Following the survey the search started with the common peroneal (CP) cuff and proceeded until the upper (UB) and lower bounds (LB) on the recruitment threshold for this cuff were within 0.25 nC/phase. Although the search started with CP, the detection algorithm was run on all the other cuffs, such that by iteration four the threshold had been found for both CP and dCP. Execution continued in this manner until the threshold for all cuffs was determined.

The threshold search was performed on each recruited nerve sequentially, but the multichannel headstage allowed simultaneous measurements from all nerves to be captured and analyzed at each stimulation amplitude that was tested. For each iteration of the binary search (Figure 4.3), the response of a single nerve to stimulation was used to select the subsequent intensity, but the upper and lower bound on the threshold estimate for all other nerves was updated in parallel. Intensities chosen to find the recruitment threshold of a single nerve informed subsequent testing on the remaining nerves and in many instances obviated the need for additional iterations for one or more nerve branches. This approach reduced the overall number of search iterations across all experiments by an estimated 77% and significantly shortened experiment duration.

4.3 RESULTS

An example threshold search is shown in Figure 4.3. An initial high amplitude survey trial determined which nerves could be recruited by this particular electrode (Cat H, L7-DRG). In this example only the common peroneal, distal common peroneal, tibial, distal tibial, and medial and lateral gastrocnemius nerves were recruited. The algorithm then performed a binary search on the common peroneal nerve by testing an amplitude midway between the survey and minimum possible (0.16 nC/phase) amplitudes. A response was detected on the first iteration, therefore the amplitude was reduced on the second iteration. No response was detected at the second amplitude so the amplitude was increased on the third trial, and the search continued until the upper and lower bounds (denoted UB and LB) on the common peroneal nerve threshold were

determined to within 0.25 nC/phase. This condition was satisfied on iteration four. After determining threshold for the common peroneal nerve, the search algorithm switched to find threshold for the distal common peroneal nerve, however by this point the threshold bounds for this cuff were already within 0.08 nC/phase. The search then continued with proximal and distal portions of the tibial nerve, and gastrocnemius nerves. Upon completion of the threshold search on the medial gastrocnemius nerve, thresholds had been found for all cuffs, including the lateral gastrocnemius nerve, and the algorithm started again with a new stimulation electrode. This continued until the threshold for recruiting all cuffs had been determined for all stimulation electrodes. The binary search algorithms parameters for each cat are summarized in Table 4.1.

Table 4.1 Penetrating electrode binary search parameters and selectivity results. Threshold resolution denotes the maximum allowable difference in the upper and lower estimates of threshold, separated here into the values used for each ganglion. Total electrode number is the number of electrodes that were capable of recruiting any nerve at any intensity tested. Selective electrodes were those that recruited only a single nerve, or multiple nerves within a common innervation pathway, at threshold

Cat	**Threshold Resolution (nC/phase)**			**Max Charge (nC/phase)**	**# Total**	**% Selective**
	L5	**L6**	**L7**			
E	N/A	0.08	0.08	1.23	30	76.7
F	N/A	0.08	0.08	3.28	28	85.7
G	0.08	0.12	0.41	2.46	95	92.6
H	0.25	0.25	0.25	3.28	83	79.5

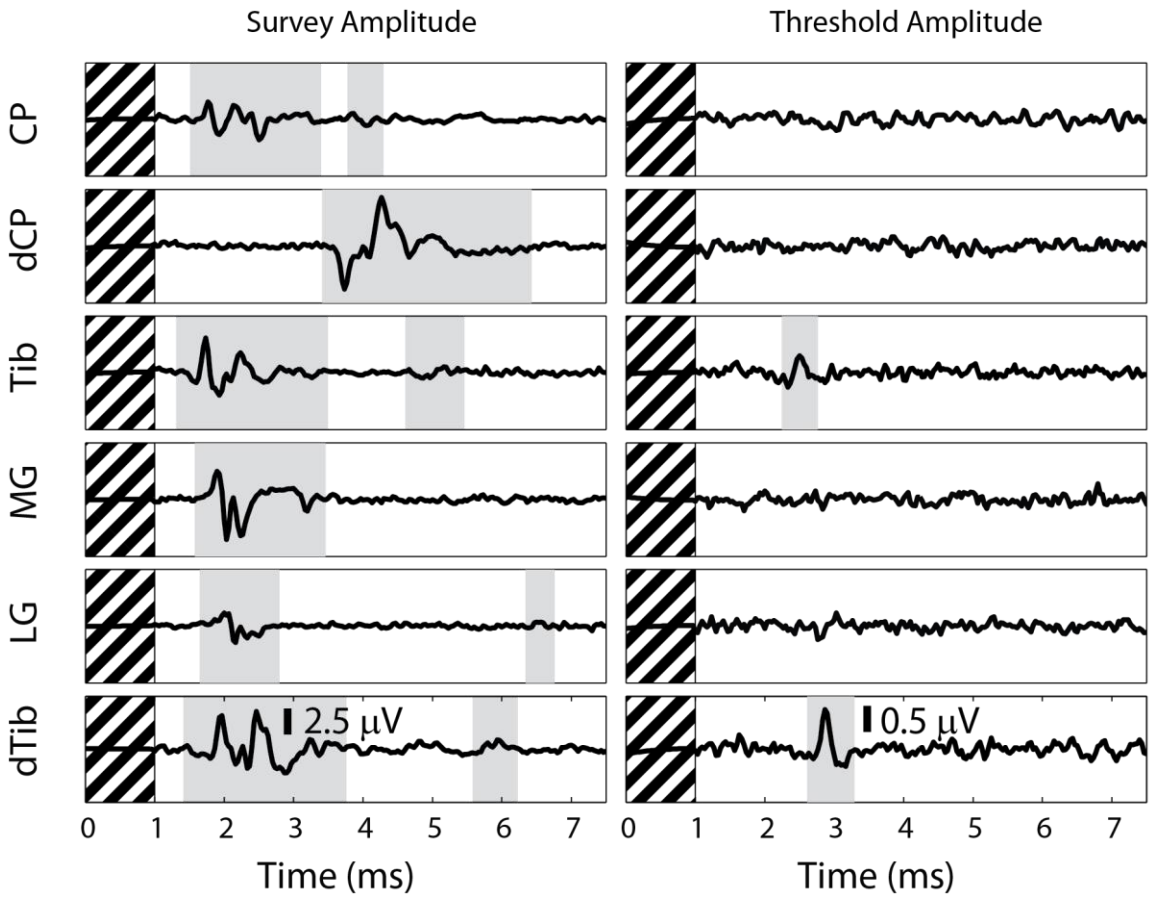

Figure 4.4 Compound action potentials recorded on distal branches of the sciatic nerve at the survey amplitude (left column) and at the lowest amplitude at which any response was detected (right column). Detected responses are highlighted in gray. This example highlights a DRG electrode (same as in Figure 4.3) which, at high amplitude, recruited many of the nerves innervating the ankle and foot but at low amplitude was selective for only the nerves projecting to the plantar surface of the paw. Hashed regions denote 1 ms blanking period.

Over the intensity range used in this example search there was a large change in recruitment. This particular stimulation electrode recruited many distal branches of the sciatic nerve (Figure 4.4) to the exclusion of the femoral nerve branches (not shown). At the survey amplitude, the likely projected fields of this stimulation electrode were the medial and lateral

gastrocnemius, the plantar surface of the foot via the distal portion of the tibial nerve, and the proximal and distal portions of the common peroneal nerve, which innervates the ankle dorsiflexors and the foot dorsum respectively. At threshold, however, this electrode recruited only the proximal and distal portions of the tibial nerve without co-activation of the common peroneal nerve and its branches. It was expected that proximal and distal portions of the same nerve would be co-activated, therefore the stimulation at this intensity was considered selective.

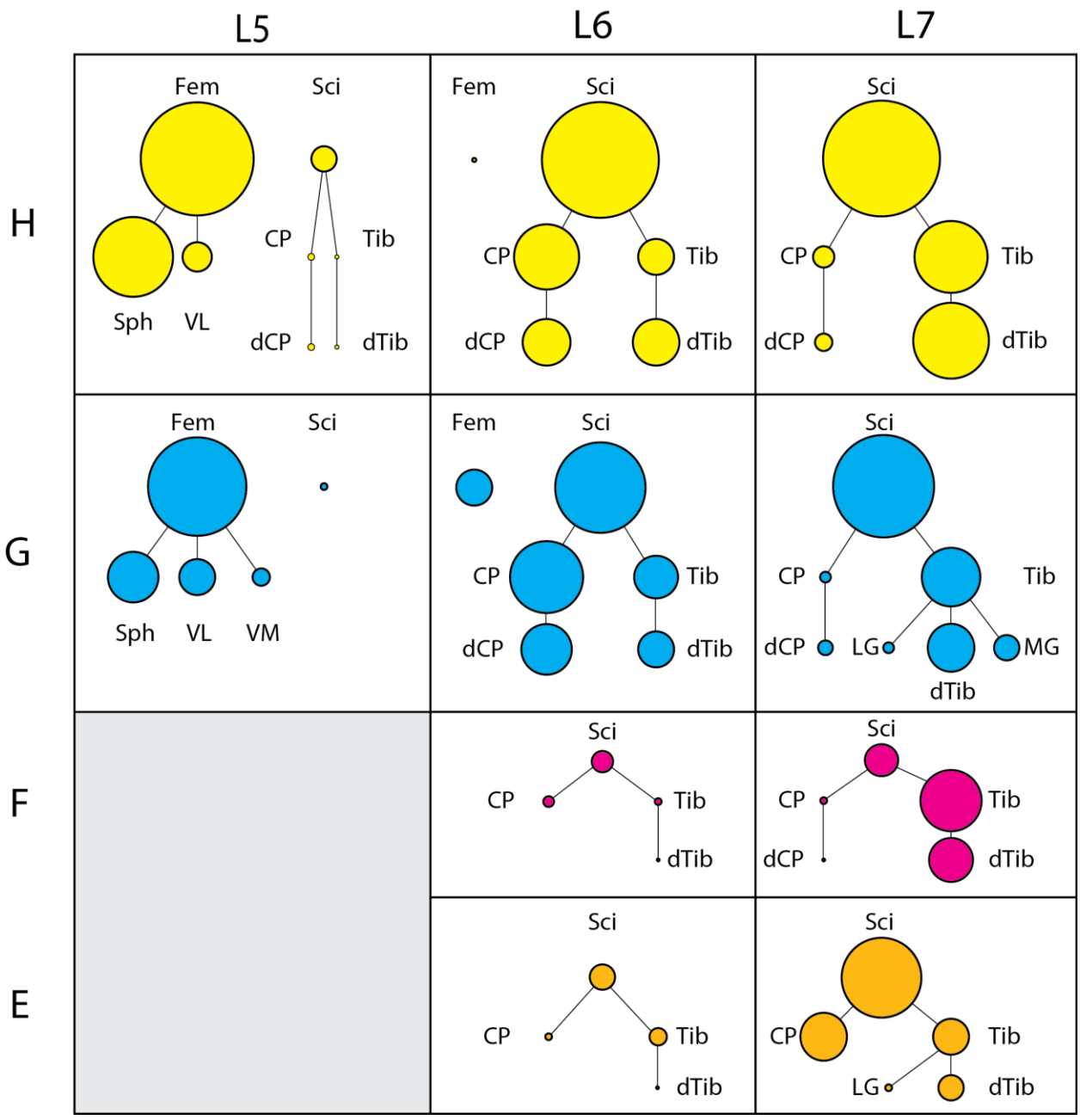

Figure 4.5 Innervation trees in which each circle represents a selectively recruited nerve. Each of the four cats (row) is shown separately and the trees have been split by ganglion (column). The relative size of each circle represents the number of DRG electrodes that selectively recruited that nerve. Lines denote innervation of each nerve.

Threshold responses for each DRG electrode were used to map the corresponding innervation target, providing an overview of the selectivity achieved at each DRG (Figure 4.5). These maps were used to validate results with the known innervation of the hindlimb [128] and to determine coverage of the leg by each electrode array. The diameter of the circle for each distal nerve was set using the number of electrodes able to selectively recruit that nerve at threshold. The local cross correlation (LCC) algorithm, detailed elsewhere [123], was used to detect responses on the femoral and sciatic trunks. From these plots, and in accordance with the physiology, it is clear that L5 stimulation predominantly activates neurons innervating the femoral nerve and its distal branches, L6 stimulation predominantly activates neurons from the plantar and dorsal regions of the foot and the ankle dorsiflexors, and L7 stimulation predominantly activates neurons from the ankle plantarflexors and plantar surface of the foot.

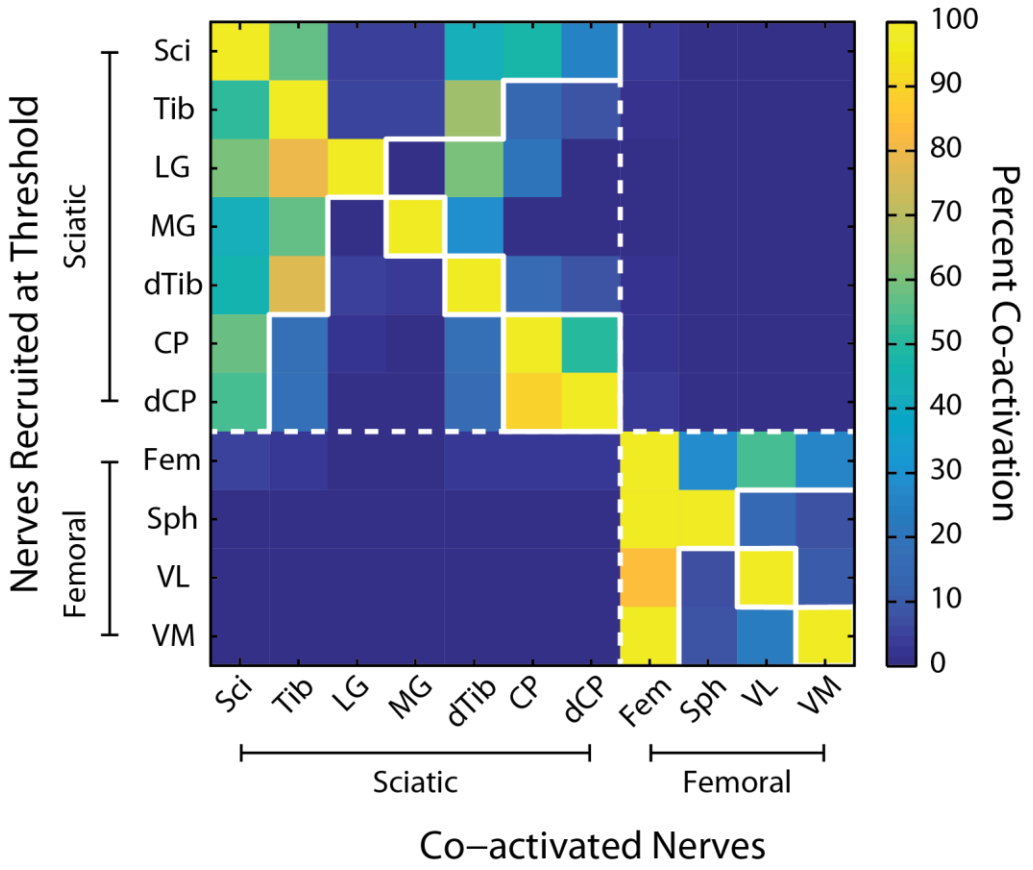

Figure 4.6 Coactivation matrix. Normalized counts of instances in which a nerve was recruited at threshold and identities of the co-activated nerves. Nerves which were never activated at threshold have been omitted from this figure. The dashed lines indicate the division between the sciatic and femoral nerves and their branches. Some nerves, such as the tibial, were expected to be recruited along with other nerves in their innervation pathway, such as the distal tibial and branches to the gastrocnemius muscles. These relationships have been highlighted with white borders. Responses on the sciatic and femoral trunks were detected using the Local Cross Correlation (LCC) algorithm [59,119].

In addition to selectivity at threshold, we also quantified the tendency of multiple nerves to be coactivated at threshold. Given the branching structure of the nerves and our use of multiple cuffs on proximal and distal portions of the same nerve, it was expected that some

nerves would be co-activated frequently. For example, the distal ends of the common peroneal and tibial nerve were expected to be co-activated with their respective proximal trunks. A matrix was produced to visualize co-activation relationships (Figure 4.6) and to help summarize whether stimulation was selective or not. The matrix was produced by counting the number of times for each nerve (rows) that another nerve was also recruited at threshold (columns). The counts in each row were then normalized by dividing by the total number of times that nerve was recruited. The regions of this matrix that represent expected co-activation are highlighted with white borders, and the division between sciatic (upper left) and femoral innervation (lower right) is shown with the dashed white line. There was negligible co-activation of femoral and sciatic branches (upper-right and lower-left quadrants), and within the sciatic and femoral branches co-activation tended to occur between co-located regions. Six nerves were never recruited selectively at threshold: sural, sartorious, biceps femoris, the superficial and deep peroneal nerves, and the cutaneous branch of the sciatic nerve. These non-responding nerves have been omitted from the matrix.

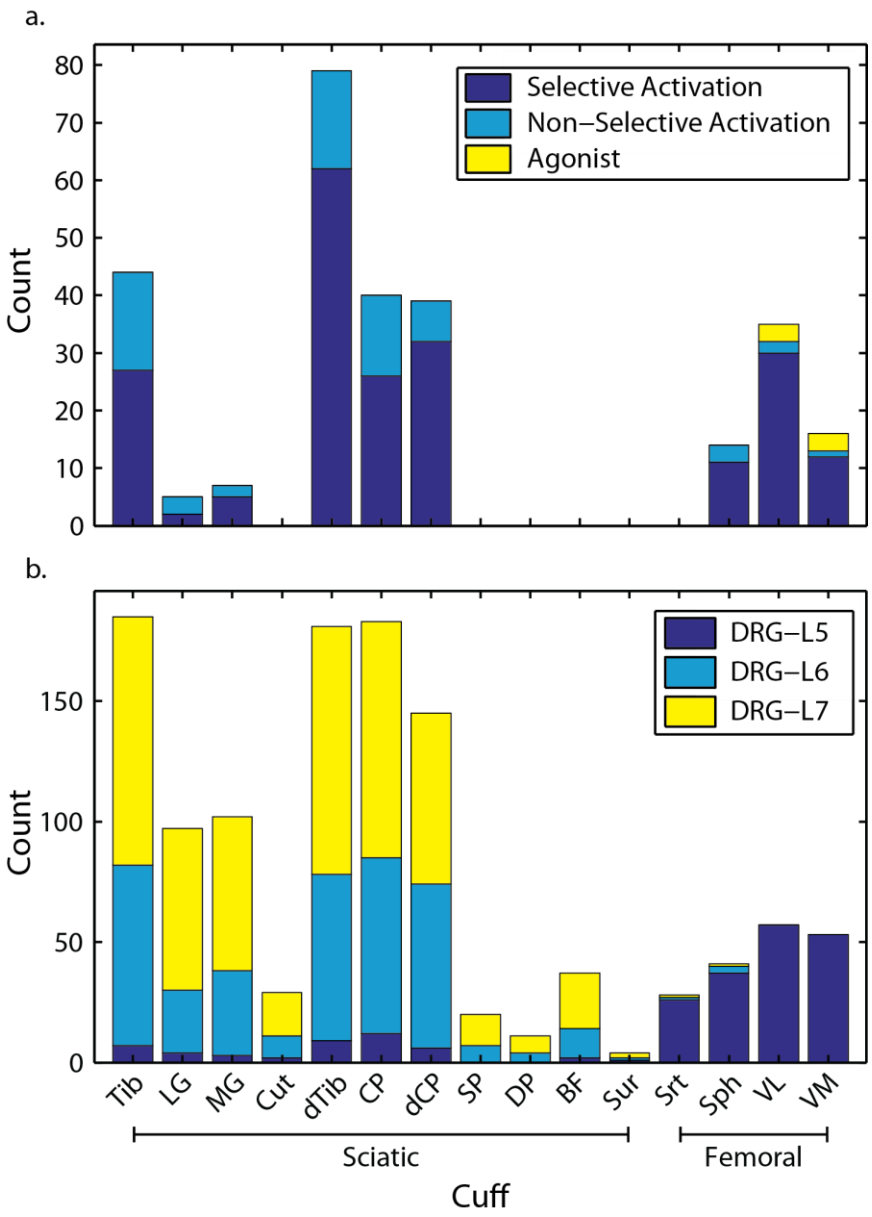

Figure 4.7 Summary of selectively recruited nerves. a.) Counts of selective (dark blue) and non-selective (light blue) instances of nerves recruited at threshold. Nerves in the same innervation path (e.g. tibial and distal tibial) were allowed to be co-activated while still being considered selective, however only activation of the distal most nerve was counted to highlight differential recruitment of proximal branches. Cases where agonists, such as vastus lateralis and medialis, were co-activated are identified separately (yellow) from selective and non-selective counts. b.) Nerves activated during the high amplitude survey, split by stimulation location.

The data from the co-activation matrix were used to summarize the likelihood of selectively recruiting a particular nerve. The instances of selective recruitment of each nerve was tallied using each row of the co-activation matrix (without normalization) and subtracting the number of instances of co-activation with other nerves (Figure 4.7). In the event of co-activation of multiple nerves within the same innervation pathway only recruitment of the most distal nerves was counted. Proximal nerves that were recruited to the exclusion of anything else indicated activity that was likely projecting to uninstrumented distal nerve branches. For example, in the case of the common peroneal nerve any activation of the proximal portion not concomitant with the distal portion suggested possible recruitment of the uninstrumented ankle dorsiflexor nerves (Figure 4.1). For functional groups of agonist muscles, namely the two gasctrocnemius muscles and the vastus lateralis and medialis, co-activation was counted for each nerve branch as well as for each functional group. For the purposes of comparison the raw recruitment numbers at the survey intensity were also summarized. Most of the instrumented nerves could be recruited selectively, and in only a minority of cases were multiple nerves recruited at threshold (Figure 4.7). There was an overall bias for recruiting branches of the sciatic nerve because these populations are highly represented in the L6 and L7 DRG, though there was significant selective recruitment of the femoral nerve via the L5 DRG. Across all experiments 84.7% of electrodes (N=201) achieved selective activation.

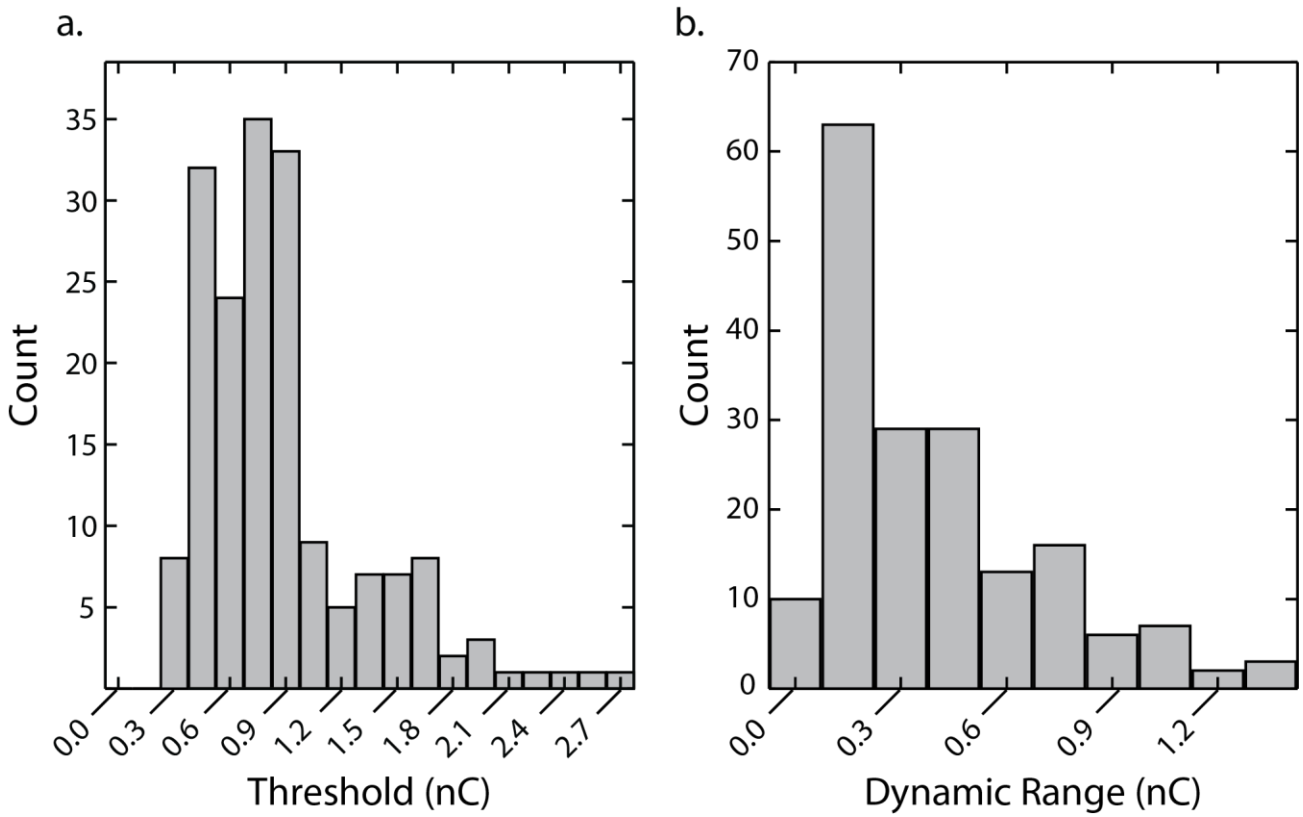

Figure 4.8 Threshold and dynamic range distributions. a.) Distribution of recruitment thresholds, median = 0.68 nC/phase. b.) Distribution of dynamic range, the amount that charge can be increased above threshold before recruitment becomes non-selective, median = 0.36 nC/phase.

The selective range of stimulation intensity was summarized by the recruitment threshold and the dynamic range of stimulation (Figure 4.8). The dynamic range was defined as the difference between the threshold intensity and the intensity that recruited a second nerve non-selectively. As in the other selectivity metrics, recruitment was considered to be selective until a nerve was recruited outside the innervation pathway of the first selectively recruited nerve. Electrodes that did not achieve selective recruitment at threshold and outliers (> 95th quantile)

were not included in this figure. The median threshold was 0.68 nC/phase and the median dynamic range was 0.36 nC/phase.

4.4 DISCUSSION

The goal of this study was to further characterize the recruitment properties of threshold-level microstimulation in the lumbar DRG. First, we wanted to identify which of the major nerve branches in the leg could be accessed with stimulation applied to the L5-L7 DRG. Second, we wanted to know if these nerve branches could be recruited selectively to achieve activation of a localized group of sensory nerve fibers. Finally we wished to characterize the dynamic range of stimulation within which selective recruitment could be achieved.

Overall, 85% of electrodes achieved selective recruitment and those that did not tended to recruit nerves from similar parts of the hindlimb as shown in the co-activation matrix (Figure 4.6). For example, the common peroneal nerve was frequently co-activated with the tibial nerve and not any of the femoral branches. There were also three cases in which the agonists vastus lateralis and vastus medialis were co-activated (Figure 4.7). Recruitment of these two nerves is not strictly selective, but because these muscles are agonists it may not affect sensory feedback. The division of hindlimb innervation between multiple DRG is such that, even without somatotopy within an individual DRG, the likelihood of recruiting two nerves projecting to wholly different parts of the limb was low. Therefore, the functional consequences of non-selective recruitment may be minimal. This is important because the dynamic range of

stimulation was small; increasing stimulus intensity 0.36 nC/phase above threshold recruited at least one other nerve.

Through extensive instrumentation of the nerves of the hindlimb this study provides insight into the distribution of muscular and non-muscular targets of DRG. If DRG microstimulation is to restore proprioceptive feedback it must selectively recruit a diverse population of muscular afferents. In these four cats DRG stimulation selectively recruited all instrumented muscular nerves except for biceps femoris and sartorious. Furthermore, the recruitment of the proximal portion of the common peroneal nerve to the exclusion of the distal may indicate recruitment of ankle dorsiflexor nerves. This pattern of activation supports our hypothesis, based on dermatome mapping [58] and anatomy, that stimulation of three ganglia is sufficient to achieve coverage of the majority of the hindlimb. The L7 DRG alone may be sufficient to provide feedback to trans-tibial amputees based on its ability to selectively recruit both ankle plantar flexors and the distal portions of the common peroneal and tibial nerves (Figure 4.5).

Previous studies have demonstrated the ability of penetrating microelectrodes to recruit medium and large diameter fibers both acutely [61] and chronically [123], but because only the sciatic trunk was instrumented, the specific peripheral targets were unknown. We have also recorded from area 3a, in primary somatosensory cortex, to characterize the recruitment of DRG microstimulation [129] but using this method it was not possible to infer the distal targets of recruited neurons. Conscious reports from human subjects have been crucial in developing an understanding of sensory stimulation, but not all afferents produce conscious percepts when stimulated [42]. Likewise researchers have found the threshold for evoking behavioral responses in cats using muscular afferent stimulation to be higher than that of cutaneous afferent stimulation

[130]. We developed the method of instrumenting many nerves to enable us to make definitive statements about specific peripheral targets, recruitment selectivity, and dynamic range of many electrodes which would not have been possible otherwise.

That neurons can be recruited selectively via microstimulation is a naïve result, however the diversity of afferents and lack of a clear somatotopic organization in the DRG suggested selective recruitment would be challenging. Modeling of perithreshold recruitment of peripheral nerves using microelectrodes [123] predicted that the reverse recruitment principle would no longer hold. In this model, recruitment favored medium diameter fibers over large ones owing to their relative abundance and closer internode spacing. Our strategy for achieving a diverse recruitment profile and selective activation of large fibers is to use a large number of electrodes spread across multiple ganglia. In this study, this strategy appears to have been successful as representatives from all major hindlimb muscle groups were recruited selectively (Figure 4.5), excluding the hamstrings and ankle dorsiflexors, which were under-instrumented.

Although many of the distal branches of the sciatic and femoral nerves were instrumented, it was still a relatively coarse sampling due to our desire to limit muscle dissection. The largest groups of missing muscles were the hamstrings, aside from biceps femoris which was only tested in Cat G. The sciatic nerve branch innervating the hamstrings was generally too proximal to access. The sciatic cuff was always placed distal to this branch, so it was not possible to infer semitendinosus or semimembranosus activity from the sciatic recordings. On the other hand, the co-activation matrix suggests the cuff on the proximal portion of the tibial nerve could be removed from future experiments, as it is so frequently recruited with the distal portion of the nerve. The same was not true of the proximal common peroneal cuff which was

used to infer activation of ankle dorsiflexor nerves when differentially recruited to the exclusion of the distal portion of the nerve.

In this experiment a very strict definition of selectivity was applied: only nerves within a given innervation pathway could be recruited to the exclusion of all others. In practice, co-activation of synergistic nerves may be acceptable for cases in which broad activation is desired (e.g recruiting both the common peroneal and tibial nerves to signal ground contact by recruiting afferents from the entire foot). Co-activation may also be acceptable if there is a large difference in the perceived intensities produced by the recruitment of each neural population, such that feedback is still largely unimodal. We chose not to compare relative ENG response magnitudes, because there is not necessarily a functional relationship between ENG magnitude and intensity of sensory feedback. In contrast, studies of selective muscle recruitment can rely on EMG [122], tendon forces [127] or the induced torque about a joint [42,127] all of which provide unambiguous interpretations of the functional consequences of non-selective recruitment.

The ultimate utility of this model developed here is that it can be used to directly compare the recruitment properties of electrode technologies. Future work will focus on characterizing the selectivity of epineural stimulation. It is anticipated that epineural electrodes will provide an easier path to clinical translation as minimally invasive techniques exist to implant cervical [132] and lumbar [86,87] DRG.

4.5 CONCLUSIONS

Current prosthesis technology provides limited sensory feedback, a shortcoming that could potentially be addressed by DRG microstimulation. We have demonstrated in four animals that this technology is capable of selective recruitment in the acute setting. Using a binary search algorithm, selective recruitment of distal branches of the sciatic and femoral nerves was achieved by nearly 85% of tested electrodes. Median threshold across all selective electrodes was 0.68 nC/phase and the median dynamic range was 0.36 nC/phase. Implanting multiple lumbar ganglia enabled selective recruitment of sensory fibers in most major nerves of the hindlimb, and non-selective recruitment tended to recruit nerves innervating similar regions of the hindlimb. Recruitment at threshold suggested that implanting the L7 ganglion alone may be sufficient for restoring sensation to trans-tibial amputees as it innervates the ankle dorsiflexors and nerves projecting to the foot. These results suggest that DRG microstimulation may be an effective method for restoring sensation to lower limb amputees.

5.0 EPINEURAL STIMULATION OF THE DRG SELECTIVELY RECRUITS A DIVERSE POPULATION OF HINDLIMB AFFERENTS

5.1 ABSTRACT

Microstimulation of the dorsal root ganglion (DRG) with microelectrode arrays has been shown to selectively recruit distal branches of the sciatic and femoral nerves in acute preparations. Penetrating microelectrodes are able to selectively recruit neural populations owing to their physical closeness to neurons, small active areas, and high charge densities. However, the immune response to indwelling penetrating electrodes remains a problem that diminishes long-term viability. Additionally, chronic stimulation at high charge densities may result in tissue damage. Epineural electrodes may provide a compromise between selectivity, long term stability, and safety but they have not been tested in against the challenge of selectively recruiting neurons within the DRG. Many distal branches of the sciatic and femoral nerves were implanted with nerve cuffs in two anesthetized cats to test the ability of epineural electrodes to selectively recruit neurons within the DRG. A binary search was used to generate recruitment thresholds for custom fabricated epineural arrays placed on the L5-S1 DRG. Recruitment on 73.5% of all electrodes (25/34) was found to be selective at threshold, and in one placement each of the four electrodes recruited separate nerves. Both the median threshold (5.81 nC/phase) and dynamic range (0.89 nC/phase) of epineural stimulation were significantly larger (kruskal-wallis,

$p << 0.01$) than their penetrating counterparts. Epineural electrodes were able to recruit a similar population of nerves within each DRG as their penetrating counterparts. These results suggest that despite having high recruitment thresholds epineural electrodes may provide both sufficient selectivity and coverage for use in a sensory neuroprosthesis.

5.2 INTRODUCTION

Penetrating microelectrodes arrays are well suited for selective recruitment of neurons because they are able to focally deliver small amounts of current [84]. This makes them a popular choice for investigations into sensory [65] and motor restoration [127] which require many independent channels of stimulation to approximate the function of the healthy nervous system. Unfortunately, there are a host of safety issues associated with implanting a foreign object in neural tissue. Electrode insertion results in mechanical damage to the tissue followed by an acute immune response [85]. Indwelling electrodes provoke glial scarring which isolates the electrode from the neurons it is attempting to recruit [79] and in the periphery shifts the fiber composition towards smaller fibers [86]. Devices relying on microelectrodes must ensure that they do not exceed the narrow safety window to avoid the electrolysis of water and dissolution of the electrode materials into toxic species [84]. A study that attempted to approximate the operating conditions of a sensory neural prosthesis found that chronic daily stimulation of 7 to 8 hours would result in additional cell death above the chronic immune response [113]. Histology from studies using shorter duration periods of stimulation still found hypo-myelination in stimulation versus control groups [48].

The safety concerns associated with indwelling microelectrode arrays have restricted their use to only a small number of clinical studies. Penetrating arrays have only been implanted in the peripheral nerves of humans in a few separate studies in which they were used to signal grip force [133] and a variety of cutaneous sensations [50]. In the central nervous system custom fabricated 'Hat-Pin' style electrodes were implanted in the visual cortex of a blind subject where they were able to evoke phosphenes [134].

Microstimulation of the dorsal root ganglion (DRG) has been shown to selectively recruit distal branches of the sciatic and femoral nerves in acute preparations **(**Chapter 4**)**. A neuroprosthesis based on those methods would need to contend with all the issues listed above. An additional consideration, particular to implanting devices within the DRG, is the risk of inducing neuropathic pain. Unlike in the peripheral nerve, even minor DRG compression can lead to chronic pain [135]. It is unknown whether implanting penetrating electrodes arrays in the DRG would be painful, however the arrays used in previous studies [59,119,125] require high velocity insertion which causes at least short term compression. Spontaneous firing of neurons, which can potentially be attributed to both acute and chronic compression of the DRG [136], has been observed in acute recordings using electrode arrays [124]. However, despite the potential for neuropathic pain, chronically implanted animals tend to recover quickly and exhibit normal behavior post-implant.

One method of overcoming these disadvantages is to use non-penetrating epineural electrodes. Non-penetrating electrodes have been favored for clinical translation due to their overall biocompatibility (e.g. vagal nerve stimulators [87], phrenic pacers [88], bladder control [89]). Epineural electrodes can be designed to conform to neural tissue to minimize the gap between neurons and the active region. Epineural electrodes may be amenable for use in DRG

based sensory neuroprosthesis. Existing minimally invasive surgical techniques for accessing the spinal cord [90], and specifically for implanting DRG with epinural electrodes for pain management [91], can potentially be adapted for implanting epineural arrays on the DRG. Clinically approved epineural stimulation leads, such as those used for sacral root [89], may be amenable to use in sensory feedback easing the clinical translation process.

In this study, we report on the use of custom fabricated epineural electrodes to selectively recruit neurons from within the lumbar and sacral DRG. This work builds directly on the methods introduced in Chapter 4**,** which also serves as a direct comparison as these two studies were performed in the same animals. As epineural electrodes don't damage tissue they were implanted multiple times on each DRG to maximize the amount of recruitment data that could be collected. Ease of placement enabled testing of stimulation of the first sacral ganglia which we have not typically investigated using penetrating arrays.

5.3 METHODS

Acute experiments were performed in two anesthetized male cats (G-H). All experimental procedures were performed under the approval of the University of Pittsburgh IACUC.

5.3.1 Electrode Implantation Procedures

Isoflurane (1-2%) was used to maintain the animals at a surgical anesthetic plane throughout the experiment and vitals signs were monitored continuously. Distal nerve branches

(Figure 5.1) were instrumented with two-contact nerve cuffs, which were either custom made or purchased (Microprobes, Gaithersburg, MD). Both types of electrodes were made from split silicone tubing with circumferential fine-wire stainless steel electrodes with an interelectrode spacing of 3 or 4 mm. The nerve cuff inner diameters ranged from 1 mm to 3 mm depending on the size of the targeted nerve. The sciatic and femoral nerves were instrumented with 5-pole nerve cuffs (Ardiem Medical, Indiana, PA), which had an interelectrode spacing of 4 mm. Proximal, center, and distal contacts were shorted together and were used as a reference in a virtual tripole configuration when recording from the second and fourth contacts within the cuff [14] .

Where possible, nerves projecting to members of each major muscle group innervated by the sciatic and femoral trunks were instrumented. The sciatic branches innervating the hamstrings were often too proximal to instrument safely, although a cuff was implanted around the nerve innervating biceps femoris in cat G. It was not possible to instrument the branch of the common peroneal nerve innervating ankle dorsiflexors without reflecting the biceps femoris tendon, however the common peroneal nerve was always instrumented proximal and distal to this important branch point. Nerve identities were determined using known anatomical landmarks and verified by stimulation using a voltage-controlled stimulator (Grass, Warwick, RI) and finding coarse motor thresholds. Sensory nerves, such as the sural and the sciatic cutaneous branch, were tested to the maximum stimulation intensity (20 V) to verify that there were no evoked movements. After nerve cuff implantation, the left L5, L6 and L7 DRG were exposed via laminectomy and the cat was placed in a spinal frame for duration of the experiment. Motor thresholds were measured again after transfer to the frame to verify that the cuffs still made adequate contact and that the instrumented nerves were still intact. Epineural electrode

arrays were placed on the L5 through S1 DRG. A stainless steel screw in the iliac crest was used as the return for stimulation.

5.3.2 Electrode Design

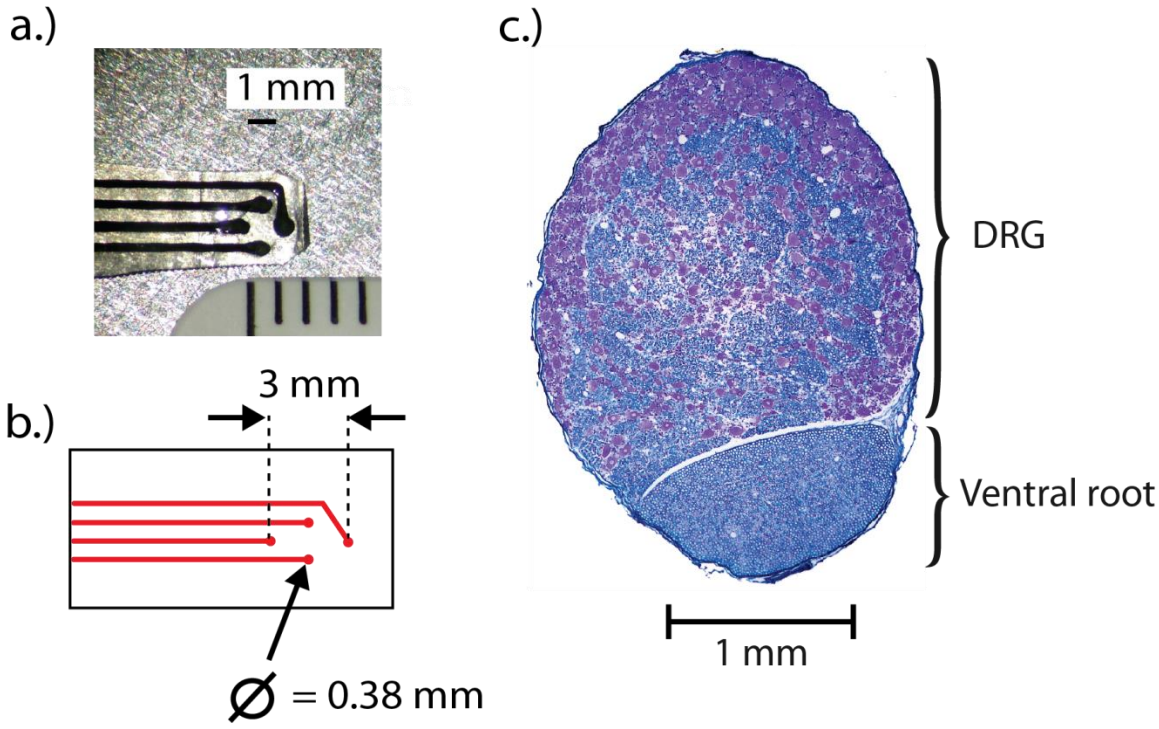

Figure 5.1: Epineural electrode array design**.** a.) Epineural array b.) Array schematic b.) Cross section of an example right L6 DRG. Tissue has been stained using Nissl (violet, cell bodies) and Luxol fast blue (myelin).

The epineural electrode array fabrication process was based on patterned robotic deposition of alternating layers of insulating medical-grade silicone/polyurethane co-polymer and a conductive polymer. The conductive polymer traces and electrode sites were formed by

mixing platinum microparticles with the silicone/polyurethane substrate material. This provided mechanical matching of all the materials throughout the device for high flexibility and flexural durability. The flexibility of these electrodes allowed for conformation to the surface of neural tissue. The polymer material in the electrodes is similar to those used for pacemaker leads. The diameter of the exposed electrode contact was 380 µm (Figure 5.1).

5.3.3 Experiment Design

The objective of these experiments was to identify the minimum stimulus intensity in the DRG that elicited activity in any of the instrumented nerve cuffs (threshold), and whether or not activity occurred in one or more nerves (selectivity) at threshold. The range of intensities over which recruitment was selective (dynamic range) was also characterized.

Table 5.1 Epineural electrode binary search parameters and selectivity results

Cat	Threshold Resolution (nC/phase)				Max Charge (nC/phase)	# Total	% Selective
	L5	L6	L7	S1			
G	0.08	0.81	0.81	0.81	15.36 - 16.38	12	66.7
H	0.41	0.41	0.41	.41	16.38	22	77.3

Experiment design has been discussed at length in Chapter 4. Briefly, many distal branches of the sciatic and femoral nerves were implanted with bipolar nerve cuffs. An epineural array was placed on a single DRG, L5 through S1, at a time and held in place with

light pressure. A binary search for recruitment threshold was performed over stimulation intensities for each of the four electrodes. Electrodes that only recruited nerves within a single innervation pathway were said to be selective. The threshold accuracy and maximum injected charge parameters are summarized in Table 5.1. Epineural arrays were tested at least twice per spinal level. Following epineural array testing penetrating arrays were implanted in the L5-L7 DRG and the selectivity of each electrode was found (Chapter 4). Testing epineural arrays first prevented tissue damage from impacting recruitment performance.

The detection algorithm used for the penetrating arrays (Chapter 4) was modified to account for movement induced non-monotonicity in the evoked responses. as a function of stimulation intensity. Occasionally, CAPs were evoked at low and high intensities with a single electrode, but not in intervening intensity range. This behavior was unexpected as antidromic propagation should by definition always occur at superthreshold intensities. The failure for superthreshold intensities to evoke a response was attributed to poor fixation of the epineural arrays which were only held in place by light pressure. To account for this behavior responses were first detected at each stimulation intensity using the same algorithm developed for testing the penetrating electrodes. Then, responses were accepted or rejected at each intensity based on whether there was a response on that same nerve within a 250 μs window at the next lower or higher intensity. This gating procedure allowed responses to disappear and then reappear over the tested intensities but also rejected spurious transients that did not fall within reasonable time windows.

5.4 RESULTS

The epineural arrays used in these experiments conformed partially to the curvature of the DRG, but inevitably some electrodes were not in contact with the tissue either due to the stiffness of the material or the geometry of the placement. Electrodes not in contact with the DRG were either not tested at all or did not recruit any nerves during the survey trial. These ineffective electrodes are not counted as part of the total number of electrodes used in the experiments (Table 5.1).

The epineural arrays were not sutured in place to facilitate multiple placements of a single array on multiple ganglia. During the testing of some electrodes there was significant non-monotonicity in the recruited responses which was attributed to movement of the array due to respiration or reflexive movement of the animal during stimulation. Electrodes whose recruitment properties changed dramatically with time were not included in analysis. Restrictions on timing and monotonic behavior were relaxed versus the penetrating electrodes to facilitate post-hoc analysis of the remaining electrodes. Responses were allowed to vanish and reappear between tested amplitudes so long as they met the time window restrictions described in the methods.

Epineural electrode survey trials were performed at significantly higher intensities than those used for the penetrating electrodes (Table 5.1**)**. This was done under the assumption that the distance from the neural tissue and relatively low charge densities of the electrode would require a higher injected charge. Use of high intensity stimulation was enabled by a lack of large reflexive movements, which are frequently evoked during high intensities stimulation with penetrating microelectrodes. The threshold accuracy used for epineural testing was lowered

relative to penetrating electrode testing (i.e. intensity was sampled more coarsely) to compensate for the high starting intensity and to reduce the time spent generating recruitment curves.

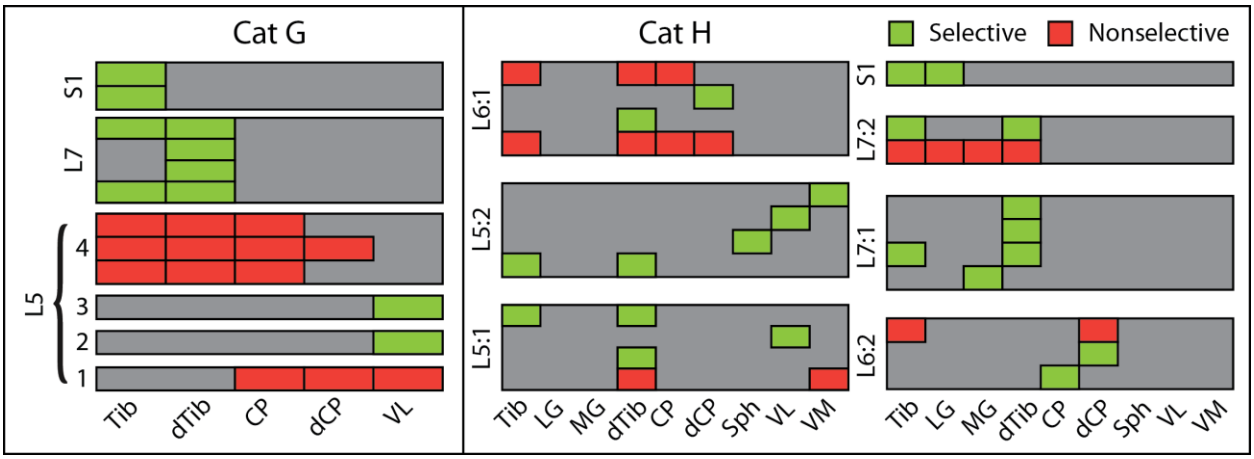

Figure 5.2 Threshold recruitment pattern for each tested electrode. Each sub-axis is a different array placement (colons denote multiple placement per DRG), and each row within an axis is an electrode. Each column is a distal nerve and colored squares denote a nerve was recruited at threshold by a particular electrode. Nerves that were never recruited and placements that did not recruit any nerves have been omitted for clarity. Nerves in the same innervation path, such as Tib and LG, could be coactivated while still being considered selective. Electrodes which were selective at threshold have been highlighted in green, electrode which were not are red

Most of the array placements had multiple electrodes that selectively recruited nerves at threshold (Figure 5.2). Some placements (e.g. Cat H L5:2) had multiple electrodes all of which selectively recruited a different subpopulation of neurons. Other placements (e.g. Cat G L5:4) had multiple non-selective electrodes that recruited the same nerves. Recruitment from stimulating the S1 DRG is likely deceptively selective as most of its innervation (i.e. pudendal, caudal cutaneous, and rectal nerves) were not instrumented in these experiments. Overall

stimulation was selective on 73.5% (N=25) of tested electrodes, across 14 placements in the two cats (total count = 34)(Table 5.1).

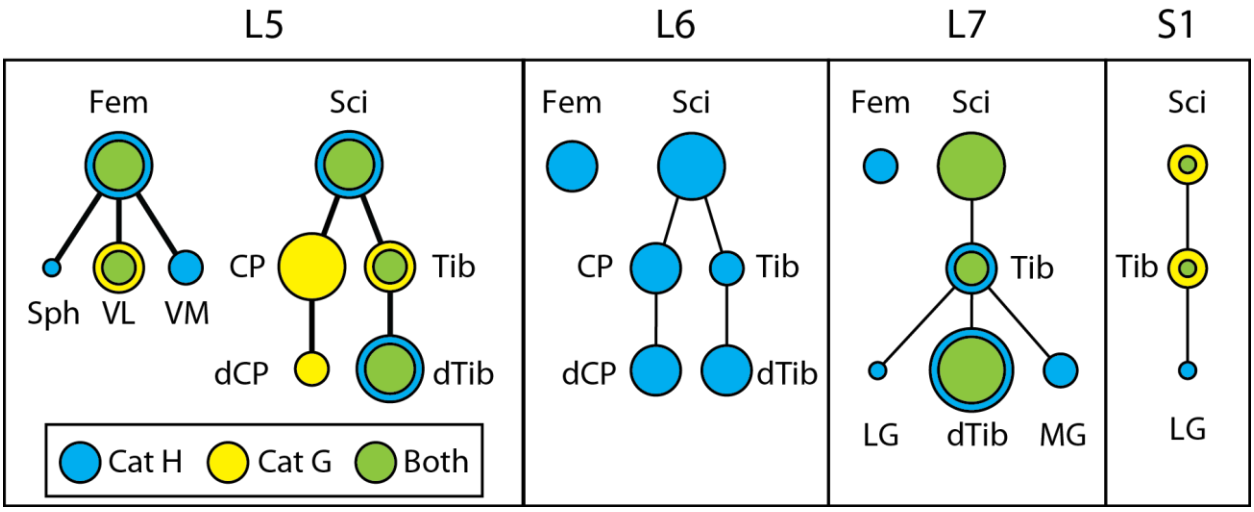

Figure 5.3 Innervation trees in which each circle represents a recruited nerve. Each cat is shown using a separate color, except where overlap occurs. The trees have been split by ganglion (column). The relative diameter of each circle represents the number of DRG electrodes that selectively recruited that nerve (max = 4). Lines denote innervation of each nerve. Cat G did not have any data for the L6 DRG.

The overall pattern of recruitment between the penetrating and epineural electrodes is in good agreement within and across the experiments (Figure 5.3). Stimulation on L5 recruited distal branches of both the femoral and sciatic nerves, L6 recruitment was split between the common peroneal and tibial nerves and L7 stimulation favored the tibial nerve and ankle plantar flexors. Both the median threshold (5.81 nC/phase) and dynamic range (0.89 nC/phase) of epineural stimulation were significantly different (kruskal-wallis, $p << 0.01$) than their penetrating counterparts (0.68 nC/phase and 0.30 nC/phase respectively) (Figure 5.4).

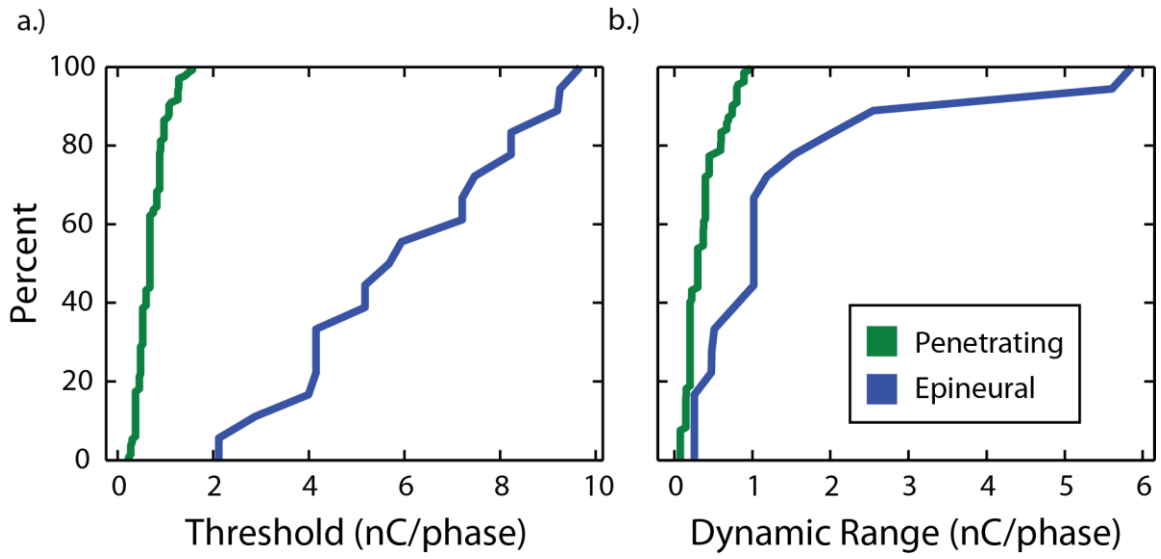

Figure 5.4 Comparison of threshold and dynamic range between electrode types. a.) Threshold cumulative distribution function for penetrating (green) and epineural (blue) electrodes b.) Dynamic range cumulative distribution function. The differences between threshold and dynamic range medians were significantly different (kruskal-wallis $p << 0.01$)

5.5 DISCUSSION

The goal of this study was to determine whether epineural stimulation of the DRG could selectively recruit distal branches of the sciatic and femoral nerves. We also wanted to identify which nerves could be recruited at each spinal segment to create a functional map. Finally, we wished to compare performance of epineural electrodes, as defined by thresholds, dynamic range, and electrode independence, with penetrating electrodes.

A major finding of this study was that the majority of epineural electrodes tested (73.5%) were capable of selective recruitment. This degree of selectivity is not much lower than that

achieved using penetrating electrodes (84.7%). Indeed epineural stimulation in cat G was on par with stimulation in cats E and H using penetrating electrodes, both of which had fewer instrumented nerves and thus should appear to be more selective as a result. This is encouraging given the heterogeneous afferent population and distribution within the DRG and the diffuse nature of epineural stimulation which caused us to anticipate less selective recruitment.

Recruitment thresholds were higher for epineural than penetrating electrodes as expected due to the much lower charge density and separation between electrode and neurons. However, it was not anticipated that the dynamic range would be higher. The dynamic range granularity is determined by threshold accuracy, which was coarser for testing the epineural electrodes. It will be necessary to increase the threshold accuracy in subsequent testing to perform a more direct comparison of dynamic range. If the dynamic range of epineural stimulation is still higher than that of penetrating stimulation after parameter adjustments this will represent another distinct benefit of the technology. A higher dynamic range will add resilience to electrode migration; increasing stimulation intensity may still selectively recruit the same neural population on electrodes with a high dynamic range. Less sensitivity to stimulation intensity, i.e. high dynamic range, means that parameterizing stimulation is easier and potentially less time can be spent in search if the completion criteria is not absolute threshold but only selectivity.

One shortcoming of the large electrode contacts on the epineural arrays is the potential for multiple electrodes to recruit redundant neural populations. Each electrode on an array ideally recruits only a separate population of neurons to provide multiple channels of feedback. An example of this was Cat H placement L5:2 in which each electrode recruited a different nerve. Waveform shape alone is not sufficient to disentangle whether multiple electrodes that elicited responses on the same nerves (e.g. Cat G L7) were recruiting the same neurons.

Electrode independence can be determined experimentally using a masking paradigm [137]. The masking paradigm relies on the fact that neurons recruited by one electrode are unable to be recruited by a second when stimulation delay periods are small. Such a test is necessary to determine what interelectrode distance, channel counts, and active area yields the highest degree of recruitment independence between channels.

Successful array placement and fixation determined the success of stimulation. Each DRG has a several millimeter radius (Figure 5.1) and the arrays were unable to cover the entire structure due to its curvature. Most placements only had two or three electrodes that could be confirmed visually as being in contact with the tissue, although five of the 14 placements did have all four electrodes capable of recruiting nerves. Poor fixation resulted in array movements during some trials which resulted in data being discarded. Problems related to fixation will be resolved by adding tabs to the arrays for fixation to the spinal cord dura and a flap to provide closure about the DRG and ventral root.

Maximizing the utility of epineural electrodes will likely require pursuing bipolar stimulation and more complex current steering techniques to achieve more focal recruitment. Current steering techniques to target particular fascicles using cuff electrodes has been investigated for decades both through computer modelling [45,134] and in animal studies [139]. The treatment of neuropathic pain has also benefited significantly from multipolar stimulation which has allowed the steering of the evoked paresthesia without physical movement of the electrode [81]. The development of the instrumentation model discussed in Chapter 4, combined with optimization techniques to automate the parameterization of multiple stimulation electrodes, will enable the development of future stimulation paradigms.

This study was motivated by the desire to transition from basic research that demonstrates chronic recruitment of medium and large diameter sensory fibers through DRG stimulation [123] to clinical studies where penetrating electrodes are currently unsuited due to the safety concerns related to chronic stimulation [113]. Epineural electrodes represent a compromise between selectivity, safety and stability and are the basis of many successful deployed neuromodulation devices [83,84,85]. In the context of DRG stimulation non-penetrating electrodes may also reduce the risk of neuropathic pain secondary to compression as they can be implanted using minimally invasive techniques [86,87] and don't require high velocity insertion [140]. However even epineural electrodes can damage tissue with excessive stimulation [141] and so care must be taken to monitor the stimulation intensity. Fortunately the threshold intensities of this experiment are much lower than the values found to be damaging [141].

5.6 CONCLUSION

Previous investigations of DRG stimulation have demonstrated its potential as the basis for a somatosensory neuroprosthesis, however the reliance on penetrating electrodes created a barrier to clinical translation. It was anticipated that epineural electrodes, due to their relatively large exposed area and distance from neural tissues, would not approach the recruitment selectivity of penetrating electrodes. These experiments have demonstrated that it is possible to use epineural arrays to selectively recruit distal branches of the sciatic and femoral nerves. Epineural stimulation was selective on 73.5% of electrodes (N=24) across four ganglia in two cats.

Recruitment thresholds for epineural stimulation (median = 5.81 nC/phase) were significantly higher than for penetrating electrodes (kruskal-wallis $p << 0.01$) as was the dynamic range (median = 0.89 nC/phase). The nerves recruited by stimulating a DRG at a particular spinal segment were similar for both epineural and penetrating electrodes. An example of recruiting four separate nerves using a single epineural array suggested that it may be possible to increase the number of contacts and/or increase the electrode pitch in future revisions of the arrays. In conclusion, epineural stimulation appears to be a viable path forward for clinical translation of DRG based neuroprostheses.

6.0 SUMMARY OF RESULTS AND FUTURE WORK

This body of work sought to determine whether DRG PAMS could serve as the basis for a SSNI through model development and the assessment of its stability, selectivity, and safety. There remains a significant amount of work to translate the technique into a therapeutic device, but progress was made towards validating the efficacy DRG PAMS. What follows is a summary of relevant results, discussion and suggestions for future work.

6.1 CORTICAL RECORDING ASSAY

Microstimulation in the L6 and L7 DRG elicited discriminable percepts at a variety of intensities. The cortical responses evoked by stimulation on individual electrodes were analyzed by training naïve bayes classifiers to discriminate between stimulation and baseline epochs as well as between stimulation on separate electrodes. There were several major findings presented in this work, the first of which was that recordings from primary somatosensory cortex could be used to detect stimulation and to discriminate between stimulation locations. Second, we found interactions between stimulation pulse rate, intensity, and location that significantly affected the evoked cortical response. Larger regions of cortex could be recruited either by increasing stimulation intensity and recruiting more afferents, or by increasing pulse rate and relying on

downstream temporal summation. Finally, a first attempt was made at describing the effect that stimulation on two electrodes had on recruitment.

At the time, establishing an assay based on recordings from somatosensory cortex was viewed as a critical step in the development of DRG PAMS. It was thought that behavioral paradigms, a traditional method for investigating proprioception, lacked sufficient sensitivity. Cortical recordings were pursued as an alternative to decerebrate models, which have dominated the study of proprioceptive feedback, and as an objective means of comparing complex limb state encoding models. It was expected that cortical recordings would provide direct access to subconscious proprioceptive feedback. Additionally, given the vast stimulation parameter space we had hoped that cortical recordings would facilitate high throughput testing of encoding models.

Interactions between pulse rate and intensity suggested that for simple stimulation trains the parameter space may be smaller than initially anticipated. For example, both intensity and pulse rate could be increased on a particular stimulation channel to produce supra-threshold cortical recruitment. However, responses evoked by nearby stimulation electrodes at high intensities tended to recruit similar patterns of cortical activity. The overlap between recruited cortical populations suggested that scaling the number of stimulation electrodes and pulse rate, rather than intensity, would maximize the effectiveness of stimulation without sacrificing selectivity. Only a cursory analysis was performed on multi-electrode stimulation, but 5.5% of the tested stimulation channel pairs were found evoke a more vigorous response than that driven by either individual electrode.

Unfortunately, early success using the cortical recording assay was difficult to reproduce. The intent was to evaluate the ability of PAMS to deliver meaningful proprioceptive information

to the central nervous system using cortical activity as an assay. Cortical responses to stimulation habituated within several hundred milliseconds. The surgical and instrumentation procedures required for these experiments strained personnel before data collection even began resulting in mistakes in collecting data. Incorrect anesthesia selection and titration abolished cortical activity [38,39] rendering an otherwise successful implant useless. Chronic implantation of both DRG and cortical arrays was pursued, but unfortunately, the ability to record neurons in the DRG degraded rapidly leaving nothing with which to inform stimulation paradigms.

Despite difficulties, the cortical assay remains a compelling method for investigating artificial proprioceptive feedback [101]. A single well executed acute experiment could yield more data in a shorter time period than chronic testing which is limited to only several hours a week. Unpublished observations of high quality post-closure cortical recordings following chronic implant surgeries suggest that some problems with the acute procedures could be mitigated by closing the craniotomy.

The threshold search methods developed in Chapter 4 should be leveraged to rapidly characterize the cortical responses to stimulation. First, recruitment thresholds for both cortical and primary afferents should be determined. Physiologically based encoding models are only useful to the extent that the appropriate afferents can be recruited selectively, which is likely to occur at perithreshold intensities. Electrodes which are not capable of selective recruitment should be ignored as this is an unnecessary confounding factor. The binary search experimental control framework, which in essence is feedback control of stimulation, should be extended to support optimization techniques. Rather than rely on recordings of afferents to generate models, the stimuli on each electrode could be chosen from a predetermined set of afferent models in a manner that maximizes cortical response probability.

A separate study must be undertaken to understand why cortical responses to stimulation tended to adapt so rapidly. Stimulation on electrode pairs suggested that habituation to stimulation could be overcome simply by using additional electrodes. Non-linear growth in recruitment resulting from stimulation on neighboring electrodes [142] is likely to be a significant concern that must be addressed as part of this work.

6.2 ASSESSING RECRUITMENT STABILITY

Chronic recruitment thresholds were initially low and increased over time. Additionally the number of electrodes with thresholds less than or equal to 15 μA decreased over time. Approximately 12% of tested electrodes continued to elicit responses at 15 μA up to 26 weeks after implantation. Higher stimulation intensities were tested in one cat at 23 weeks post-implantation yielding responses on over 20 additional electrodes. Within the first six weeks after implantation, approximately equal numbers of electrodes elicited only responses at threshold, but the relative proportion of Group II/Aβ responses decreased over time.

The failure of experiments due to infection or lead wire breakage is not a reflection on the stability of DRG PAMS, so much as it is on contemporary electrode technology and lab surgical ability. An obvious solution to both of these problems would be to use fully implantable systems such that the wound can be closed to avoid infection and prevent damage to delicate lead wires. Testing an implantable system is a necessary step to ultimately bring a DRG PAMS based device to market, but outside the purview of this dissertation. However, cats A and C both provided insight into the performance of an implantable system, as these experiments were not terminated

prematurely. The implants in these animals were still effective after 20 weeks, and in cat C higher intensity testing, up to 30 μA, increased the number of effective stimulation electrodes from 2 to 23. Unfortunately, the stimulation intensities used for this work were chosen *a prioi* which was a limitation of the experiments.

Thresholds are currently being calculated more accurately and over a greater intensity range using the binary search methodology developed in Chapter 4. Response latency is also being calculated more accurately using a sliding RMS window. The experimental focus has changed from characterizing stability to developing a behavioral assay for DRG PAMS, but the functional lifetime of each implant is still determined as a result. Stability testing has evolved into an essential, if simple, system identification procedure. A logical next step is to compare the results presented in Chapter 3 against the P_{15} values found using the new binary search method.

Evaluating the stability of epineural stimulation is an important next step in the development of a chronic DRG SSNI. It is expected that once surgical techniques have been developed, epineural arrays will be more stable than their penetrating counterparts due to the greatly reduced immune response. There is still internal lab debate as to longevity of specific types of penetrating MEAs and stability testing could be used to determine which type lasts the longest. That having been said this is a tertiary concern that should not interfere with other ongoing investigations, unless funding is acquired specifically for more testing.

6.3 ASSESSING RECRUITMENT SELECTIVITY

We have demonstrated in four animals that DRG PAMS is capable of selective recruitment of distal nerve branches in an acute procedure. Using a binary search algorithm, selective recruitment of distal nerve branches was achieved by nearly 85% of tested electrodes. Implanting multiple lumbar ganglia enabled selective recruitment of sensory fibers in most major nerves of the hindlimb. Non-selective recruitment tended to recruit nerves innervating adjacent regions of the hindlimb rather than distant targets. These results suggest that despite the heterogeneous composition of the DRG, selective recruitment is possible using optimization techniques.

Recruitment patterns at threshold suggested that implanting the L7 DRG alone may be sufficient for restoring sensation to a feline trans-tibial amputee. Microstimulation of the L7 DRG tended to recruit ankle dorsiflexors and distal portions of the common peroneal and tibial nerves both of which innervate the foot. The resulting innervation patterns provided compelling evidence that DRG PAMS may be an effective method for restoring sensation. In humans, the lower leg and foot are innervated by the L4-S1 DRG, which may preclude a single DRG from providing sufficient coverage for all but the most distal amputations. However, the division of limb innervation across more ganglia should enable selective recruitment because an individual ganglion innervates a smaller region of the limb. Non-selective recruitment will be less problematic because the potential limb region over which neurons can be co-activated is smaller.

A major accomplishment of this dissertation was successfully designing and implementing a new animal model for assessing the performance of DRG PAMS. Previous investigations relied on either recordings from the sciatic nerve or somatosensory cortex to

provide very coarse information about the modality and distal targets of recruited neurons. Instrumenting a large number of nerve branches and producing recruitment curves is inherently a brute force approach, but as lab surgical and engineering skills improved the duration of the experiments decreased and the amount of data collected increased. Improvements can be made to the algorithm to further reduce run time, notably the decision to find the recruitment threshold for every nerve and stimulation electrode is likely excessive. Performing a search for the nerves recruited at threshold and then finding the first intensity resulting in non-selective recruitment is sufficient to describe the dynamic range and innervation of recruited neurons.

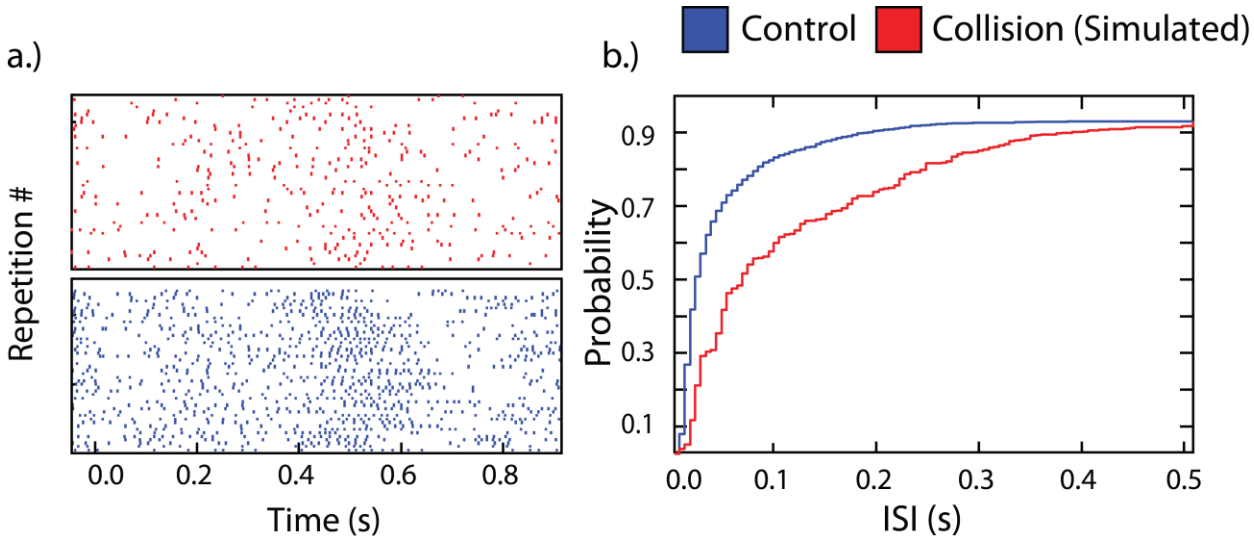

Figure 6.1 Collision block simulation. Recordings from a neuron sensitive to ramp and hold movements (blue) were collided with DRG stimulation on the same channel to produce a reduced firing rate (red). a.) Pre and post collision rasters b.) Pre and post collision ISI cumulative distribution.

Statements about the innervation of recruited neurons can be corroborated by collision block [143]. The specific identity of a recruited afferent can be determined by stimulating and abolishing action potentials recorded on that same electrode. Successful collision is measured by a shift in the ISI CDF towards longer intervals (Figure 6.1) during stimulation. The peripheral target and modality of mechanical stimulation that excited the recorded afferent should be in agreement with the distal nerves that were recruited by stimulation on that electrode. That is, if passive ankle dorsiflexion results in muscle spindle activity on an electrode, stimulation should recruit ankle plantarflexor nerves. This procedure relies on DRG electrodes driven by headstages that can rapidly switch between stimulation and recording, and therefore can stimulate and monitor the outcome on the same electrode. Combining collision block with instrumentation of distal nerve branches will enable experimenters to state with confidence the identity of recruited neurons.

Afferents can also be "marked" using prolonged high frequency stimulation [41] allowing their subsequent identification during passive mechanical movement. Neurons that have been marked by stimulation fire ectopically when driven naturally. Experimenters thus can unambiguously identify which neurons have been marked by performing a careful unit identification of all the neurons that can be recorded by the stimulation electrode. The marked neurons should innervate portions of the limb recruited by stimulation on that same electrode.

Measurement of recruitment selectivity should transition to a routine system identification procedure like chronic threshold monitoring. Stimulus encoding models that attempt to reproduce the firing rate profiles of muscle spindles and tendon organs [53,54,139] are only valid when applied to those specific afferents. For these models to be useful experimenters must know the identities of the neurons recruited by each electrode. The marking and collision

block procedures should be validated during a selectivity experiment so that they can be used during chronic testing. If the precise identities of neurons can be identified in chronic experiments this will greatly aid our understanding of results from future behavioral experiments.

6.4 EPINEURAL STIMULATION OF THE DRG

Epineural electrodes implanted on the L5-S1 DRG were able to selectively recruit neurons projecting to a diverse set of peripheral targets in the hindlimb. The recruitment pattern generated by stimulating each DRG was qualitatively similar to that of penetrating counterparts, and the overall percentage of selective electrodes was only slightly lower. These results were achieved despite difficulties maintaining adequate fixation of the epineural arrays to the DRG. Revisions to array geometry will improve fixation and make placement easier thus increasing the amount of data that can be collected. Some array placements produced selective recruitment of four wholly distinct neural populations which suggested that these arrays are not yet limited by current spread, and that electrode count can be increased.

If DRG PAMS is to be developed into a useful clinical tool, it must be safe in addition to being efficacious. Inserting penetrating electrodes into neural tissue is an inherently damaging process. Neural interfaces that rely upon penetrating MEAs may require future developments in electrode technology that minimize cell death before they are clinically viable. However, if DRG PAMS can achieve performance goals using non-penetrating epineural electrodes, then clinical translation is likely to be much easier. Fortunately, the coverage and selectivity of DRG PAMS

using epineural arrays approached that of using penetrating MEAs implanted in the same animals. The relative performance of epineural arrays in the DRG suggests that they will be amenable for use in a SSNI.

Future revisions of the epineural arrays should include higher electrode counts and reduced active areas to potentially recruit a more independent and diverse neural populations. An important next step is establishing whether electrodes that elicit activity in the same nerves are doing so with independent populations of neurons. This will determine the useful lower limit in electrode pitch, although fabricating arrays with an even smaller pitch may allow enhanced stability. Oversampling the DRG with low pitch arrays can mitigate the effects of array migration by providing multiple electrodes that are able to recruit the same neurons. In the event of electrode migration these extra electrodes can potentially restore recruitment of the previously recruited neurons.

Developing models of current steering may be a necessary next step towards producing a viable neuroprosthesis using epineural electrodes. Current steering can provide both enhanced selectivity and recruitment of different neural populations via "virtual" channels [139]. Steering is another technique to contend with electrode migration, which is a larger risk for epineural electrodes than with self-anchoring penetrating electrodes. Instrumenting many distal nerves provides a means for evaluating the effects of current steering, which in other experiments has been evaluated using correlates of muscle recruitment.

6.5 FINAL THOUGHTS AND CONCLUSIONS

This dissertation chronicles the development of DRG PAMS from the first demonstration of its ability to entrain cortical activity to suggesting a path towards clinical testing. It was, of course, not as straightforward a path as this document might suggest. The complexity and pitfalls of the cortical recording assay stalled development for several years. Eventually, cortical recordings were abandoned and replaced by the instrumentation of many distal nerves which has proven to be significantly more fruitful. Instrumenting many nerves has enabled direct measurement of selectivity and the means to demonstrate the clinical viability of epineural electrodes.

Experimental validation remains one of the largest challenges in investigating artificial proprioceptive feedback. Proprioception defies investigation, requiring the integration of many afferent modalities to create a sense of body. Artificial proprioceptive feedback must be interpretable by the central nervous system so that artificial limbs can operate within the context of the intact body, e.g. to implement the cross-extension reflex. This is in stark contrast to other sensory systems in which rehabilitative intervention is not pursued until sensory loss is complete. By way of example, individuals with unilateral deafness can still hear, therefore a cochlear implant is not a necessity. The need for integrating a SSNI with the intact sensory feedback system may require researchers to develop complex encoding schemes. However, history has shown that simple encoding methods are workable [54], and that function can be improved with even crude feedback. Whatever encoding model is ultimately deemed sufficient, this body of work has shown that DRG PAMS is a viable method for implementing it.

APPENDIX

ANALYSIS OF P_{15}

The contents of this appendix are published in: *Fisher LE, Ayers CA, Ciollaro M, Ventura V, Weber DJ, Gaunt RA (2014) Chronic Recruitment of Primary Afferent Neurons By Microstimulation in the Feline Dorsal Root Ganglia. Journal of Neural Engineering vol. 11, no. 3, p. 036007, Jun. 201*

Below is a detailed description of the statistical analysis performed on P_{15} data to determine effects of factors such as time since implant, animal, DRG (L6 vs. L7), electrode tip size, and stimulated fiber type (CV_{fast} vs. CV_{slow}) on threshold. We found that electrode impedances remained constant over the course of the study, and as such could not account for changes in P_{15}. Therefore, we did not include them in the following models.

Logistic regression models of P_{15}

Let $P_{15}(s, g, t)$ be the probability at time *t* that electrodes with tip size *s* for fibers of type g generate a CAP when stimulated at or below 15 μA, for an implanted array in a particular DRG in a particular cat. We consider $P_{15}(s, g, t)$ separately for each implant because their estimates are visibly different across cats (A, B, C, D) and DRG (L6, L7); see Figure 5. We estimate

$P_{15}(s,g,t)$ using a logistic regression fitted to the observed proportions of electrodes with tip size *s* that activate fibers of type g at time *t*. We start by modeling the logit of $P_{15}(s,g,t)$ according to

$$\text{logit}\big(P_{15}(s,g,t)\big)=\log\left(\frac{P_{15}(s,g,t)}{1-P_{15}(s,g,t)}\right)=\alpha_{s,g}+\beta_{s,g}\times t; \qquad \text{(Model 1)}$$

i.e. we assume that, on the logit scale, the probability of a CAP is linear in time, with different intercepts and different slopes for each of the 4×2 combinations of tip size and fiber type. This is **Model 1**; it only assumes that given a particular cat, implant, electrode tip size, and fiber type, the time course of $P_{15}(s,g,t)$ is a smooth function of time that is linear on the logit scale. **Model 2** is the same as **Model 1**, but with equal slopes, $\beta_{s,g}=\beta$, i.e.

$$\text{logit}\big(P_{15}(s,g,t)\big)=\log\left(\frac{P_{15}(s,g,t)}{1-P_{15}(s,g,t)}\right)=\alpha_{s,g}+\beta\times t; \qquad \text{(Model 2)}$$

and implies that the effect of time is the same for all electrodes on an array. Sequential analysis of variance (ANOVA) tests performed at the 5% significance level revealed that **Model 2** provides a better fit than **Model 1**, from which we conclude that there are no significant interactions between time since implant, and tip size or fiber type.

Next, we investigate if tip size and fiber type have baseline effects on P_{15} values, and if those factors interact. We consider **Model 3**:

$$\text{logit}\big(P_{15}(s,g,t)\big)=\big(\alpha_g+\gamma_s\big)+\beta\times t, \qquad \text{(Model 3)}$$

an extension of **Model 2** that assumes no interactions between tip size and fiber type; i.e. the intercepts $\alpha_{s,g}$ in **Model 2** can be decomposed into additive effects of electrode size, γ_s, and fiber type, α_g. We set $\alpha_1 = 0$ so that parameters are uniquely defined. Sequential ANOVA tests suggest that **Model 3** fits the data on all implants better than **Model 2**.

Finally, **Model 4** specifies that the effect of tip size on P_{15} is proportional to tip size, i.e.

$$\text{logit}\big(P_{15}(s,g,t)\big) = \alpha_g + (\gamma_0 + \gamma_1 \times s/25) + \beta \times t, \qquad \text{(Model 4)}$$

where $\alpha_1 = 0$, α_2 measures the differential effect between CV_{fast} and CV_{slow} fibers, $\gamma_1 \times s/25$ is the linear effect of tip size, and $\beta \times t$ is the linear effect of time. We rescaled the tip size by 25, so that the magnitude of the corresponding coefficient γ_1 is comparable to the other regression coefficients. **Models 3** and **4** are not embedded so we compare them using Akaike Information Criterion (AIC) scores rather than sequential ANOVA tests. **Model 4** provides better fits to the data of all implants, except for the L7 DRG for Cat A, for which **Model 3** has a slightly better AIC score. This difference is because the tip size effect is not linear for that implant. However, we verified that the effect was ordered, i.e. the larger the tip size is, the higher the P_{15} of the electrode.

Results

Table A1 reports the estimated coefficients of **Model 4** for all implants. The P_{15} values predicted by that model are plotted in Figure 3.5 in the main text. **Model 4** is not the best model for the L7 DRG implant for Cat A, but γ_1 nevertheless captures qualitatively the P_{15} increase associated with the increase in the tip size, which facilitates comparisons between cats and implant locations.

Table A1 Estimated coefficients of Model 4 for all implants

	Array Location	α_2 *(SD)*	*p*	γ_1*(SD)*	*p*	β*(SD)*	*p*
Cat A	L6	-1.95 (0.19)	**	0.40 (0.07)	**	-0.10 (0.01)	**
	L7	-1.76 (0.28)	**	0.52 (0.10)	**	0.06 (0.05)	
Cat B	L6	-0.05		0.09		-1.03 (0.11)	**
	L7	0.29		0.19 (0.08)	0.01	-0.45 (0.06)	**
Cat C	L6	-2.59 (0.41)	**	0.10 (0.06)	0.13	-0.14 (0.02)	**
	L7	-1.00 (0.37)	0.006	0.24 (0.13)	0.07	-0.08 (0.03)	0.003
Cat D	L6	0.20		0.13		-1.06 (0.13)	**

We conclude from Table A1 that:

1. With the exception of the time coefficient β for the L7 DRG for Cat A, which is not significantly different from 0 at the 5% significance level, all β's are negative and significant: P_{15} for all electrodes decayed with time. Using two-samples t-tests, we determined that P_{15} decayed significantly faster for the two implants of Cat B, and that Cats A and C had the same rates of decay at L6, and also at L7.
2. For all cats, the estimate of β at L7 is significantly larger than the estimate of β at L6: P_{15} decayed with time more slowly for the electrodes implanted at L7.

3. We detect a fiber type effect in Cats A and C: the estimate of α_2 is negative, which means that P_{15} for all electrodes on these implants are lower for CV_{slow} fibers. We detect no fiber type effects for Cats B and D, possibly because the samples are too small.
4. There is a clear effect of electrode tip size for the implants of Cat A, and a smaller effect for the implants of Cat C, and the L7 DRG of Cat B: the estimate of γ_1 is positive, i.e. the larger the tip size is, the higher the P_{15} is.
5. We fitted a model with common slope and common intercept to the data of Cats B and D. We found that model provided a better fit than **Model 4**: these data have no significant effects of tips size and fiber type.

Model diagnostics and outliers

On particular days, the electrodes on specific implants all failed to produce CAPs. This suggests that local time effects exist across all factor combinations, which do not follow the general time trend of the rest of the data. These outliers may be caused by abnormal week-specific behavior of the electrodes or other unobserved causes. After removing the outliers, all residual diagnostics and goodness of fit measures suggested an adequate fit of the models we considered for the data. However, we found that a model like **Model 4**, but with the linear time effect $\beta \times t$ replaced by a non-parametric smooth function of time, provided a better fit, especially for Cat C. The qualitative conclusions from the parametric and non-parametric models were the same, so we reported the parametric model to ease interpretability.

BIBLIOGRAPHY

[1] K. Ziegler-Graham, E. MacKenzie, P. Ephraim, T. Travison, and R. Brookmeyer, "Estimating the prevalence of limb loss in the United States: 2005 to 2050.," *Arch. Phys. Med. Rehabil.*, vol. 89, no. 3, pp. 422–9, Mar. 2008.

[2] W. C. Miller, M. Speechley, and B. Deathe, "The prevalence and risk factors of falling and fear of falling among lower extremity amputees," *Arch. Phys. Med. Rehabil.*, vol. 82, no. 8, pp. 1031–1037, Aug. 2001.

[3] G. H. Kejlaa, "Consumer concerns and the functional value of prostheses to upper limb amputees.," *Prosthet. Orthot. Int.*, vol. 17, no. 3, pp. 157–63, Dec. 1993.

[4] R. Stein and M. Walley, "Functional comparison of upper extremity amputees using myoelectric and conventional prostheses.," *Arch. Phys. Med. Rehabil.*, vol. 64, no. June, pp. 243–248, 1983.

[5] M. S. Johannes, J. D. Bigelow, J. M. Burck, S. D. Harshbarger, M. V. Kozlowski, and T. Van Doren, "An overview of the developmental process for the modular prosthetic limb," *Johns Hopkins APL Tech. Dig.*, vol. 30, no. 3, pp. 207–216, 2011.

[6] M. Goldfarb, B. E. Lawson, and A. H. Shultz, "Realizing the promise of robotic leg prostheses.," *Sci. Transl. Med.*, vol. 5, no. 210, p. 210ps15, Nov. 2013.

[7] C. Behrend, W. Reizner, J. Marchessault, and W. Hammert, "Update on advances in upper extremity prosthetics.," *J. Hand Surg. Am.*, vol. 36, no. 10, pp. 1711–7, Oct. 2011.

[8] R. K. Aaron, H. M. Herr, D. M. Ciombor, L. R. Hochberg, J. P. Donoghue, C. L. Briant, J. R. Morgan, and M. G. Ehrlich, "Horizons in prosthesis development for the restoration of limb function.," *J. Am. Acad. Orthop. Surg.*, vol. 14, no. 10 Spec No., pp. S198–S204, 2006.

[9] D. S. Childress, "Closed-loop control in prosthetic systems: historical perspective.," *Ann. Biomed. Eng.*, vol. 8, no. 4–6, pp. 293–303, 1980.

[10] E. Biddiss, D. Beaton, and T. Chau, “Consumer design priorities for upper limb prosthetics,” *Disabil. Rehabil. Assist. Technol.*, vol. 2, no. 6, pp. 346–357, Jan. 2007.

[11] T. W. Wright, a D. Hagen, and M. B. Wood, “Prosthetic usage in major upper extremity amputations.,” *J. Hand Surg. Am.*, vol. 20, no. 4, pp. 619–22, Jul. 1995.

[12] J. Marchessault, P. L. McKay, and W. C. Hammert, “Management of upper limb amputations.,” *J. Hand Surg. Am.*, vol. 36, no. 10, pp. 1718–26, Oct. 2011.

[13] B. Rybarczyk, D. L. Nyenhuis, J. J. Nicholas, S. M. Cash, and J. Kaiser, “Body image, perceived social stigma, and the prediction of psychosocial adjustment to leg amputation.,” *Rehabil. Psychol.*, vol. 40, no. 2, pp. 95–110, 1995.

[14] W. C. Miller, A. B. Deathe, M. Speechley, and J. Koval, “The influence of falling, fear of falling, and balance confidence on prosthetic mobility and social activity among individuals with a lower extremity amputation,” *Arch. Phys. Med. Rehabil.*, vol. 82, no. 9, pp. 1238–1244, 2001.

[15] D. M. Ehde, J. M. Czerniecki, D. G. Smith, K. M. Campbell, W. T. Edwards, M. P. Jensen, and L. R. Robinson, “Chronic phantom sensations, phantom pain, residual limb pain, and other regional pain after lower limb amputation,” *Arch. Phys. Med. Rehabil.*, vol. 81, no. 8, pp. 1039–1044, 2000.

[16] R. Gailey, K. Allen, J. Castles, J. Kucharik, and M. Roeder, “Review of secondary physical conditions associated with lower-limb amputation and long-term prosthesis use.,” *J. Rehabil. Res. Dev.*, vol. 45, no. 1, pp. 15–29, 2008.

[17] A. M. Karmarkar, D. M. Collins, T. Wichman, A. Franklin, S. G. Fitzgerald, B. E. Dicianno, P. F. Pasquina, and R. A. Cooper, “Prosthesis and wheelchair use in veterans with lower-limb amputation.,” *J. Rehabil. Res. Dev.*, vol. 46, no. 5, pp. 567–576, 2009.

[18] P. J. Whelan, “Control of locomotion in the decerebrate cat.,” *Prog. Neurobiol.*, vol. 49, no. 5, pp. 481–515, Aug. 1996.

[19] T. Sinkjaer, J. B. Andersen, M. Ladouceur, L. O. Christensen, and J. B. Nielsen, “Major role for sensory feedback in soleus EMG activity in the stance phase of walking in man.,” *J. Physiol.*, vol. 523 Pt 3, no. 2000, pp. 817–827, 2000.

[20] J. M. Donelan and K. Pearson, “Contribution of sensory feedback to ongoing ankle extensor activity during the stance phase of walking,” *Can. J. Physiol. Pharmacol.*, vol. 598, pp. 589–598, 2004.

[21] G. W. Hiebert and K. Pearson, “Contribution of sensory feedback to the generation of extensor activity during walking in the decerebrate Cat.,” *J. Neurophysiol.*, vol. 81, no. 2, pp. 758–770, 1999.

[22] P. J. Whelan, G. W. Hiebert, and K. Pearson, “Stimulation of the group I extensor afferents prolongs the stance phase in walking cats.,” *Exp. Brain Res.*, vol. 103, no. 1, pp. 20–30, Jan. 1995.

[23] J. P. Roll and J. P. Vedel, “Kinaesthetic role of muscle afferents in man, studied by tendon vibration and microneurography.,” *Exp. Brain Res.*, vol. 47, no. 2, pp. 177–190, 1982.

[24] J. Roll, J. Vedel, and E. Ribot, “Alteration of proprioceptive messages induced by tendon vibration in man: a microneurographic study,” *Exp. Brain Res.*, vol. 76, no. 1, pp. 213–222, 1989.

[25] A. Prochazka and M. Gorassini, “Ensemble firing of muscle afferents recorded during normal locomotion in cats.,” *J. Physiol.*, vol. 507 (Pt 1, no. October 1997, pp. 293–304, Feb. 1998.

[26] K. Pearson, “Proprioceptive regulation of locomotion.,” *Curr. Opin. Neurobiol.*, vol. 5, no. 6, pp. 786–91, Dec. 1995.

[27] Y. Lajoie, N. Teasdale, J. D. Cole, M. Burnett, C. Bard, M. Fleury, R. Forget, J. Paillard, and Y. Lamarre, “Gait of a deafferented subject without large myelinated sensory fibers below the neck.,” *Neurology*, vol. 47, no. 1, pp. 109–15, Jul. 1996.

[28] R. W. M. van Deursen and G. G. Simoneau, “Foot and Ankle Sensory Neuropathy, Proprioception, and Postural Stability,” *J. Orthop. Sport. Phys. Ther.*, vol. 29, no. 12, pp. 718–726, Dec. 1999.

[29] J. G. Buckley, D. O. Driscoll, and S. J. Bennett, “Postural Sway and Active Balance,” *Am. J. Phys. Med. Rehabil.*, no. January, pp. 13–20, 2002.

[30] V. Macefield, S. Gandevia, B. Bigland-Ritchie, R. B. Gorman, and D. Burke, “The firing rates of human motoneurones voluntarily activated in the absence of muscle afferent feedback.,” *J. Physiol.*, pp. 429–443, 1993.

[31] R. L. Sainburg, H. Poizner, and C. Ghez, “Loss of Proprioception Produces Deficits in Interjoint Coordination,” *J. Neurophysiol.*, vol. 70, no. 5, pp. 2136–2147, 1993.

[32] J. Monzée, Y. Lamarre, and A. M. Smith, “The effects of digital anesthesia on force control using a precision grip.,” *J. Neurophysiol.*, vol. 89, no. 2, pp. 672–83, Feb. 2003.

[33] R. Jacobs, R. Brånemark, K. Olmarker, B. Rydevik, D. van Steenberghe, and P. Brånemark, “Evaluation of the psychophysical detection threshold level for vibrotactile and pressure stimulation of prosthetic limbs using bone anchorage or soft tissue support,” *Prosthet. Orthot. Int.*, vol. 24, no. 2, pp. 133–142, Jan. 2000.

[34] J. A. Sabolich and G. M. Ortega, “Sense of feel for lower limb amputees: a phase one study,” *J. Porsthetics Orthot.*, vol. 6, no. 2, pp. 36–41, 1994.

[35] R. E. Fan, M. O. Culjat, C. H. King, M. L. Franco, R. Boryk, J. W. Bisley, E. Dutson, and W. S. Grundfest, “A haptic feedback system for lower-limb prostheses,” *IEEE Trans. Neural Syst. Rehabil. Eng.*, vol. 16, no. 3, pp. 270–277, 2008.

[36] R. E. Fan, C. Wottawa, A. Mulgaonkar, R. J. Boryk, T. C. Sander, M. P. Wyatt, E. Dutson, W. S. Grundfest, and M. O. Culjat, “Pilot testing of a haptic feedback rehabilitation system on a lower-limb amputee,” *2009 ICME Int. Conf. Complex Med. Eng. C. 2009*, 2009.

[37] A. Branner and R. A. Normann, “A multielectrode array for intrafascicular recording and stimulation in sciatic nerve of cats,” *Brain Res. Bull.*, vol. 51, no. 4, pp. 293–306, 2000.

[38] J. Viton, L. Mouchnino, M. L. Mille, M. Cincera, A. Delarque, A. Pedotti, A. Bardot, and J. Massion, “Equilibrium and movement control strategies in trans-tibial amputees,” *Prosthet. Orthot. Int.*, vol. 24, no. 2, pp. 108–116, Jan. 2000.

[39] A. Anani, K. Ikeda, and L. Korner, “Prosthesis Sensory Feedback Properties Of Afferent Nerve Stimulation In Below-Elbow Amputees,” in *Proceedings of the European Conference on Electrotechnics*, 1977, pp. 190–195.

[40] A. Anani and L. Körner, “Afferent electrical nerve stimulation: Human tracking performance relevant to prosthesis sensory feedback,” *Med. Biol. Eng. Comput.*, vol. 17, no. 4, pp. 425–434, 1979.

[41] H. E. Torebjörk and J. Ochoa, “Specific sensations evoked by activity in single identified sensory units in man.,” *Acta Physiol. Scand.*, vol. 110, no. 4, pp. 445–7, Dec. 1980.

[42] G. Macefield, S. C. Gandevia, and D. Burke, “Perceptual responses to microstimulation of single afferents innervating joints, muscles and skin of the human hand.,” *J. Physiol.*, vol. 429, no. 1, pp. 113–129, Oct. 1990.

[43] J. Ochoa, “Intraneural microstimulation in humans,” *Neurosci. Lett.*, vol. 470, pp. 162–167, 2010.

[44] D. Tyler and D. Durand, “Functionally selective peripheral nerve stimulation with a flat interface nerve electrode,” *IEEE Trans. Neural Syst. Rehabil. Eng.*, vol. 10, no. 4, pp. 294–303, Dec. 2002.

[45] N. M. Ledbetter, C. Ethier, E. R. Oby, S. D. Hiatt, A. Wilder, J. H. Ko, S. P. Agnew, L. E. Miller, and G. A. Clark, “Intrafascicular stimulation of monkey arm nerves evokes coordinated grasp and sensory responses.,” *J. Neurophysiol.*, no. October 2012, pp. 580–590, Oct. 2012.

[46] T. Akin, K. Najafi, R. H. Smoke, and R. M. Bradley, “A micromachined silicon sieve electrode for nerve regeneration applications.,” *IEEE Trans. Biomed. Eng.*, vol. 41, no. 4, pp. 305–13, Apr. 1994.

[47] J. Sweeney, D. Ksienski, and J. Mortimer, “A Nerve Cuff Technique for Selective Excitation of Peripheral Nerve Trunk Regions,” *IEEE Trans. Biomed. Eng.*, vol. 31, no. 7, 1990.

[48] A. Branner, R. Stein, E. Fernandez, Y. Aoyagi, and R. A. Normann, “Long-term stimulation and recording with a penetrating microelectrode array in cat sciatic nerve.,” *IEEE Trans. Biomed. Eng.*, vol. 51, no. 1, pp. 146–57, Jan. 2004.

[49] G. S. Dhillon, S. M. Lawrence, D. T. Hutchinson, K. Horch, and S. L. City, “Residual Function in Peripheral Nerve Stumps of Amputees : Implications for Neural Control of Artificial Limbs,” *Hand Surg.*, pp. 605–615, 2004.

[50] G. A. Clark, S. Wendelken, D. M. Page, T. Davis, H. A. C. Wark, A. Richard, D. Warren, and D. Hutchinson, “Using Multiple High-Count Electrode Arrays in Human Median and Ulnar Nerves to Restore Sensorimotor Function after Previous Transradial Amputation of the Hand,” pp. 1977–1980, 2014.

[51] D. Tan, M. Schiefer, M. W. Keith, R. Anderson, and D. Tyler, “Stability and selectivity of a chronic, multi-contact cuff electrode for sensory stimulation in a human amputee,” *Int. IEEE/EMBS Conf. Neural Eng. NER*, vol. 12, no. 2, pp. 859–862, 2013.

[52] K. Horch, S. Meek, T. G. Taylor, and D. T. Hutchinson, “Object discrimination with an artificial hand using electrical stimulation of peripheral tactile and proprioceptive pathways with intrafascicular electrodes,” *IEEE Trans. Neural Syst. Rehabil. Eng.*, vol. 19, no. 5, pp. 483–489, 2011.

[53] H. Flor, T. Elbert, S. Knecht, C. Wienbruch, C. Pantev, N. Birbaumer, W. Larbig, E. Taub, and others, “Phantom-limb pain as a perceptual correlate of cortical reorganization following arm amputation,” *Nature*, vol. 375, no. 6531, pp. 482–484, 1995.

[54] F. Clippinger, A. V Seaber, J. H. McElhaney, J. M. Harrelson, and G. M. Maxwell, “Afferent sensory feedback for lower extremity prosthesis.,” *Clin. Orthop. Relat. Res.*, no. 169, pp. 202–206, 1982.

[55] M. P. Mileusnic, I. E. Brown, N. Lan, and G. Loeb, “Mathematical Models of Proprioceptors. I. Control and Transduction in the Muscle Spindle,” *J. Neurophysiol.*, pp. 1772–1788, 2006.

[56] M. P. Mileusnic and G. Loeb, “Mathematical models of proprioceptors. II. Structure and function of the Golgi tendon organ.,” *J. Neurophysiol.*, vol. 96, no. 4, pp. 1789–802, Oct. 2006.

[57] M. Häggström, “Medical gallery of Mikael Häggström 2014,” *Wikiversity J. Med.*, vol. 1, no. 2, 2014.

[58] P. B. Brown and H. Koerber, “Cat hindlimb tactile dermatomes determined with single-unit recordings.,” *J. Neurophysiol.*, vol. 41, no. 2, pp. 260–267, Mar. 1978.

[59] H. Burton and J. J. McFarlane, “The organization of the seventh lumbar spinal ganglion of the cat,” *J. Comp. Neurol.*, vol. 149, no. 2, pp. 215–231, 1973.

[60] J. M. Peyronnard, J. P. Messier, M. Dubreuil, L. Charron, and F. Lebel, “Three-dimensional computer-aided analysis of the intraganglionic topography of primary muscle afferent neurons in the rat,” *Anat. Rec.*, vol. 227, no. 4, pp. 405–417, 1990.

[61] R. Gaunt, J. Hokanson, and D. Weber, “Microstimulation of primary afferent neurons in the L7 dorsal root ganglia using multielectrode arrays in anesthetized cats: thresholds and recruitment properties.,” *J. Neural Eng.*, vol. 6, no. 5, p. 055009, Oct. 2009.

[62] A. S. Koivuniemi, O. B. Regele, J. H. Brenner, and K. J. Otto, “Rat behavioral model for high-throughput parametric studies of intracortical microstimulation,” in *2011 Annual International Conference of the IEEE Engineering in Medicine and Biology Society*, 2011, vol. 2011, pp. 7541–7544.

[63] D. C. Bradley, P. Troyk, J. A. Berg, M. Bak, S. Cogan, R. Erickson, C. Kufta, M. Mascaro, D. McCreery, E. Schmidt, V. L. Towle, and H. Xu, “Visuotopic mapping through a multichannel stimulating implant in primate V1.,” *J. Neurophysiol.*, vol. 93, no. 3, pp. 1659–70, Mar. 2005.

[64] R. Romo, A. Hernández, A. Zainos, C. D. Brody, and L. Lemus, “Sensing without touching: psychophysical performance based on cortical microstimulation.,” *Neuron*, vol. 26, no. 1, pp. 273–8, Apr. 2000.

[65] J. A. Berg, F. V Tenore, L. Jessica, R. J. Vogelstein, and S. J. Bensmaia, “Restoring the sense of touch with a prosthetic hand through a brain interface,” *Proc. Natl. Acad. Sci.*, vol. 111, no. 2, pp. 875–875, 2013.

[66] M. Nicolelis, J. E. O’Doherty, M. a. Lebedev, P. J. Ifft, K. Z. Zhuang, S. Shokur, and H. Bleuler, “Active tactile exploration using a brain–machine–brain interface,” *Nature*, pp. 1–5, Oct. 2011.

[67] B. Edin, “Cutaneous afferents provide information about knee joint movements in humans.,” *J. Physiol.*, vol. 531, no. Pt 1, pp. 289–97, Feb. 2001.

[68] S. Gandevia, “Illusory movements produced by Electrical Stimulation of Low-Threshold Muscle Afferents from the Hand,” *Brain*, pp. 965–981, 1985.

[69] J. Swett and C. Bourassa, “Comparison of sensory discrimination thresholds with muscle and cutaneous nerve volleys in the cat.,” *J. Neurophysiol.*, 1967.

[70] G. S. Dhillon and K. Horch, “Direct Neural Sensory Feedback and Control of a Prosthetic Arm,” *IEEE Trans. Neural Syst. Rehabil. Eng.*, vol. 13, no. 4, pp. 468–472, Dec. 2005.

[71] G. S. Dhillon, S. M. Lawrence, D. T. Hutchinson, and K. W. Horch, “Residual function in peripheral nerve stumps of amputees: implications for neural control of artificial limbs.,” *J. Hand Surg. Am.*, vol. 29, no. 4, pp. 605–15; discussion 616–8, Jul. 2004.

[72] C. G. Phillips, T. P. S. Powell, and M. Wiesendanger, “Projection from low-threshold muscle afferents of hand and forearm to area 3a of baboon’s cortex,” *J. Physiol.*, vol. 217, no. 2, pp. 419–446, Sep. 1971.

[73] T. McKenna, B. Whitsel, D. Dreyer, and C. Metz, “Organization of cat anterior parietal cortex: Relations among cytoarchitecture, single neuron functional properties, and interhemispheric connectivity,” *J. Neurophysiol.*, vol. 45, no. 4, pp. 667–697, 1981.

[74] S. Kim, A. Badi, and R. A. Normann, “Selective activation of cat primary auditory cortex by way of direct intraneural auditory nerve stimulation,” *Laryngoscope*, vol. 34, no. 2, pp. 300–9, Feb. 2007.

[75] M. E. Clark, M. J. Bair, C. C. Buckenmaier, R. J. Gironda, and R. L. Walker, “Pain and combat injuries in soldiers returning from Operations Enduring Freedom and Iraqi Freedom: implications for research and practice.,” *J. Rehabil. Res. Dev.*, vol. 44, no. 2, pp. 179–194, 2007.

[76] J. Maurer, N. Marangos, and E. Ziegler, “Reliability of cochlear implants,” *Otolaryngol. - Head Neck Surg.*, vol. 132, no. 5, pp. 746–750, 2005.

[77] W. G. Ondo, C. Meilak, and K. D. Vuong, “Predictors of battery life for the Activa Soletra 7426 Neurostimulator,” *Park. Relat. Disord.*, vol. 13, no. 4, pp. 240–242, 2007.

[78] D. Y. Deng, M. Gulati, M. Rutman, S. Raz, and L. V. Rodríguez, “Failure of Sacral Nerve Stimulation Due to Migration of Tined Lead,” *J. Urol.*, vol. 175, no. 6, pp. 2182–2185, 2006.

[79] V. S. Polikov, P. Tresco, and W. M. Reichert, “Response of brain tissue to chronically implanted neural electrodes.,” *J. Neurosci. Methods*, vol. 148, no. 1, pp. 1–18, Oct. 2005.

[80] J. Volkmann, J. Herzog, F. Kopper, and G. Geuschl, “Introduction to the programming of deep brain stimulators,” *Mov. Disord.*, vol. 17, no. SUPPL. 3, 2002.

[81] K. M. Aló, J. Holsheimer, M. Stanton-Hicks, A. R. Rezai, Y. Kanpolat, A. Savas, and K. J. Burchiel, "New trends in neuromodulation for the management of neuropathic pain," *Neurosurgery*, vol. 50, no. 4, pp. 690–704, 2002.

[82] T. Powell and V. Mountcastle, "Some aspects of the functional organization of the cortex of the postcentral gyrus of the monkey: a correlation of findings obtained in a single unit analysis with cytoarchitecture.," *Bull. Johns Hopkins Hosp.*, vol. 105, pp. 133–162, 1959.

[83] B. S. Wilson and M. F. Dorman, "Cochlear implants: a remarkable past and a brilliant future," *Hear. Res.*, vol. 242, no. 1–2, pp. 3–21, Aug. 2008.

[84] S. Cogan, "Neural stimulation and recording electrodes.," *Annu. Rev. Biomed. Eng.*, vol. 10, pp. 275–309, Jan. 2008.

[85] S. Schmidt, K. Horch, and R. A. Normann, "Biocompatibility of silicon-based electrode arrays implanted in feline cortical tissue," *J. Biomed. Mater. Res.*, vol. 27, no. 11, pp. 1393–1399, 1993.

[86] M. B. Christensen, S. M. Pearce, N. M. Ledbetter, D. J. Warren, G. A. Clark, and P. Tresco, "The foreign body response to the Utah Slant Electrode Array in the cat sciatic nerve," *Acta Biomater.*, vol. 10, no. 11, pp. 4650–4660, 2014.

[87] D. Lulic, A. Ahmadian, A. A. Baaj, S. R. Benbadis, and F. L. Vale, "Vagus nerve stimulation," *Neurosurg. Focus*, vol. 27, no. 3, p. E5, Sep. 2009.

[88] G. Creasey, J. Elefteriades, A. DiMarco, P. Talonen, M. Bijak, W. Girsch, and C. Kantor, "Electrical stimulation to restore respiration.," *J. Rehabil. Res. Dev.*, vol. 33, no. 2, pp. 123–132, 1996.

[89] N. Kohli and D. Patterson, "InterStim® Therapy: A Contemporary Approach to Overactive Bladder," *Rev. Obstet. Gynecol.*, vol. 2, no. 1, pp. 18–27, 2009.

[90] S. M. Pirris, S. Dhall, P. V Mummaneni, and A. S. Kanter, "Minimally invasive approach to extraforaminal disc herniations at the lumbosacral junction using an operating microscope: case series and review of the literature," *Neurosurg. Focus*, vol. 25, no. 2, p. E10, Aug. 2008.

[91] L. Liem, M. Russo, F. J. P. M. Huygen, J.-P. Van Buyten, I. Smet, P. Verrills, M. Cousins, C. Brooker, R. Levy, T. Deer, and J. Kramer, "A Multicenter, Prospective Trial to Assess the Safety and Performance of the Spinal Modulation Dorsal Root Ganglion Neurostimulator System in the Treatment of Chronic Pain," *Neuromodulation Technol. Neural Interface*, vol. 16, no. 5, pp. 471–482, Sep. 2013.

[92] V. Mooney, "Sensory feedback in upper-extremity amputees," *Clinical Orthopaedics and Related Research*. pp. 274–275, 1976.

[93] D. Atkins, D. C. Y. Heard, and W. H. Donovan, “Epidemiologic Overview of Individuals with Upper-Limb Loss and Their Reported Research Priorities,” *JPO J. Prosthetics Orthot.*, vol. 8, no. 1, pp. 2–11, 1996.

[94] A. Anani, K. Ikeda, and L. M. Körner, “Human ability to discriminate various parameters in afferent electrical nerve stimulation with particular reference to prostheses sensory feedback.,” *Med. Biol. Eng. Comput.*, vol. 15, no. 4, pp. 363–73, Jul. 1977.

[95] W. J. Wessels and E. Marani, “A rostrocaudal somatotopic organization in the brachial dorsal root ganglia of neonatal rats.,” *Clin. Neurol. Neurosurg.*, vol. 95 Suppl, pp. S3–S11, 1993.

[96] J. Ochoa and E. Torebjörk, “Sensations evoked by intraneural microstimulation of single mechanoreceptor units innervating the human hand.,” *J. Physiol.*, pp. 633–654, 1983.

[97] L. Resnik, M. R. Meucci, S. Lieberman-Klinger, C. Fantini, D. L. Kelty, R. Disla, and N. Sasson, “Advanced upper limb prosthetic devices: implications for upper limb prosthetic rehabilitation.,” *Arch. Phys. Med. Rehabil.*, vol. 93, no. 4, pp. 710–7, Apr. 2012.

[98] R. L. Sainburg, M. F. Ghilardi, H. Poizner, and C. Ghez, “Control of limb dynamics in normal subjects and patients without proprioception.,” *J. Neurophysiol.*, vol. 73, no. 2, pp. 820–35, Feb. 1995.

[99] S. G. Millstein, H. Heger, and G. a Hunter, “Prosthetic use in adult upper limb amputees: a comparison of the body powered and electrically powered prostheses.,” *Prosthet. Orthot. Int.*, vol. 10, no. 1, pp. 27–34, Apr. 1986.

[100] T. R. Farrell, R. F. Weir, C. W. Heckathorne, and D. S. Childress, “The effects of static friction and backlash on extended physiological proprioception control of a powered prosthesis.,” *J. Rehabil. Res. Dev.*, vol. 42, no. 3, pp. 327–41, 2005.

[101] D. J. Weber, B. M. London, J. A. Hokanson, C. A. Ayers, R. A. Gaunt, R. R. Torres, B. Zaaimi, and L. E. Miller, “Limb-State Information Encoded by Peripheral and Central Somatosensory Neurons: Implications for an Afferent Interface,” *IEEE Trans. Neural Syst. Rehabil. Eng.*, vol. 19, no. 5, pp. 501–513, Oct. 2011.

[102] F. Clippinger, R. Avery, and B. R. Titus, “A sensory feedback system for an upper-limb amputation prosthesis.,” *Bull. Prosthet. Res.*, vol. 22, pp. 247–58, Jan. 1974.

[103] C. B. Novak, H. Mehdian, and H. P. von Schroeder, “Laxity of the ulnar nerve during elbow flexion and extension.,” *J. Hand Surg. Am.*, vol. 37, no. 6, pp. 1163–7, Jun. 2012.

[104] V. V. Patel, F. P. Heidenreich, R. R. Bindra, K. Yamaguchi, and R. H. Gelberman, “Morphologic changes in the ulnar nerve at the elbow with flexion and extension: a

magnetic resonance imaging study with 3-dimensional reconstruction.," *J. Shoulder Elb. Surg.*, vol. 7, no. 4, pp. 368–74, 1998.

[105] P. Banczerowski, R. Veres, and J. Vajda, "Modified minimally invasive surgical approach to cervical neuromas with intraforaminal components: hemi-semi-laminectomy and supraforaminal burr hole (modified foraminotomy) technique.," *Minim. Invasive Neurosurg.*, vol. 52, no. 1, pp. 56–8, Feb. 2009.

[106] M. Bruneau, J. Cornelius, and B. George, "Microsurgical Cervical Nerve Root Decompression by Anterolateral Approach," *Neurosurgery*, vol. 58, no. Supplement 1, p. ONS–108–ONS–113, Feb. 2006.

[107] R. Riso, "Strategies for providing upper extremity amputees with tactile and hand position feedback – moving closer to the bionic arm," *Technol. Heal. Care*, vol. 7, pp. 401–409, 1999.

[108] D. Weber, B. M. London, J. A. Hokanson, C. Ayers, R. A. Gaunt, R. R. Torres, B. Zaaimi, and L. E. Miller, "Limb-state information encoded by peripheral and central somatosensory neurons: implications for an afferent interface.," *IEEE Trans. Neural Syst. Rehabil. Eng.*, vol. 19, no. 5, pp. 501–13, Oct. 2011.

[109] I. Boyd and K. Kalu, "Scaling factor relating conduction velocity and diameter for myelinated afferent nerve fibres in the cat hind limb.," *J. Physiol.*, pp. 277–297, 1979.

[110] D. P. C. Lloyd and H. T. Chang, "Afferent fibers in muscle nerves," *J. Neurophysiol.*, vol. 11, no. 3, p. 199, 1948.

[111] C. Hunt and A. K. Mcintyre, "An analysis of fibre diameter and receptor characteristics of myelinated cutaneous afferent fibres in cat," *J. Physiol.*, pp. 99–112, 1960.

[112] A. Vallbo, "Sensations evoked from the glabrous skin of the human hand by electrical stimulation of unitary mechanosensitive afferents.," *Brain Res.*, vol. 215, no. 1–2, pp. 359–63, Jun. 1981.

[113] D. McCreery, V. Pikov, and P. Troyk, "Neuronal loss due to prolonged controlled-current stimulation with chronically implanted microelectrodes in the cat cerebral cortex," *J. Neural Eng.*, vol. 036005, 2010.

[114] A. S. Koivuniemi and K. J. Otto, "Asymmetric Versus Symmetric Pulses for Cortical Microstimulation," *IEEE Trans. Neural Syst. Rehabil. Eng.*, vol. 19, no. 5, pp. 468–476, Oct. 2011.

[115] X. Cui, J. Wiler, M. Dzaman, R. A. Altschuler, and D. C. Martin, "In vivo studies of polypyrrole/peptide coated neural probes.," *Biomaterials*, vol. 24, no. 5, pp. 777–87, Feb. 2003.

[116] D. J. Bourbeau, J. A. Hokanson, J. E. Rubin, and D. J. Weber, “A computational model for estimating recruitment of primary afferent fibers by intraneural stimulation in the dorsal root ganglia,” *J. Neural Eng.*, vol. 8, no. 5, p. 056009, Oct. 2011.

[117] Z. P. Fang and J. T. Mortimer, “A method to effect physiological recruitment order in electrically activated muscle,” *Biomed. Eng. IEEE Trans.*, vol. 38, no. 2, pp. 175–179, 2002.

[118] F. Downs, “Prosthetics in the VA: Past, Present and Fure,” *Proceedings, US Nav. Inst.*, vol. 6, 2008.

[119] K. Etter, M. Borgia, and L. Resnik, “Prescription and repair rates of prosthetic limbs in the VA healthcare system: implications for national prosthetic parity,” *Disabil. Rehabil. Assist. Technol.*, vol. 10, no. 6, pp. 493–500, Nov. 2015.

[120] T. M. Quai, S. G. Brauer, and J. C. Nitz, “Somatosensation, circulation and stance balance in elderly dysvascular transtibial amputees.,” *Clin. Rehabil.*, vol. 19, no. 6, pp. 668–676, 2005.

[121] M. Schiefer, K. H. Polasek, R. J. Triolo, G. C. J. Pinault, and D. Tyler, “Selective stimulation of the human femoral nerve with a flat interface nerve electrode.,” *J. Neural Eng.*, vol. 7, no. 2, p. 26006, Apr. 2010.

[122] M. Schiefer, M. Freeberg, G. J. C. Pinault, J. Anderson, H. Hoyen, D. Tyler, and R. J. Triolo, “Selective activation of the human tibial and common peroneal nerves with a flat interface nerve electrode.,” *J. Neural Eng.*, vol. 10, no. 5, p. 056006, 2013.

[123] L. Fisher, C. Ayers, M. Ciollaro, V. Ventura, D. Weber, and R. Gaunt, “Chronic recruitment of primary afferent neurons by microstimulation in the feline dorsal root ganglia.,” *J. Neural Eng.*, vol. 11, no. 3, p. 036007, Jun. 2014.

[124] Y. Aoyagi, R. Stein, A. Branner, K. Pearson, and R. A. Normann, “Capabilities of a penetrating microelectrode array for recording single units in dorsal root ganglia of the cat,” *J. Neurosci. Methods*, vol. 128, no. 1–2, pp. 9–20, Sep. 2003.

[125] M. Kausz and M. Réthelyi, “Lamellar Arrangement of Neuronal Somata in the Dorsal Root Ganglion of the Cat,” *Somatosens. Mot. Res.*, vol. 2, no. 3, pp. 193–204, Jan. 1985.

[126] P. B. Yoo, M. Sahin, and D. Durand, “Selective stimulation of the canine hypoglossal nerve using a multi-contact cuff electrode.,” *Ann. Biomed. Eng.*, vol. 32, no. 4, pp. 511–9, Apr. 2004.

[127] A. Branner, R. Stein, and R. A. Normann, “Selective Stimulation of Cat Sciatic Nerve Using an Array of Varying-Length Microelectrodes,” *J. Neurophysiol.*, vol. 85, no. 4, pp. 1585–1594, 2001.

[128] J. E. Crouch, *Text-Atlas of Cat Anatomy*. Lea & Febiger, 1969.

[129] J. Hokanson, C. Ayers, R. Gaunt, T. Bruns, and D. Weber, "Effects of spatial and temporal parameters of primary afferent microstimulation on neural responses evoked in primary somatosensory cortex of an anesthetized cat.," *Conf. Proc. IEEE Eng. Med. Biol. Soc.*, vol. 2011, pp. 7533–6, Jan. 2011.

[130] J. E. Swett, C. M. Bourassa, and S. Inoue, "Effects of Cutaneous and Muscle Sensory Nerve Volleys in Awake Cats: A Study in Perception," *Science (80-.).*, vol. 145, no. 3636, pp. 1071–1073, Sep. 1964.

[131] L. Fisher, D. Tyler, J. S. Anderson, and R. J. Triolo, "Chronic stability and selectivity of four-contact spiral nerve-cuff electrodes in stimulating the human femoral nerve.," *J. Neural Eng.*, vol. 6, no. 4, p. 046010, 2009.

[132] P. J. Lynch, T. McJunkin, E. Eross, S. Gooch, and J. Maloney, "Case report: Successful epiradicular peripheral nerve stimulation of the C2 dorsal root Ganglion for postherpetic neuralgia," *Neuromodulation*, vol. 14, no. 1, pp. 58–61, 2011.

[133] K. Warwick, M. Gasson, B. Hutt, I. Goodhew, P. Kyberd, B. Andrews, P. Teddy, and A. Shad, "The application of implant technology for cybernetic systems.," *Arch. Neurol.*, vol. 60, no. 10, pp. 1369–73, Oct. 2003.

[134] E. M. Schmidt, M. J. Bak, F. T. Hambrecht, C. V Kufta, D. K. O'Rourke, and P. Vallabhanath, "Feasibility of a visual prosthesis for the blind based on intracortical microstimulation of the visual cortex.," *Brain*, vol. 119 (Pt 2, pp. 507–522, 1996.

[135] B. Rydevik, M. Brown, and G. Lundborg, "Pathoanatomy and Pathophysiology of Nerve Root Compression," *Spine*, vol. 9, no. 1. pp. 7–15, 1984.

[136] J. F. Howe, J. D. Loeser, and W. H. Calvin, "Mechanosensitivity of dorsal root ganglia and chronically injured axons: A physiological basis for the radicular pain of nerve root compression," *Pain*, vol. 3, no. 1, pp. 25–41, 1977.

[137] A. N. Badi, A. O. Owa, C. Shelton, and R. A. Normann, "Electrode independence in intraneural cochlear nerve stimulation.," *Otol. Neurotol.*, vol. 28, no. 1, pp. 16–24, Jan. 2007.

[138] N. Brill and D. Tyler, "Optimizing Nerve Cuff Stimulation of Targeted Regions through Use of Genetic Algorithms," *IEEE Eng. Med. Biol. Mag.*, no. Table 1, pp. 5811–5814, 2011.

[139] C. Veraart, W. Grill, and J. Mortimer, "Selective control of muscle activation with a multipolar nerve cuff electrode.," *IEEE Trans. Biomed. Eng.*, vol. 40, no. 7, pp. 640–53, Jul. 1993.

[140] P. J. Rousche and R. A. Normann, “A method for pneumatically inserting an array of penetrating electrodes into cortical tissue,” *Ann. Biomed. Eng.*, vol. 20, no. 4, pp. 413–422, 1992.

[141] D. McCreery, W. F. Agnew, T. G. Yuen, and L. Bullara, “Charge density and charge per phase as cofactors in neural injury induced by electrical stimulation.,” *IEEE Trans. Biomed. Eng.*, vol. 37, no. 10, pp. 996–1001, Oct. 1990.

[142] J. Hokanson, “Mathematical and Experimental Models for Studying Somatosensory Feedback via Primary Afferent Microstimulation,” 2013.

[143] H. O. Handwerker, S. Kilo, and P. W. Reeh, “Unresponsive afferent nerve fibres in the sural nerve of the rat.,” *J. Physiol.*, vol. 435, no. 1991, pp. 229–242, 1991.

[144] A. Prochazka and M. Gorassini, “Models of ensemble firing of muscle spindle afferents recorded during normal locomotion in cats.,” *J. Physiol.*, vol. 507 (Pt 1, pp. 277–91, Feb. 1998.